Polar Constituents of Coal Gasification Oil Samples

Leo A. Raphaelian

Argonne National Laboratory
9700 S. Cass Avenue
Argonne, Illinois 60439

In preliminary analyses by GC/MS, it was found that HYGAS oil samples contain a variety of compounds, including toluene, the start-up and make-up oil, aromatic hydrocarbons, phenols, anilines, pyridines, thiophenes, benzonitriles, and PNAs. Direct analysis of the mixture by GC/MS or capillary column GC/MS is at best difficult for at least two reasons: (1) Due to the large number (probably over 400) of compounds present in the mixture, many overlapping peaks occur, resulting in mass spectra that are often confusing; (2) Capillary columns that give good separation of non-polar compounds are not adequate for the separation of polar compounds. Therefore, there is a definite need for a preliminary separation into fractions of the complex mixtures in HYGAS oil samples.

For the separation of petroleum, fractional distillation, extraction, complex formation, and column chromatography, including adsorption, partition, and gel permeation, are among the methods that have been used. Each method has certain advantages and disadvantages: With fractional distillation, the toluene, which represents a major portion of a HYGAS oil sample, could be removed. However, this method suffers from the fact that any distillation, fractional or otherwise, requires heat and decomposition and reaction between components in the mixture typically takes place, altering the composition. With such extractions as the acid/base liquid-liquid type, recoveries of individual components of the mixture are not only variable but also often low, particularly with polar compounds; moreover, some matrix effects frequently occur affecting recoveries. Complex formation is not only too limited to be of use but also not applicable in this case since the complexes would not be chromatographable by GC. Column chromatography, although useful, suffers from being long and tedious and requires the use and workup of large amounts of solvent; it is not recommended for a large number of samples.

It can be stated, generally, that separations that can be done by column chromatography can also be done considerably better by HPLC. When compared to column chromatography, HPLC gives much better resolution, much shorter run times, and much less solvent. However, the amount of sample that can be processed per run is considerably less than with column chromatography. To overcome this disadvantage, several runs of the sample can be made with the attendant advantages of time, workup of much less solvent, and resolution.

In the petroleum field, HPLC has been used predominantly for identification of components in a mixture or for fingerprinting oil samples. Little attention has been paid to the use of HPLC as a means of performing gross separations although, in certain instances, investigators have isolated peaks and identified the compound or compounds by GC/MS or mass spectrometry. Although HPLC/MS instruments are available, HPLC does not have the resolution capillary column GC has and, as a result, HPLC/MS is not as useful as capillary column GC/MS for the analysis of complex mixtures.

It was found that the use of the μBondapak NH_2 as a stationary phase in HPLC was excellent for the separation of non-polar or weakly polar compounds; however, with polar compounds, the phase was too retentive and, although moderately polar compounds might pass through the column with a gradient, highly polar compounds are retained. It is possible to backwash the highly polar compounds but separation into fractions of the polar compounds can not be achieved. However, if one is

interested only in non-polar or weakly polar PNAs, a nice separation according to the number of rings of the parent PNAs and their alkyl derivatives can be accomplished with μBondapak NH_2, as shown in Table 1.

Table 1. Retention Time Range of Selected Benzenoid PNAs and Alkyl PNAs as a Function of the Number of Rings (μBondapak NH_2, Hexane Solvent, Flow Programmed 1-4 mL/min)

Number of Rings	Retention Time Range (Minutes)	
	Noncondensed	Condensed
1	4.2 (1)	NA
2	5.0-5.8 (3)	NA
3	6.8-7.5 (7)	NA
4	9.3-10.9 (5)	7.7-8.3 (3)
5	13.7-15.1 (3)	11.5-12.1 (2)

( ) Number of compounds from which range was determined
NA Not Applicable

Such a separation into fractions can be very useful for identifying a complex mixture that contains predominantly compounds that are relatively non-polar, since GC conditions can be tailor-made to each fraction. It is particularly useful for identifying the higher PNAs.

Whereas HPLC with a μBondapak NH_2 column affords a good separation of non-polar compounds, it appeared that the weakly polar stationary phases, μBondapak Phenyl and μBondapak CN, might be more useful for separating the polar compounds into fractions. In experiments with these columns under a variety of conditions, it was found that, with μBondapak CN, a satisfactory separation could be accomplished using a rather complex gradient of hexane to THF, as shown in Figure 1.

Fraction 1 (Figure 1) contained a variety of the typical PNAs and alkyl PNAs, including naphthalenes, biphenyls, benzothiophenes, acenaphthenes, fluorenes, phenanthrenes, anthracenes, dibenzothrophenes, aceanthrenes, and pyrenes. (There was also a series of alkyl benzenes present in fraction 1.) Since the remaining fractions were more polar, they were derivatized with Tri-Sil Concentrate, BSA, or Methyl-8. Surprisingly, Fractions 2, 3, and 4 contained, along with some alkyl phenols, a number of hydroxy PNAs, including hydroxy styrenes, indans, benzofurans, indenes, naphthols, benzothiophenes, biphenyls, and fluorenes. In Table 2, a summary of the hydroxy PNAs and, in Figure 2, their retention time ranges on a 50 meter OV-101 column programmed from 20 to 240°C are shown. It can be seen from Table 2 that the more alkylation there is in the molecule the lower the fraction, as would be expected, since the compound would be less polar or more non-polar.

The mass spectra of the alkylated derivatives of the hydroxy PHAs typically had a M-15 ion as the base peak from loss of a methyl from the trimethyl silyl grouping. There was a M-31 peak indicative of a $R\text{-}O\text{-}Si{=}CH_2$ ion. The parent ion was also a prominant ion. Occasionally, a M-89 ion indicative of loss of $(CH_3)_3SiO$- was found. In the case of hydroxy biphenyls, an ion corresponding to the loss of the underivatized phenyl ring is found.

Fractions 5 and 6 contained dihydroxy benzenes. No dihydroxy PNAs were found in these fractions, possibly, because they might not get through the column under the conditions used.

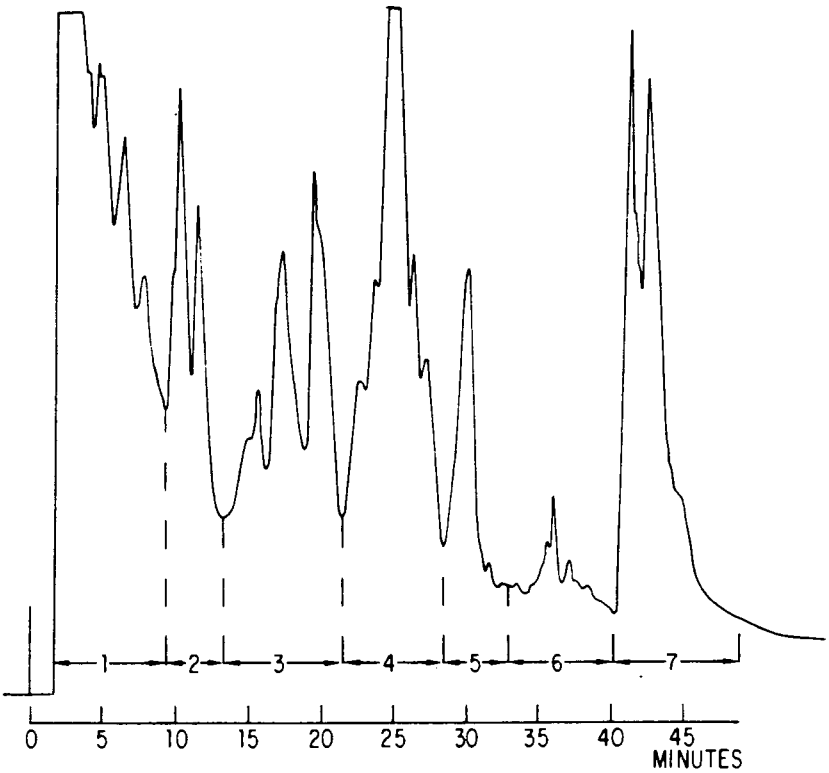

Figure 1. Hygas Oil Samples, HPLC on μBondapak CN Column, 2 mL/min Flow, 16 Minutes Hexane Alone, Linear Gradient, 0-1% in 10 Minutes, 1-5% in 10 Minutes, and 5-100% THF in Hexane in 10 Minutes; UV Detection at 254 nm

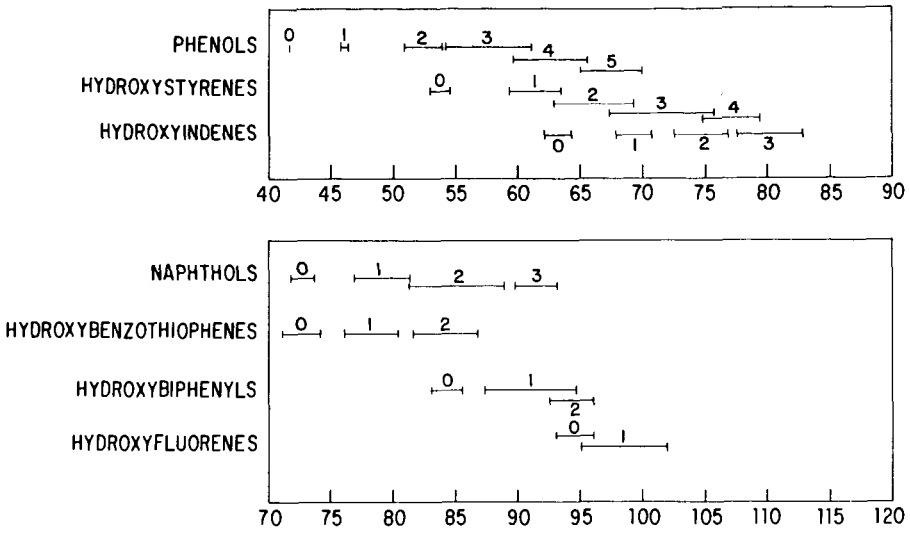

Figure 2. Retention Time Ranges of Some Phenols and Hydroxy PNAs, Derivatized with BSA, in Fractions 2,3, and 4

Table 2. Comparisons of Total Ion Count (in thousands) of Classes of Phenols and Hydroxy PNAs Versus Fraction

Type of Compound	Fraction 2	Fraction 3	Fraction 4
Phenols			
C_0	-	-	2(1)
C_1	-	202(2)	4(2)
C_2	92(4)	669(5)	8(4)
C_3	213(9)	419(9)	-
C_4	84(8)	255(7)	-
C_5	9(3)	17(2)	-
Hydroxystyrenes			
C_0	-	-	13(2)
C_1	27(1)	97(3)	19(4)
C_2	144(8)	154(7)	19(7)
C_3	80(15)	77(13)	3(1)
C_4	14(2)	8(4)	2(1)
Hydroxyindenes			
C_0	-	19(2)	32(3)
C_1	-	24(8)	6(1)
C_2	4(2)	8(4)	-
C_3	20(7)	2(1)	-
Naphthols			
C_0	-		368(2)
C_1	-	47(2)	277(6)
C_2	-	73(12)	95(10)
C_3	-	12(3)	2(1)
Hydroxybenzothiophenes			
C_0	-	-	152(4)
C_1		15(3)	92(6)
C_2	4(2)	23(5)	42(10)
C_3	-	-	3(1)
Hydroxybiphenyls			
C_0	-	-	71(2)
C_1	-	30(5)	101(7)
C_2	-	-	53(5)
C_3	2(1)	-	9(1)
Hydroxyfluorenes			
C_0	-	-	48(4)
C_1	-	-	6(3)

( ) Number of compounds found, inside parentheses

SYNTHETIC MIMICS FOR VISCOSITY AND SPECTRA OF H-COAL ASPHALTENES

Peter A. S. Smith, James C. Romine, and Mustafa El-Sheikh

Department of Chemistry, University of Michigan, Ann Arbor, MI 48109

Asphaltenes from liquefaction of coal have characteristic properties of solubility, viscosity, and spectroscopy that on the one hand require explanation, and on the other hand could provide insight into the complex chemical nature of these substances. Knowing that asphaltenes can be separated into neutral, acidic and basic fractions and that the acids are phenolic and the bases are apparently pyridine derivatives, we turned our attention to the hypothesis that phenolic structures having two or more hydroxyl groups per molecule and heterocyclic bases of the pyridine type with two or more basic sites might when mixed display properties similar to those observed in asphaltenes.

In choosing model compounds, we noted that asphaltenes have nuclear magnetic resonance spectra showing some absorption in the region δ 3 to 4. This is too far upfield to be due to aromatic or olefinic hydrogens, and too far downfield to be due to simple alkyl groups, even when they bear phenyl substituents. However, the greater electron-withdrawing power of the pyridine ring might be enough to shift aliphatic resonance to that region. We therefore chose structures having two or more phenol or pyridine rings linked by a series of methylene groups ranging between one and six. Such compounds would be capable of multiple hydrogen bonding with each

other, analogous to asphaltenes (1), and their mixtures could be anticipated to have high viscosities. Furthermore, we had already demonstrated the presence of chains of methylene groups in asphaltenes (2).

Methylene-4,4'-bisphenol and its 2,2'-isomer are commercially available. Bisphenols with a two-carbon bridge were synthesized from the appropriate benzaldehyde by the benzoin condensation and reduction. Bisphenols with other bridges were prepared as shown in the equations, utilizing the Fries rearrangement. Trisphenols were prepared by a double Fries rearrangement, and tetrakisphenols were prepared from bisphenol ethers by a double Friedel-Crafts reaction using methoxyphenylalkanoyl chlorides, reduction, and demethylation.

$$2\text{-ArCH=O} \rightarrow \text{Ar-CHOH-CO-Ar} \rightarrow \text{Ar-CH}_2\text{CH}_2\text{-Ar}$$

$$\text{HOArCH=O} + \text{CH}_3\text{COAr'OH} \rightarrow \text{HOArCH=CHCOAr'OH} \rightarrow \text{HOAr-(CH}_2)_3\text{-Ar'OH}$$

$$\text{HOArH} + \text{ClCO(CH}_2)_n\text{-2COCl} \rightarrow \rightarrow \text{HOArCO(CH}_2)_{n-2}\text{COArOH} \rightarrow \text{HOAr(CH}_2)_n\text{ArOH}$$

Bispyridines and bisquinolines were prepared as shown, or were prepared from quinolylmethyllithium and an α,Ω-dibromoalkane.

$$\text{PyCH=O} + \text{PyCH}_3 \rightarrow \text{PyCH=CHPy} \rightarrow \text{Py(CH}_2)_2\text{Py}$$

1-(2-Pyridyl)-2-(2-hydroxyphenyl)ethane was prepared analogously from α-picoline and salicylaldehyde and reduction of the resulting stilbene analog with H_2/Pd.

The compounds and their properties are listed in Table I. The nmr spectra of the bispyridines, and especially the bisquinolines, simulate the aliphatic region of asphaltene spectra, including the downfield end, reasonably well.

Mixtures of a phenol and a pyridine from this group were more difficult to dissolve than the pure compounds, and tetrahydrofuran was the only inert solvent that showed a general ability to dissolve them. In this respect, there is a similarity to preasphaltenes of H-coal vacuum bottoms.

Table I
Phenols and Pyridines

No.	Compound	mp, °C	"aliphatic"[a] NMR, ppm
	$4\text{-}HOC_6H_4(CH_2)_nC_6H_4\text{-}OH$		
1.	n = 2	198-99	2.9
2.	n = 3	96-98	1.6-2.8
3.	n = 4	158-59	1.5-2.5
	$3\text{-}HOC_6H_4(CH_2)_nC_6H_4\text{-}3\text{-}OH$		
4.	n = 3	131-33	2.0, 2.8
	$2\text{-}HOC_6H_4(CH_2)_nC_6H_4\text{-}2\text{-}OH$		
5.	n = 1	115-17	4.2
6.	n = 3	83-85	1.0-2.8, 5.3
	$2\text{-}HO\text{-}5\text{-}CH_3C_6H_3(CH_2)_nC_6H_3\text{-}5\text{-}CH_3\text{-}2\text{-}OH$		
7.	n = 5	103-05	2.7, 4.8
8.	n = 6	123-24	1.4, 2.2
	$C_5H_4N\text{-}2\text{-}(CH_2)_n\text{-}2\text{-}C_5H_4N$		
9.	n = 2	107-10	3.4
10.	n = 3	liq.	2.0-2.5, 2.6-3.1
	$C_5H_4N\text{-}4\text{-}(CH_2)_n\text{-}4\text{-}C_5H_4N$		
11.	n = 2	109-109.5	2.95
12.	n = 3	57-60	1.9-2.4, 2.5-3.0
13.	$C_5H_4N\text{-}2\text{-}(CH_2)_2\text{-}4\text{-}C_5H_4N$	liq.	2.95
14.	$C_5H_4N\text{-}3\text{-}(CH_2)_2\text{-}4\text{-}C_5H_4N$	34-36	2.95
15.	$C_5H_4N\text{-}2\text{-}(CH_2)_2\text{-}3\text{-}C_5H_4N$	liq.	2.90
	2-quinolyl$(CH_2)_n$-2-quinolyl		
16.	n = 2	162-63	3.55
17.	n = 6	90-91.5	1.3-2.2, 2.9-3.3
18.	$2\text{-}C_5H_4N\text{-}(CH_2)_2\text{-}2\text{-}C_6H_4OH$	87.5-88	3.18

a. In all compounds, aromatic ^1H resonance occurred in the region 7-9 ppm.

Initially, we planned to measure viscosity in solution, owing to the facts that most of the compounds were solids, and the quantities

were in most cases small, owing to the laborious syntheses. The solvents used by previous workers to study the effect of hydrogen bonding on viscosity (benzene, ethanol, ethyl or amyl acetate) would not dissolve sufficient quantities of our materials, and we were driven to use tetrahydrofuran. This solvent had already been used to study association in asphaltenes by Schwager, Lee and Yen (1), using vapor pressure osmometry.

Measurements of solutions of single phenols or pyridines and mixtures of them were made in 0.1 molar solutions in THF on an Ubbelohde viscometer at 25.00±0.02°, calibrated against water, dimethyl sulfoxide, and THF. The values of η so obtained are shown in Table II.

Table II
Viscosities of 0.1 M Solutions in Tetrahydrofuran

Solutes	θ (sec)	ρ (g/ml)	η (cp)
None			0.461
17	107.2	0.8930	0.5017
6	106.0	0.8909	0.4948
6 + 17	108.2	0.8952	0.5076
15	104.1	0.8880	0.4845
6 + 15	105.0	0.8906	0.4901
15 + methylene-2,2'-bisphenol	105.8	0.8896	0.4933

The results show that the viscosities, η, do not distinguish the solutions in which O-to-N hydrogen bonding can occur from those in which it cannot. This fact appears to arise from the nature of the solvent, which can itself act as an acceptor in hydrogen bonding. The energy of formation of the phenol-THF hydrogen bond has been reported to be 2.6 kcal/mol (3) and that of the phenol-pyridine hydrogen bond to be 8.0 kcal/mol (4). However, in the 0.1 M solutions, the concentration of the solvent THF is two orders of magnitude greater than that of the pyridine, such that the solvent can compete effectively with the pyridine for the phenol. This leveling effect greatly reduces the validity of studies of hydrogen bonding between substrates in THF; unfortunately, the solubility characteristics of the substrates did not allow a more inert solvent to be used.

The foregoing results demonstrated that viscosities would have to be measured on undiluted melts in order to investigate the role of hydrogen bonding. Such experiments require much larger samples than we had been able to prepare of most of the substrates, and we therefore limited these experiments to those substances that were available in sufficient quantity. Furthermore, the necessity to work with melts at elevated temperatures dictated a change in measurement technique, and we therefore used a Brookfield Engineering Laboratories model LVT rotational viscometer, using a Brookfield UL sample cell suitable for viscosities of 1 to 10 cp, or a specially designed small sample cell (1.5-2.0 ml) for viscosities in the range 100-10,000 cp. The entire apparatus was enclosed in a glass container which was immersed in a thermoregulated bath of silicone oil. Measurements on model compounds were made on 15-g. samples under an argon atmosphere at a series of increasing temperatures. Measurements were reproducible after cooling and remelting for the model compounds, but not for coal-derived materials until the sample had been subjected to several heating/cooling cycles.

Although a range of temperatures was used in each case, variations in melting point and viscosity precluded comparing all samples at the same temperature. Changes in shear rate (6, 30, 60 rpm) showed some non-Newtonian behavior (shear thinning), which was pronounced with some samples. Comparison of samples is thus more reliable at higher shear rates, and only values at 60 rpm are shown here. Representative results are given in Table III.

Table III
Viscosities of Undiluted Melts at 60 rpm and Activation Parameters
$\ln\eta = A + E_\eta/RT$

Sample	at 160° (cp)	at 180° (cp)	at 210° (cp)	A	E_η [a]
11	1.25			-5.1	4.6
12	1.39			-5.2	4.9
$CH_2(4\text{-}C_6H_4OH)_2$		3.99	2.70	-5.6	6.3
$CH_2(2\text{-}C_6H_4OH)_2$	4.84	3.45	2.13	-6.2	6.7
$CH_2(4\text{-}C_6H_4OH)_2$ + 11	6.55	4.19	2.26	-8.0	8.4
$CH_2(2\text{-}C_6H_4OH)_2$ + 11		4.24	2.12	-10.0	10.4
$CH_2(2\text{-}C_6H_4OH)_2$ + 12	3.58	2.45		-10.2	9.9
$CH_2(4\text{-}C_6H_4OH)_2$ + 12			2.48	--4.8	5.6
2 + 11	5.17	3.68		-6.3	6.9
18	2.77	2.08		-8.1	7.8
"oils & resins" [b]	3.84	2.70		-7.5	7.6
"low mol. wt." asphaltenes [c]		6.95	4.68	-5.7	6.9
"high mol. wt." asphaltenes [c]			1550.0 [d]	-5.2	55.5

a. kcal/mol. b. Pentane-soluble fraction of H-coal vacuum bottoms.
c. See text. d. At 200°.

The measurements at different temperatures (a greater range and number of points than given in Table III) allow the activation energy for viscous flow, E_η, to be determined from the Eyring equation (5), $\ln\eta = A + E_\eta/RT$. These values are given in Table III, although this equation is of uncertain validity for molecules that are far from spherical (6). The linearity of a plot of $\ln\eta$ vs. $1/T$ may be used as a gauge of its applicability to a given system; the data for the various model systems were closely linear, with a correlation coefficient of 0.97-0.99. For coal-derived materials, the equation is less reliable (correlation coefficient 0.91-0.96), some curvature being noticeable at higher temperatures.

The activation energies are of the same order of magnitude as the energy of the hydrogen bond, except for the "high molecular weight" asphaltenes (soluble in toluene, but insoluble in 75% pentane/25% toluene), the value for which is more than five-fold those of the others, and in particular, is eight times as high as that for "low molecular weight" asphaltenes (soluble in 75% pentane/25% toluene).

Among the foregoing data, the system 2 + 11 provides a reasonably good simulation of the viscosity characteristics of "low molecular weight" asphaltenes. Both the activation parameters and the manifestation of non-Newtonian behavior vary with the length of the connecting chain of methylene groups and the position of the

H-bonding sites, and further study of the relationship may provide a more precise delineation of the structural possibilities for coal-derived liquids. It appears, however, even at this stage, that the "high molecular weight" asphaltenes owe their viscosity to a major extent to other causes.

We have made similar comparisons of the infrared spectra of melted asphaltenes and of model systems at elevated temperatures, using an electrically heated cell with internal temperature sensing, and recording the spectra over a range of temperatures. As was expected, the absorptions due to associated O-H decreased in comparison to unassociated O-H as the temperature was raised. The general form and the temperature sensitivity for asphaltenes and for mixtures of model phenols and pyridines were qualitatively similar.

REFERENCES

(1) I. Schwager, W. Lee and T. Yen, Anal. Chem., 49 (14), 2323 (1977).
(2) P. A. S. Smith, J. C. Romine and S.-S. P. Chou, Div. Petrol. Chem., Am. Chem. Soc., Preprints, 24, 974 (Sept. 1979).
(3) N. Nametkin, A. Kashevnik, M. Kurashev and T. Veretyakhina, J. Gen. Chem. (USSR), 47, 2168 (1977).
(4) R. Drago, G. Vogel and T. Needham, J. Am. Chem. Soc., 93, 6014 (1971).
(5) H. Eyring, J. Chem. Phys., 4, 283 (1936).
(6) S. Brush, Chem. Rev., 62, 5131 (1962); S. Breitting and J. Magill, J. Appl. Phys., 45 (10), 4167 (1974).

Reducing Viscosity of Coal Liquefaction Products With Additives

T. S. Chao, H. W. Kutta and A. C. Smith, Jr.

ARCO Petroleum Products Company
Harvey Technical Center
Harvey, IL 60426

Introduction

Viscosity is one of the critical properties hindering the development of coal liquefaction processes. A product of high viscosity is difficult to pump, filter and atomize, affecting the flow of process streams, removal of catalysts, transport from one location to another and proper atomization in combustion equipment. The use of higher temperatures to reduce viscosity is costly and is often accompanied by problems of oxidative and thermal degradation and safety.

Viscosity can be reduced by more extensive hydrogenation. This practice, however, increases the cost of product and may not be necessary. If the cause of high viscosity of coal liquefaction products is thoroughly understood, an economically attractive alternative to extensive hydrogenation can probably be found. A research program to investigate the cause of high viscosity of coal liquefaction products and to improve this critical property was carried out at Harvey Technical Center under the joint sponsorship by Electric Power Research Institute and Atlantic Richfield Company. Results of this program have been issued as an EPRI report.(1) Prior to this joint program an in-house project was also initiated by Atlantic Richfield to determine causes and remedies for high viscosity of coal liquefaction products. One result of these programs is the discovery that certain chemical compounds, when used at concentrations of 1-10%, are effective in reducing the melt viscosity and softening temperature of these coal liquefaction products. This paper summarizes our findings on this subject and expresses our thinking regarding their mechanism of action.

Experimental

Source of Coal Liquefaction Products

1. H-Coal

H-Coal was provided by Hydrocarbon Research, Inc., Trenton, NJ, and was identified as PDU Run 130-73. This pilot plant run was operated at a fuel oil mode meaning that less extensive hydrogenation was carried out. This yielded three fractions: atmospheric overhead, atmospheric bottoms and vacuum bottoms. The last-named fraction contained catalysts and other ash-forming materials. It was de-ashed in our laboratory by dissolving in tetrahydrofuran, filtering through a fine-pore filter aid (Celatom FP-2 from Eagle-Picher Industries) and removing the solvent by diluting with water, filtering, washing and drying in a vacuum oven. The de-ashed vac. bottoms was then combined with the other two fractions according to the proportions

provided by Hydrocarbon Research. To avoid oxidation all operations were carried out under N_2 atmosphere and all materials were stored in desiccators or closed containers under N_2. Analyses of the different batches of H-Coal used for this study are shown in Table 1.

2. SRC-Coal

Solvent Refined Coal was provided by Catalytic, Inc., Wilsonville, AL. It was produced from Illinois No. 6 Coal of Burning Star Mines and was used as received in our studies. Analyses are also shown in Table 1.

Source of Additives

All the additives discussed in this paper (except naphthenic acid and aromatic oils) were purchased. Suppliers and chemical structure are shown in Table 6.

Blending

In the case of H-Coal the components were weighed into a N_2-flushed screw-capped Pyrex jar, heated in an oven at 350-360°F until the solids melted and were then stirred under a N_2 blanket into a homogeneous mixture. The jar was closed, cooled to room temperature and the solid mass was pulverized into a powder under N_2 blanket. This powder was used for analysis, for melting point and softening point determinations and for blending with additives. H-Coal and less volatile additives were weighed directly into the Brookfield viscometer cup. This procedure avoided oxidation of the product during hot blending and was more convenient than carrying out the blending in an autoclave. However, it also limited the quantity of H-Coal blended in each batch and a total of six batches had to be prepared for this study. An autoclave was used when more volatile additives, e.g. propylene oxide, acetic anhydride and acetic acid were employed.

For Solvent Refined Coal the same procedure was followed except that no blending from components was required.

Viscosity Determination

Viscosity was determined in a Brookfield Viscometer (Model RVT) at temperatures of 278-500°F and shear rates of 14 and 28 sec^{-1}. These correspond to speeds of 50 and 100 rpm with the SC 4-28 spindle. All viscosity data were based on an average of three readings which were usually within 2% of each other. Temperatures shown for the viscosity data were actual temperatures based on calibration. Low and inconsistent viscosity readings obtained for non-homogeneous samples were disregarded.

Softening Point Determination

The softening point was determined according to ASTM Method D-2398. To avoid excessive oxidation, the preparation of the sample disc was carried out under N_2 atmosphere in the laboratory of one of the investigators.

Results and Discussion

The additives found to be effective at 1-10% level can be divided into two groups: those which are reactive with certain components of coal liquefaction products and those which are unreactive. These materials are defined as additives on the basis that they perform an essential function at a relatively low concentration.

Reactive Additives

The presence of acidic and basic components in coal liquefaction products is well known. Sternberg and his coworkers[2][3][4] reported that asphaltenes, the key intermediate of coal liquefaction, contains both acidic and basic components and that the hydrogen bonding between these components is responsible for the high viscosity of the products. The acidic components include phenols and pyrroles, while the basic components are pyridines.

Based on this knowledge we postulated that any chemical compound which can react with either the acidic or basic groups will reduce the viscosity of coal liquefaction products by converting the acid or basic components into neutral ones and, in so doing, eliminate the strong intermolecular forces causing high viscosity. The postulation was proved to be correct. Fig. 1 shows the viscosity of a H-Coal with and without the presence of 5% by weight of various reactive additives. Table 2 shows the effect of these additives on softening temperature and a calculated % reduction of 330°F viscosity. These additives represent the following class of chemical compounds. Only one or two compounds in each class were tested and consequently, may not represent the optimum choice. The latter is dependent on cost, availability, effectiveness and such considerations as volatility, corrosiveness, toxicity, safety and ease of handling.

a. Acids and Anhydrides

These compounds are expected to convert the basic nitrogen compounds to salts or amides, eliminating the H-bonding with the weaker phenolic compounds. Compounds tested include naphthenic acid, acetic acid, acetic anhydride and dodecenyl succinic anhydride. At a concentration of 5% W, the reduction in 330°F melt viscosity was 82-89%. In later work with 1 and 2% acetic anhydride and a different batch of H-Coal reductions of 355°F viscosity of 40.5 and 52.5% were obtained. (Table 4)

b. Amines

The amines selected for testing were Cocoamine and Duomeen C, based on considerations of volatility. At 5% W they reduced 330°F viscosity of H-Coal by 72.6-81.0%. These amines (represented by B') probably function by replacing the weaker pyridine type components (B) from the hydrogen bonding pair A---B.

$$A\text{---}B + B' \rightleftharpoons A\text{---}B' + B$$

The new hydrogen bonding pair formed A-B' will have lower viscosity, since B' is a smaller molecule than B.

c. Epoxides

Epoxides can react with the phenolic compounds in the coal liquefaction product, forming hydroxyalkyl ethers.

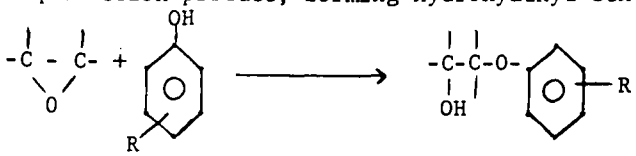

The epoxides tested included propylene oxide and Epoxide No. 7, a glycidy ether of a mixture of n-C_8 and n-C_{10} alcohols. The former lowered 355°F viscosity of one batch of H-Coal by 56.7% when used at 2% W. The latter lowered the 330°F viscosity of another batch by 84.3%, when used at 5% W. The effect of concentration of propylene oxide on viscosity of H-Coal is shown in Table 4.

Unreactive Additives

Compounds of this type are not expected to react chemically with components of coal liquefaction products. Table 3 shows their effect on viscosity and softening point of H-Coal. At a concentration of 5% W they reduced the 330°F melt viscosity of H-Coal by 76.3-95.5% and lowered the softening point by 17-81°F.

One most promising compound is N-methyl-2-pyrrolidone (NMP). At 5% W it gave the largest reduction in viscosity, 95.5%, among the compounds tested and is shown in Table 4. Subsequent concentration studies indicated that it is quite effective even at 1% W. The results of this concentration study are shown in Table 4 and illustrate that 68.0-78.4% reductions of the 330°F viscosity was achieved with 1% N-methyl-2-pyrrolidone for different batches of H-Coal. Fig. 2 shows viscosity of H-Coal as a function of temperature and concentration of NMP.

These compounds belong to the chemical classes of amides, phosphoramides, lactams and ketone. They are all polar compounds with moderate hydrogen bonding characteristics. Their ability to reduce the viscosity of H-Coal is believed to be related to their strong solvent power for the asphaltenes and preasphaltenes. Altgelt and Harle[5] reported that viscosity of solutions of petroleum asphaltenes is dependent on the nature of solvent. A good solvent such as pyridine provides a much lower solution viscosity for a petroleum asphaltene than a poor solvent such as cyclohexane. From this and related observations they concluded that viscosity of asphalts depends considerably on the intermolecular aggregation of dissolved asphaltenes and the extent of aggregation is dependent on the solvent.

The situation encountered with H-Coal is believed to be similar in the sense that good solvents did reduce viscosity and that the high viscosity is caused by aggregation. Differences may exist in the cause of aggregation. Altgelt and Harle, referring to studies by Yen et al[6], described the aggregate as the stacking of condensed aromatic rings. For coal liquefaction products, the work of Sternberg also indicated that aggregation of asphaltene molecules is caused by intermolecular H-bonding between acidic and basic groups. Regardless of the exact mechanism we can expect that aggregation of molecules does exist in coal liquefaction products and that good solvents can alter the extent of aggregation and thereby reduce its viscosity.

One important difference between the present case and that of Altgelt and Harle is the relative proportion of solvent and solute molecules. In the latter case the highest concentration of solute was 26.8% and the predominant species in the solution is that of the solvent. In the case with H-Coal and 1% NMP it is estimated that each molecule of NMP has to exert its effect on 10-15 molecules of asphaltene or preasphaltenes. This seems to indicate that these asphaltenes and preasphaltene molecules do exist in aggregates of 10-15 and more and that NMP exerts its effect not on individual molecules but on these aggregates.

Effectiveness in Solvent Refined Coal (SRC)

a. Reactive Additives

SRC from Illinois No. 6 coal was treated with 1 and 2% of propylene oxide, acetic acid and acetic anhydride in an autoclave. A reaction temperature of 500°F was maintained for 30 min. The treated product had a viscosity 15-40% lower than the original SRC (Table 5). This improvement was considerably less than that occurred with H-Coal (40.5-56.7%) under comparable test conditions.

b. Unreactive Additives

Of the many unreactive additives found effective in H-Coal only one was chosen for treatment of SRC. Results indicated that N-methyl-2-pyrrolidone gave a 48.2% reduction of 430°F viscosity at a concn. of 4% W.

However, a number of aromatic petroleum by-products were found to be effective at concentrations of 10%. Data in Table 5 show that the two aromatic extracts reduced the 440°F viscosity by 44.0-72.5%. These are by-products from solvent refining of 200 and 100 viscosity (SUS @ 100°F) lubricant base oils. The concentration of aromatic hydrocarbons by clay-gel analysis is in the range of 66-70%. The two light cycle oils reduced the 440°F viscosity by 78.0-83.5%. They are by-products of fluid catalytic cracker and contain approximately 60% aromatic hydrocarbons. The effectiveness of these additives is apparently related to the presence of high concentrations of aromatic hydrocarbons and their better solubility for the components of SRC. The greater effectiveness of light cycle oils than the aromatic extracts is believed to be related to their much lower viscosity.

REFERENCES

1. Kutta, H. W., E. H. Burk, Jr., L. H. Beckberger and T. S. Chao "Physical Property Improvement of Coal Liquefaction Products" Final Report, EPRI AF-392, Research Project 626, by Atlantic Richfield Co., for Electrical Power Research Institute, March, 1977.

2. Sternberg, H. W., R. Raymond and F. K. Schweighardt "Acid-Base Structure of Coal-Derived Asphaltenes," Science 188 49 (1975).

3. Sternberg, H. W., R. Raymond and S. Akhtar, "Synthoil Process and Product Analysis," American Chemical Society, Div. of Petroleum Chemistry, Philadelphia, April 6-11, 1975.

4. Sternberg, H. W., R. Raymond and F. K. Schweighardt "The Nature of Coal Liquefaction Products," American Chemical Society, Div. of Petroleum Chemistry, Chicago, Aug. 24-29, 1975.

5. Altgelt, K. H. and O. L. Harle "The Effect of Asphaltenes on Asphalt Viscosity," Ind. Eng. Chem. Prod. Res. Dev. 14 (4) 240 (1975).

6. Yen, T. F., J. G. Erdman, S. S. Pollack, Anal. Chem. 33 1587 (1961).

ACKNOWLEDGEMENT

The authors wish to express their appreciation to Electric Power Research Institute and Atlantic Richfield Company for permission to publish the paper, to Dr. W. C. Rovesti of EPRI and Doctors L. H. Beckberger, E. H. Burk, F. J. Chloupek and J. P. Kuebrich of Atlantic Richfield for their guidance and encouragement and to Dr. F. Eaton and Messrs. W. C. Keith and R. F. Poss for their contribution to this paper.

Table 1

Composition of Coal Liquefaction Products

Identity	H-Coal				SRC
Batch No.[a]	1	2	3	6	1
Analyses					
Wt. % C	85.65	85.65	86.75	85.34	86.90
H	6.71	7.15	7.30	7.38	5.75
O	4.66	4.11	4.12	4.80	5.00
S	0.70	0.62	0.57	-	0.67
N	1.39	1.28	1.27	1.28	2.00
Ash	0.14	0.17	0.21	0.15	0.24
H_2O	0.32	1.86	0.13	-	-
Mol. Ratio H/C	0.93	0.99	1.00	1.03	0.79

[a] Batches 4 and 5 were blended with same proportions of atmospheric overhead, atmospheric bottom and de-ashed vac. bottoms as Batch 3. They were not analyzed.

Table 2

Effect of Additives on Viscosity and Softening Point of H-Coal[a]

Additive	Wt. %	Softening Point °F		% Reduction Viscosity at 330°F
		Determined	Reduction	
None	-	275	-	-
Naphthenic Acid	5	210	65	82.1
Acetic Anhydride	5	235	40	88.8
Dodecenyl Succinic Anhydride	5	223	52	84.4
Cocoamine	5	200	75	81.0
Duomeen C	5	210	65	72.6
Epoxide No. 7	5	203	72	84.3

[a] Batch 2, Brookfield Viscosity 22.10 poise at 330°F and 28 sec^{-1}.

Table 3

Effects of Additives on Viscosity and Softening Point of H-Coal[a]

Additive	Wt. %	Softening Point °F		Brookfield Viscosity[c] Poise				% Reduction Viscosity at 330°F
		Determined	Reduction	278°F	305°F	330°F	355°F	
None	-	275	-	-	-	22.10	5.0	-
Dimethyl Acetamide	5	204	71	29.33	10.00	5.23	-	76.3
Tetramethyl Urea	5	200	75	7.50	2.77	1.03	-	95.3
N-methyl-2-Pyrrolidone	5	207	68	5.05	1.90	1.00	-	95.5
Hexamethyl Phosphoramide	5	194	81	13.41	4.92	2.25	-	89.8
Methylheptyl Ketone	5	258	17	b	b	5.30	-	76.0

[a] Batch 2
[b] Two phases
[c] At shear rate of 28 sec^{-1}

Table 4

Effect of Concentration of Additive on Viscosity of H-Coal

Additive	Wt. %	H-Coal Batch No.	Brookfield Viscosity Poise[a] 330°F	355°F	% Reduction
Acetic Anhydride	0	5	-	24.13	-
	1	"	-	14.35	40.5
	2	"	-	11.46	52.5
	4	"	-	9.00	62.7
Propylene Oxide	0	6	-	16.08	-
	2	"	-	6.97	56.7
	4	"	-	4.53	71.8
N-Methyl-2-Pyrrolidone	0	4	37.50	-	-
	1	"	8.10[b]	-	78.4
	2	"	5.58	-	85.1
	4	"	3.17	-	91.5

[a] At shear rate of 28 sec^{-1}
[b] Extrapolated from Vis. at 340 and 355°F

Table 5

Effect of Additives on Viscosity of Solvent Refined Coal

Additive	Wt. %	Brookfield Viscosity 440°F, 28 sec^{-1} Poise	% Reduction Viscosity at 440°F
None	-	10.00	-
Propylene Oxide	1.0	8.50	15.00
Acetic Acid	2.0	7.00	30.00
Acetic Anhydride	1.0	6.00	40.00
Aromatic Oils			
2095 Extract	10.0	5.60	44.0
1095 Extract	10.0	2.75	72.5
Light Cycle Oil	10.0	2.20	78.0
Hydrotreated Light Cycle Oil	10.0	1.65	83.5

Table 6

Supplier and Nature of Additives

Additive	Supplier	Chemical Nature or Structure
Naphthenic Acid (200 A.N.)	Atlantic Richfield	A mixture of carboxylic acids containing a cycloparaffinic ring and isolated from naphthenic crude oil. Avg. Mol. Wt. 260.
Acetic Anhydride	Eastman Organic Chemicals	$(CH_3CO)_2O$
Dodecenyl Succinic Anhydride	Humphrey Chem. Co.	$C_{12}H_{23}$-CH-CO | CH_2-CO > O
Propylene Oxide	Union Carbide	CH_3-CH-CH_2 O
Epoxide No. 7	Procter & Gamble	$ROCH_2$-CH-CH_2 O R = n-C_8H_{17} & n-$C_{10}H_{21}$
Cocoamine	Armak	Primary amine produced from coconut fatty acids.
Duomeen C	Armak	N-Coco-1,3-propanediamine
Dimethylacetamide	Aldrich	CH_3CONMe_2
Tetramethylurea	Aldrich	Me_2N-CO-NMe_2
Hexamethyl-phosphoramide	Aldrich	$P(O)(NMe_2)_3$
N-methyl-2-pyrrolidone	GAF	CH_2-CH_2 | CH_2-C = O N Me
Methylheptyl ketone	Armour	n-C_7H_{15} C-Me O

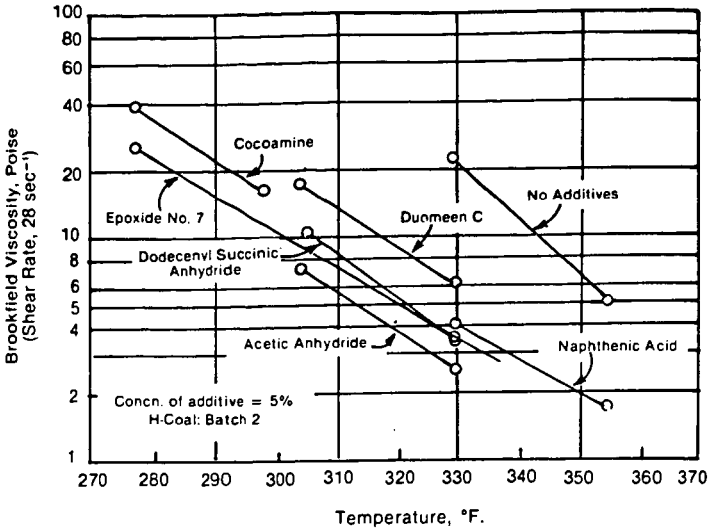

Figure 1. Effect of Additives on Viscosity of H-Coal

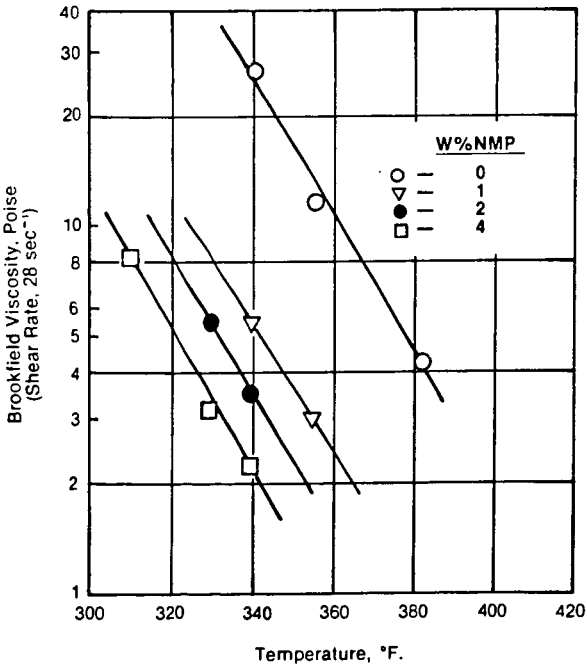

Figure 2. Effect of N-Methyl-2-Pyrrolidone (NMP) on Viscosity of H-Coal (Batch 4)

ULTRAFILTRATION DE-ASHING PROCESS FOR SOLVENT REFINED COAL

Abdelkader Bensalem*

Chemical Engineering Department, Columbia University
New York, New York 10027

*Leaving on a fellowship to: Technisch-Chemisches Laboratorium
ETH - Zurich, CH-8006 Switzerland

INTRODUCTION

Most ultrafiltration (UF) studies have focused on aqueous systems where solutions are concentrated by the removal of water[1]. References to the UF of non-aqueous solutions are infrequent. The paucity of studies on non-aqueous solutions has been due primarily to three reasons. First, present-day membrane technology is primarily directed toward the demineralization of saline and brackish waters. Second, the organic fouling in water of conventional cellulosic type membranes has limited their use in non-aqueous, organic solutions. Third, the low price of energy during the last two decades did not encourage engineers to develop low pressure, thus low energy techniques of separation which were capital intensive. But now with the necessity for energy conservation and the development of membranes made of new polymeric materials, ones which provide both good mechanical characteristics and good resistance against chemical attack, membrane technologies are being applied to non-aqueous systems[2,3].

Virtually all of the coal liquefaction processes require the separation of ash particles from the coal derived liquids in order to qualify the product as a furnace fuel. The SRC, Solvent Refined Coal, process produces a liquid having about 5% ash; a reduction of ash to below 0.1% is necessary to obviate the use of electrostatic precipitators in the furnace, thus reducing capital costs in product utilization. A further de-ashing to less than 0.005% would qualify SRC as a gas turbine fuel. Also, since most of the sulfur in SRC (0.55%) is concentrated in the ash; a UF de-ashing process would partially obviate the need for extensive desulfurization of the product[4]. A typical analysis is shown in Table 1. The asphaltenes (benzene soluble, pentane soluble) are believed to be responsible for the high viscosity of the product. A separation of these asphaltenes from the fuel could serve to avert viscosity-related problems in use. These asphaltenes could be further treated by thermal hydrocracking to produce more oil.

The objective in this investigation was to study the de-ashing (also de-sulfurization) of SRC using UF membranes including ones of fixed-charge, sulfonic acid nature. Principally such parameters as feed viscosity, temperature, use of solvents, cross-flow velocity, nature of the membrane and its fouling were of interest.

Table I

Analysis of SRC (SAMPLE from Filter feed from INDIANA V Coal)

Specific gravity at 90°C	1.087
Viscosity at 105°C	19.8 (cp)
Oils (Pentane solubles)	65.0% (wt. %)
Asphaltenes (Pentane Insolubles)	27.9% (wt. %)
Organic Benzene Insolubles	5.7% (wt. %)
Ash (Inorganic Insolubles)	5.45% (wt. %)
Sulfur	0.55% (wt.%)

EXPERIMENTAL

A. Apparatus: The system used in this investigation is shown in Fig. 1. The 2.0 l stainless steel reservoir was heated by heating tapes and its temperature controlled by a variac. The device readily withstands pressures up to 1500 psi. The operating pressures were provided by compressed nitrogen gas applied directly to the reservoir. The flow lines were made of 0.5 in. schedule - 40 pipes. Re-circulation rates were monitored with a high temperature and pressure (up to 1400 psig. and 205°C) dial indicator purgemeter Model 10A2227, manufactured by Fischer and Porter Co. of Warminster, Pennsylvania. The operating temperature was measured at the exit of the cell with a stainless steel Weston thermometer. A special positive displacement pump from the Viking Pump Division, Model GG1950 with steel external direct drive unit, acted as a feed carrier to the system. This pump can handle many types of liquids with viscosities up to 15,000 S.S.U. at temperatures up to 107°C.

B. Membranes and their Conditioning: UF membranes are usually stored and conditioned in water before use. In this study, the first treatment was to condition the membranes in a non-aqueous environment. To avoid osmotic shock this transfer was accomplished gradually at regular intervals, every 10 minutes, by increasing the concentration of the solvent with respect to water, using a water miscible solvent such as methanol. Then the membrane could be transferred directly to any other non-aqueous solvent (toluene, hexane, kerosene, ...).

The membranes used in this study were cast from a solution of polyacrylamide onto a spun bonded polyster support. The membranes pore radii were about 1.5 nm and 70% pore volume (Poiseuille).

C. 24 CB - Creosote Solvent: This solvent was obtained from Allied Chemical, Semet Solvey Division of Morristown, New Jersey. This is a specially refined creosote distillate of tar obtained by the high temperature carbonization of bituminous coal, and further processed to remove excess crystalline salts and make the oil more fluid. The 24-CB creosote oil has a specific gravity at 38°C/15.5°C of 1.06, and its viscosity is about 2.1 Cp at 100°C.

D. Analysis for Ash: A muffle furnace operating at temperatures up to 950°C was used for the analysis for inorganic ash. Weighted samples of the feeds and the permeates of SRC (each weighing about 10 g) were dried overnight at about 100°C; following this the temperature of the furnace was increased by 50°C increments every half hour until 900°C and then kept there for 2-3 hours, after which the reddish brown powder which resulted was cooled in a dessicator and

Figure 1.

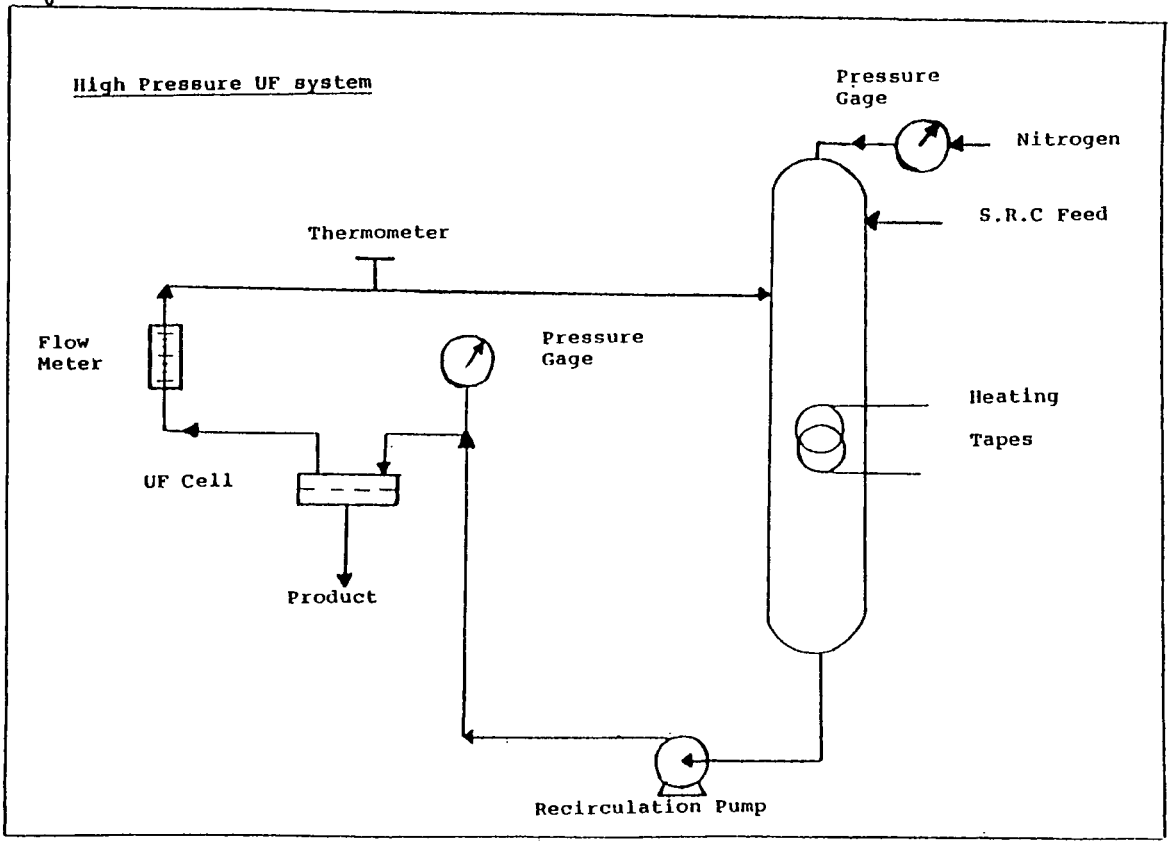
High Pressure UF system
Pressure Gage
Nitrogen
S.R.C Feed
Thermometer
Flow Meter
Pressure Gage
Heating Tapes
UF Cell
Product
Recirculation Pump

weighted. To insure total decarbonation, the process at 900°C was continued until no further weight loss was observed.

RESULTS AND DISCUSSION

As shown in Figure 2, an increase in temperature from 85°C to 100°C increased the flux by a factor of about 2.5. It is known that high temperatures reduce the viscosity of the fluid. With SRC, on going from 85°C to 100°C the viscosity was lowered from about 42.0 Cp to about 20.8 Cp, or by a factor of 2.0. As for ash rejection (99.8% at 85°C; 99.9% at 100°C) this improves with higher temperatures and with higher axial velocity of the fluid due to its lowered viscosity. From Figure 3, one can see that high pressures tend to increase the resistance to flow because under high pressures particles are forced against the membrane and possibly into the pores. These effects create a polarized boundary layer which may prevent higher fluxes. We observed that at the beginning of the run, at high pressures (15.51×10^5 Pascals or 225 psig) the rejection is low compared to the one measured at the end of the run[5]. High pressures force the smaller particles into the larger pores, which are responsible for the low rejection. After the gel slime has formed, the rejection is usually 100% but the fluxes are much lower.

UF of SRC was run, at the same temperature and pressure but at different axial velocities, as shown on Figure 4. At high axial velocities the fluxes leveled off smoothly to reach a higher steady state level; at low velocities, fluxes decreased sharply as shown by the curve for the velocity of v = 305 cm/sec. Higher velocities apparently prevented the formation of the gel slime on the surface of the membrane, and reduced the thickness of the boundary layer by promoting turbulence, in the flow of the fluid in the cell. As for ash, rejection, (99.90%[1], 99.89[2]; 99.80[3]) it increases with increasing velocities for the same reasons given above.

The permeabilities of diluted SRC with 24-CB Creosote oil is shown in Figure 5 (Curve #2). It shows that a 10% dilution almost doubled the fluxes. This again is explained by the fact that Creosote oil has a low viscosity (about 2.0 Cp at 94°C) compared with the SRC viscosity of 35.8 Cp at 94°C, this reduces the viscosity of the SRC solution and makes the fluid much easier to flow. Ash rejection also increased with dilution, 100% compared with that of pure SRC (99.9%). One observes that dilution has the same effect as temperature; both serve to reduce the SRC viscosity.

With toluene, as shown in Figure 5 (Curves #3 and 4), one can see a strong effect of dilution. A 10% dilution increased the flux by a factor of 3.5; a 25% dilution increased the flux by a factor of 6.5. Ash rejection also increased with dilution, 99.99 - 100% compared with 99.9% for undiluted SRC.

From the results shown in Figure 5, one observes that toluene served much better than 24-CB Creosote oil, primarily because it has a lower viscosity than creosote oil.

---

1 at v = 366 cm/sec.
2 at v = 335 cm/sec.
3 at v = 305 cm/sec.

ACKNOWLEDGEMENTS

The author wishes to acknowledge the generous support of Sonatrach, Co. in Houston, Texas and Professor Harry P. Gregor for his supervision and advice.

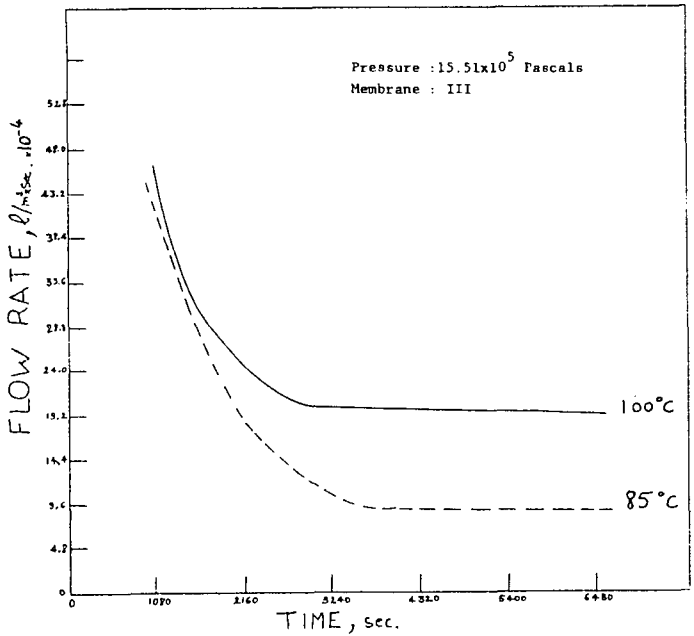

Figure 2. Pure SRC Fluxes as a Function of Temperature.

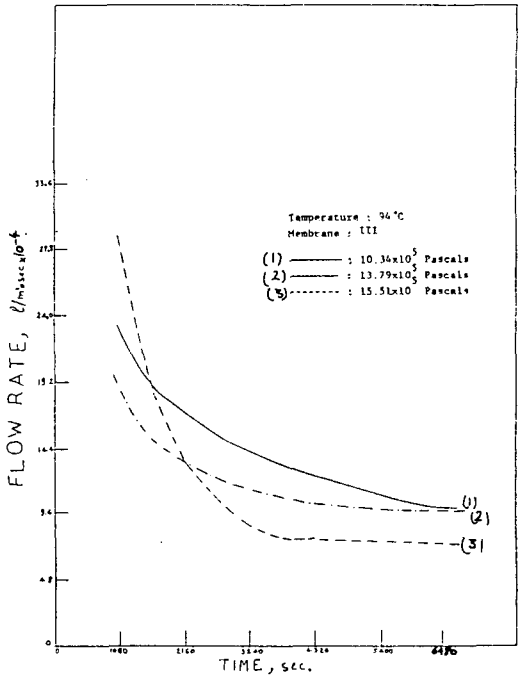

Figure 3. Pure SRC Fluxes as a Function of Pressure.

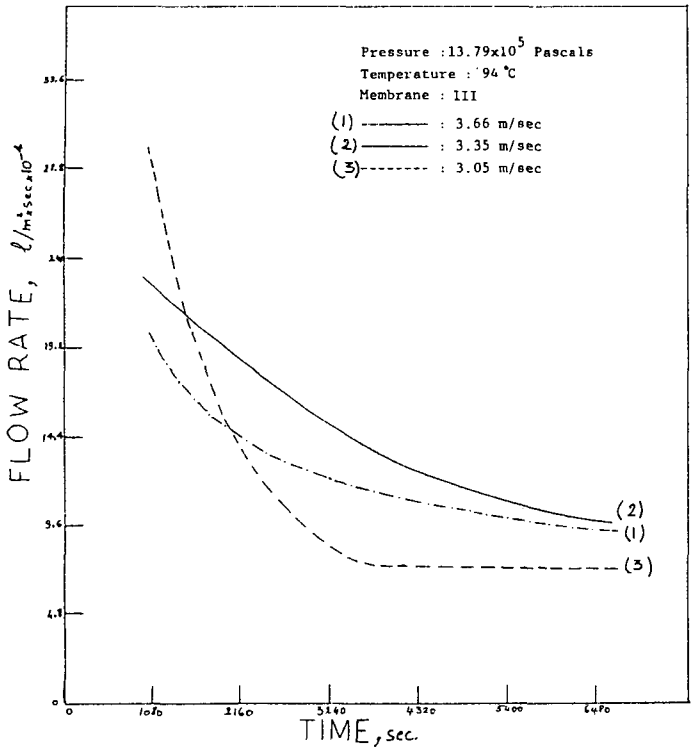

Figure 4. Pure SRC Fluxes as a Function of Axial Velocity.

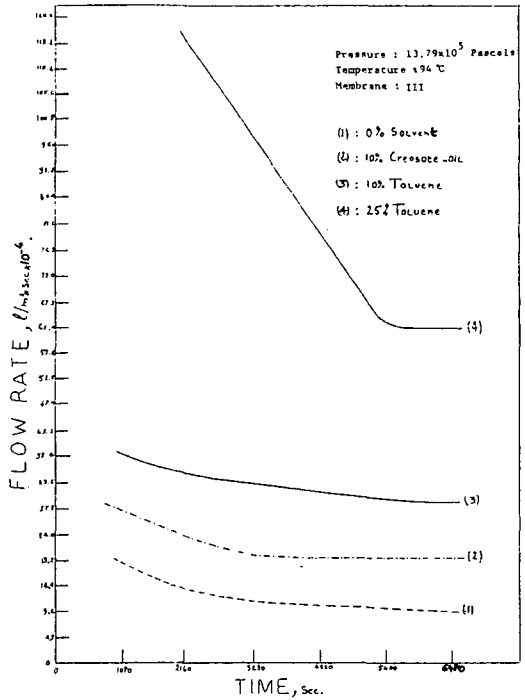

Figure 5. Comparison of Fluxes of SRC Diluted with Creosote and Toluene.

REFERENCES

1. Recent Advances in Separation Techniques, AIChE Symposium, Series No. 120, Vol. 68, 1974, p. 24.
2. Audibert, F., Defives, D., Avrillon, R. and Mimscloux, C. "Reclaiming of Spent Lubricating Oils by UF", presented at the Third International Conference on Waste Oil Recovery and Reuse", (Association of Petroleum Re-refiners), Oct. 16-18, 1978.
3. Chukumerije, O., "UF of Non-Aqueous Media", Ph.D. Thesis, Columbia University, N.Y., 1979.
4. Weintraub, M., Weiss, M.J., Akhtar, S. and Yavorsky, P.W. ACS Preprints, Fuel Chem. Div., 21(5) 1976.
5. Bensalem, A., "UF De-ashing Process for SRC", M.S. Thesis, Columbia University, N.Y. 1979.

SEPARATION OF COAL MACERALS*

Gary R. Dyrkacz, C. A. A. Bloomquist, Louis H. Fuchs, and E. Philip Horwitz

Chemistry Division, Argonne National Laboratory, 9700 South Cass Avenue, Argonne, Illinois 60439

INTRODUCTION

As coal science progresses the need for pure coal macerals becomes increasingly obvious. The chemical and physical properties of the various macerals are known to differ substantially(1), but a large portion of the work is based on European coals. Furthermore, separated macerals used for previous studies were not always of high purity. Little attention has been given to the actual procedures for separating the macerals. We are currently involved in a program to define the parameters necessary for efficient separation of macerals using differences in density and to build up stocks of macerals for additional analyses. Our technique is based on density gradient centrifugation (DGC) rather than the often used sink-float procedures. As we will show, DGC has much more latitude for separation control and has the advantage of superior resolution in less time than previous methods, *e.g.*, sink-float.

EXPERIMENTAL

Coal Samples

All coal samples used in this study were obtained from the Pennsylvania State University data bank.

Microscopic Analysis

Petrographic analysis of the fine ground coal was performed in both incident blue light and white light at 1200x. The exinites autofluoresce in blue light making them more visible. Standard procedures were used for mounting, polishing, and analyzing the coal materials.

Grinding

The grinding of the coal was performed in two steps. Initial grinding of the coal to below 200 μm particle size was performed using a planetary ball mill. The resultant ground coal from the ball mill was then used as a feed for fine grinding in a Sturtevant Micronizer fluid energy mill. This type of jet mill has no moving parts; the coal is fed into a high velocity gas stream of nitrogen moving in a circular pattern where it self-grinds. In addition, the mill is to some degree self-classifying; therefore, a narrow particle size distribution is produced.

---

*This work was performed under the auspices of the Office of Basic Energy Sciences, Division of Chemical Sciences, U. S. Department of Energy.

In the case of PSOC-297 coal, one pass through the fluid energy mill produced particles which were <6 μm in size. This size range gave particles which were largely homogeneous with respect to a given maceral. In the case of PSOC-124 coal, two passes through the mill, followed by demineralization, six freeze-thaw cycles between liquid nitrogen and 80°C, and then a final pass through the mill was required to reduce the particle size to <6 μm.

Demineralization

After fine grinding, the coal was demineralized chemically using standard procedures(2). Both coals still had ∿2.6% mineral matter present after chemical treatment.

Density Gradient Centrifugation (DGC)

DGC techniques were used for all separations. Linear density gradients were used throughout this work, and were pre-formed using a commercial density gradient former (ISCO, Model 380 or 382). Aqueous CsCl was used to form all gradients. The coal was dispersed with either Brij® 35 (polyoxyethylene-23-lauryl ether) or dodecyltrimethylammonium salt (8 g/L) added to all solutions. Two separation systems were used: analytical DGC and preparative DGC. In the analytical mode, 5-50 mg of coal was dispersed into a low density solution by mild ultrasonic treatment, layered on a 40-45 ml gradient (∿1.0 to 1.5 g/cc), and then centrifuged at 12,000 rpm (∿16,000 x g) in a Beckman J-21C centrifuge for 30 minutes. After this period the centrifuge was stopped and the contents of each of the tubes were forced out with a dense chase solution of fluorinert® FC-43. The contents leaving the centrifuge were then passed through an absorbance monitor and into a fraction collector. The density of each fraction was found by measuring its refractive index.

Large scale amounts of coal (2-3 g) were separated using a commercial zonal centrifuge rotor (Beckman, model JCF-Z) which holds a 1.6 L density gradient. After loading and centrifuging, the contents were again pumped out with the high density chase solution and collected in 30 ml fractions. Each fraction was filtered through a 1 μm pore diameter nuclepore® membrane filter. The resultant residue was washed with both room temperature and hot water to remove CsCl and surfactant, dried in a vacuum at 80°C and stored under nitrogen. Selected fractions were then microscopically analysed.

Atomic ratios for some fractions were measured using a microwave plasma detector (Applied Chromatography Systems, model MPD850) equipped with a solid probe.

RESULTS AND DISCUSSION

Two bituminous coals were used in this study, PSOC-297 and -124. PSOC-297 is a cannel-like coal, and PSOC-124 is a true cannel coal. The composition of these two coals is shown in Table I. These coals were chosen for their large inertinite and exinite concentrations; PSOC-297 was also interesting because of its high mineral matter content. We expect that any separation difficulties with mineral matter would be most evident in this coal.

Scheme I shows the sequence of procedures used to obtain separated macerals. The first and one of the most important aspects in maceral separation is the grinding stage. The initial grinding step (using a planetary ball mill) is necessary to reduce the particle size below 200 μm, which is required for the feed to the fluid energy mill. The average particle size after grinding in the fluid energy mill is 2.6 μm, with 95% of the material below 6 μm. After grinding, the coal is demineralized. We have found that demineralization is a necessary step for the two coals investigated in order to achieve a good maceral separation.

The density gradient separations were carried out using a maximum and minimum density of 1.5 and 1.0 g/cc, which encompasses the range of maceral densities. All gradients were linear (by volume). CsCl was used to form the gradients because of its relative inertness to coal, convenience in handling, and maximum density of 1.9 g/cc. However, the hydrophobic nature of coal presented a problem in dispersing the fine particles in a hydrophilic medium. In fact, very little maceral separation can be achieved without the use of surfactants to improve the dispersibility of the coal in CsCl solution. We tested three classes of surfactants: anionic, cationic, and nonionic, for their ability to disperse the two coals in aqueous density gradients. Quaternary ammonium salts, particularly dodecyltrimethylammonium bromide, and the nonionic Brij® 35 (polyoxyethylene-23-lauryl ether) were found to improve the wetting properties of the aqueous medium. However, Brij® 35 was used for all runs because it has good solubility in aqueous CsCl, is readily available, and was found to be better than the quaternary ammonium salt in regard to the stability of the dispersion of PSOC-124.

Figure 1 presents the combined results of analytical DGC runs for the two coals. All densities are solution densities corrected to 25°C. The absorbance scale can be taken as a measure of the relative amount of coal at a particular density, but the curves have not been normalized; thus direct comparison of yields per fraction between the two coals is not possible. As would be expected for such dissimilar coals, the curves are quite distinct and reflect at least crudely the proportion of the various maceral groups, with the exception of inertinite. From Dormans *et al.* (3), we expect the densities for the various macerals to be: exinities ∿1.2, vitrinites ∿1.3, and inertinites ∿1.4 g/cc. It is interesting to note that the fractograms do not show peaks where inertinite is expected to appear.

Figures 2 and 3 show the results of preparative DGC runs on PSOC-297 and PSOC-124. The top curves in each set compare very well with the analytical runs. The lower graphs show the corresponding volume percent of the three maceral groups for selected fractions. It can be seen that for both coals many fractions are better than 90% pure with respect to a maceral constituent. In the case of alginite many particles apparently split out of the coal as single entities during grinding and could be identified from other exinites by their morphology. The actual yield of alginite is probably higher but smaller particles were counted as alginite only if they exhibited the morphological characteristics of alginite.

The inertinites present an interesting case because they seemingly exhibit high concentrations in more than one density region.

This can be seen more clearly in Figures 4 and 5, where we have plotted the data in a different manner. The ordinate is the weight of coal in each equal volume fraction collected. The percentage of each maceral in a density fraction was multiplied by the weight of that fraction. The weight of vitrinite was divided by 10 in Figure 4 for convenience of plotting. We have neglected the difference between vol. % and wt. % because of the difficulty of accurately calculating wt. % from a volume distribution. Neglecting the difference in vol. and wt. % only affects the results where there is an overlap of two or more macerals, but not significantly enough to change the overall results. Note that there seems to be multiple inertinite peaks with both coals. The reason for this behavior was revealed by microscopic examinations, which showed that the low density inertinite consisted of micrinite particles bound to other macerals.

In the case of PSOC-297 the micrinite is bound to exinites and vitrinites, whereas with PSOC-124 the micrinite is bound only to exinite. In both unground coals the micrinite is highly dispersed throughout the coal rather than localized in definite regions, and thus does not seem to selectively split out of the coal on grinding. For PSOC-297 this does not constitute a major problem, but for PSOC-124 a large fraction of the inertinite is obtained as composite particles. However, these composite materials prevent us from seeing the true distribution of a particular maceral, and therefore we modified our counting procedure. If the crosslines (of the microscope) fell on a particle which contained more than 10% of a second maceral, then we described that maceral under the crosslines as being bound. The error in such a counting procedure is high (∿10%), especially where the macerals are generally of a fine nature, but for our purposes the error was not a severe problem. This procedure allows us to effectively eliminate, albeit in an artificial manner, mixed maceral particles and only observe the distributions of pure constituents. Figures 6 and 7 show this data. It is an easy task to read off from Figures 6 and 7 the maceral distribution and density peaks. For PSOC-297 coal: alginite, 1.06 g/cc; sporinite, 1.19 g/cc; vitrinite, 1.29 g/cc; and inertinite, 1.35 g/cc. Alginite constitutes only 2% of PSOC-297 and yet we achieved an excellent separation, which shows the effectiveness of the density gradient method. For the PSOC-124 separation, the alginite was present as a shoulder (1.0 to 1.1 g/cc) on the concentration profile of the exinites (see Figure 3), but was not counted because the fluorescence was not as distinctive as in the case of PSOC-297. The exinite distribution in Figure 7 shows a rather asymmetric shape. We believe this asymmetry represents two different types of exinite material, possibly different spore types; one showing higher fluorescence than the other. Vitrinite has a peak density of 1.25 g/cc and inertinite, 1.30 g/cc.

Figure 8 is a plot of the H/C and S/C for selected PSOC-297 fractions. An almost linear dependence of H/C on density is exhibited in the early fractions (<1.35 g/cc); however, the inertinite fractions show little change. The H/C behavior in the exinite-vitrinite region may be explained according to Van Krevelen's correlation between density and atomic ratios (1). However, we cannot explain the H/C independent region (>1.35 g/cc) at this time.

CONCLUSIONS

We feel the density gradient technique offers significant advantages over previous methods of maceral separation. It provides a rapid method of measuring the overall density ranges of the various macerals and of separating macerals having any density range desired. Of course, the smaller the fraction cuts, the less coal per fraction. Our current fractions range between 0.007-0.010 g/cc. To obtain the same range using sink-float techniques would require over 40 separate stages. As the results show, we have had good success with PSOC-297 and -124 coal samples using the DGC technique, although micrinite presents some problems. In the case of PSOC-297, the micrinite contribution does not drastically affect the material in which it is mixed, *e.g.*, vitrinite is still over 90% pure. In the case of PSOC-124 much more exinite material is contaminated by micrinite inclusion, undoubtedly because of the very high micrinite concentration initially present.

Two important points can be made from this study. First, the broad distribution of densities for exinite and inertinite and the corresponding large drop in H/C ratio for the exinites suggests large changes in chemical structure must be occurring. Thus, caution must be used in studying the properties of exinites and inertinites to insure that structural information is based on narrow range density fractions. In fact, this is probably why in the past the properties, both chemical and physical, have much broader limits for exinites and inertinites(1). Second, the density range for vitrinites is relatively narrow in both coals, suggesting that the properties of vitrinite should be generally less erratic and therefore considerably more predictable.

ACKNOWLEDGMENTS

We gratefully acknowledge the help of Randall E. Winans and Lynn M. Barta in obtaining the data on the atomic ratios. The authors would also like to thank Louis Petrovic and Norman Shapiro of Resource Engineering, Inc., Lexington, Massachusetts, for many helpful discussions during the early stages of this project in regard to the petrographic analysis.

REFERENCES

1. Van Krevelen, D. W., "Coal", Elsevier Publishing Company, 1961.
2. Bishop, M., and Ward, D. L., Fuel 37, 191 (1958).
3. Dormans, H. N. M., Huntjeans, F. J., and Van Krevelen, D. W., Fuel 36, 321 (1957).
4. Lowrison, G. C., "Crushing and Grinding", Butterworths, London, 1974, p. 80.
5. Kröger, C., Pohl, A., and Küthe, F., Gluckauf. 93, 123 (1957).

TABLE I. Composition Data for Coals

	Volume %	
	PSOC-297	PSOC-124
Sporinite	16.4	51.7
Resinite	0.4	1.5
Cutinite	0.4	1.7
Alginite	2.0	1.6
Vitrinite	63.0	14.6
Micrinite[a]	17.0	27.4
Semi-fusinite	0.8	1.0
Fusinite	0.4	0.4
M.M (wt. %)	22.8	10.7
% C (dmmf)	82.17	84.99
% H (dmmf)	5.62	7.20

[a]Includes: micrinite, inertodeterinite, and macrinite.

SCHEME I

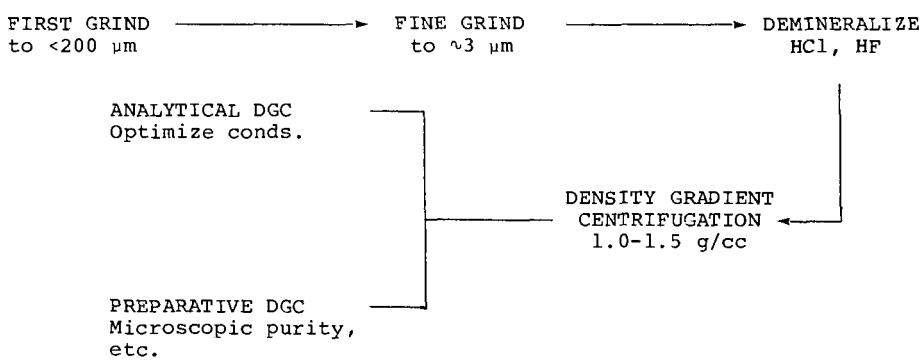

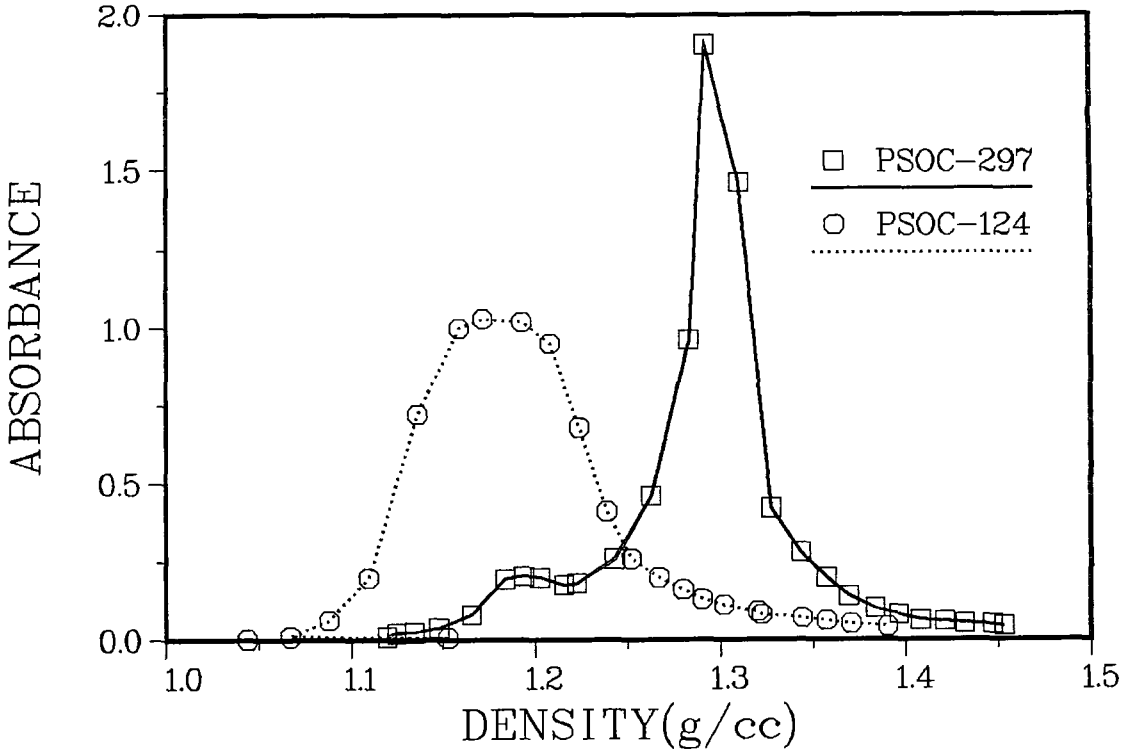

Figure 1. Analytical Density Gradient Separations for Two Coals.

Figure 2. Preparative Density Gradient Separation and Maceral Analysis of PSOC-297.

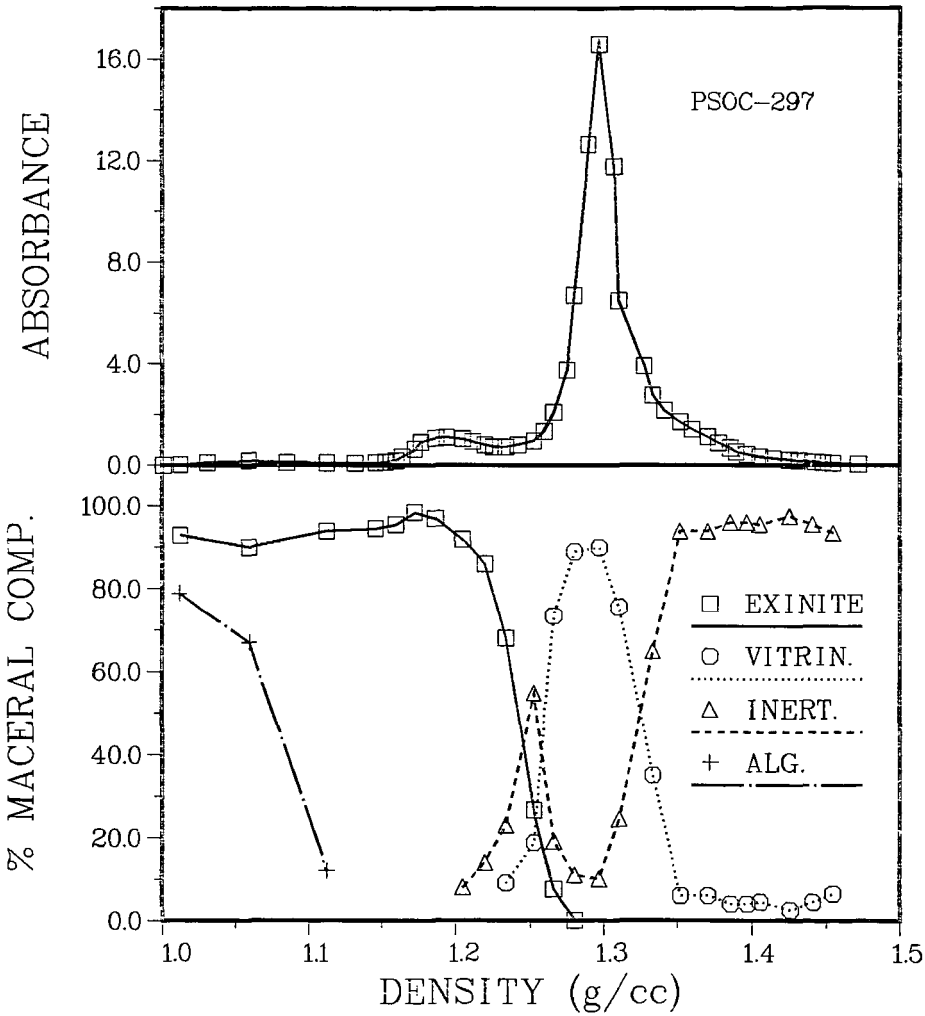

Figure 3. Preparative Density Gradient Separation and Maceral Analysis of PSOC-124.

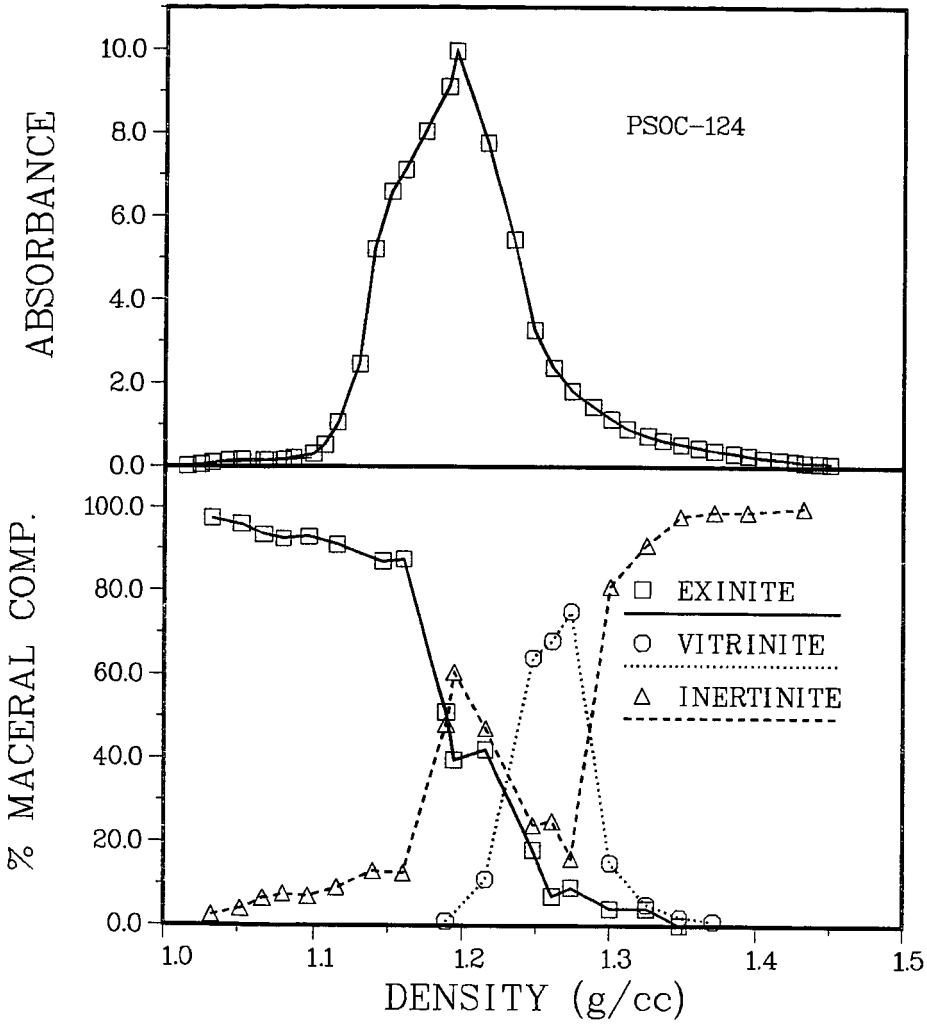

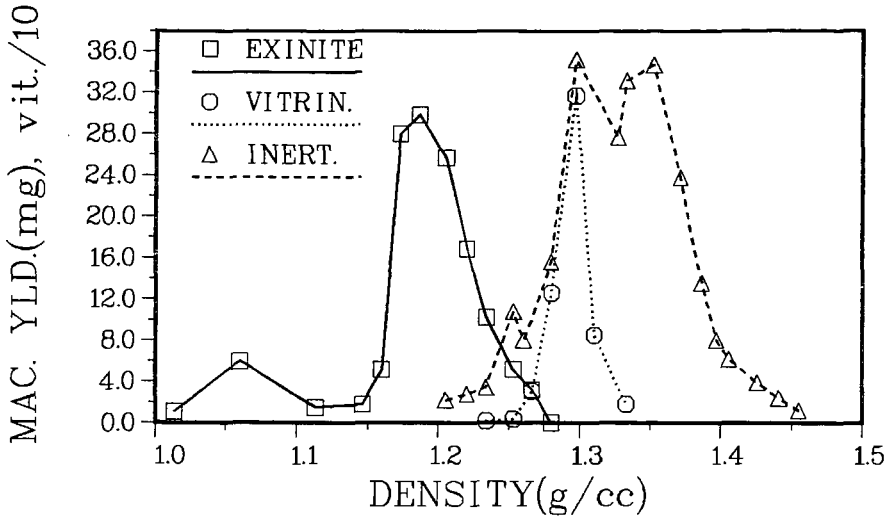

Figure 4. Amount of Each Maceral Type in Selected Density Fractions of PSOC-297.

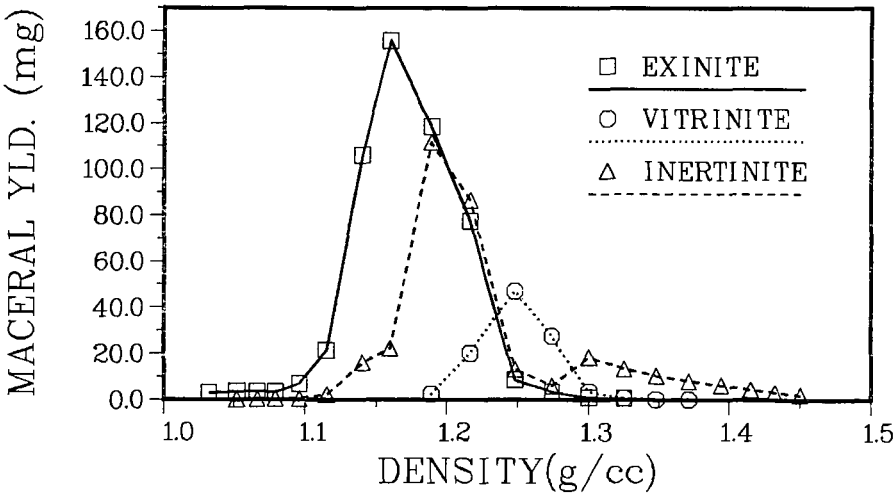

Figure 5. Amount of Each Maceral Type in Selected Density Fractions of PSOC-124.

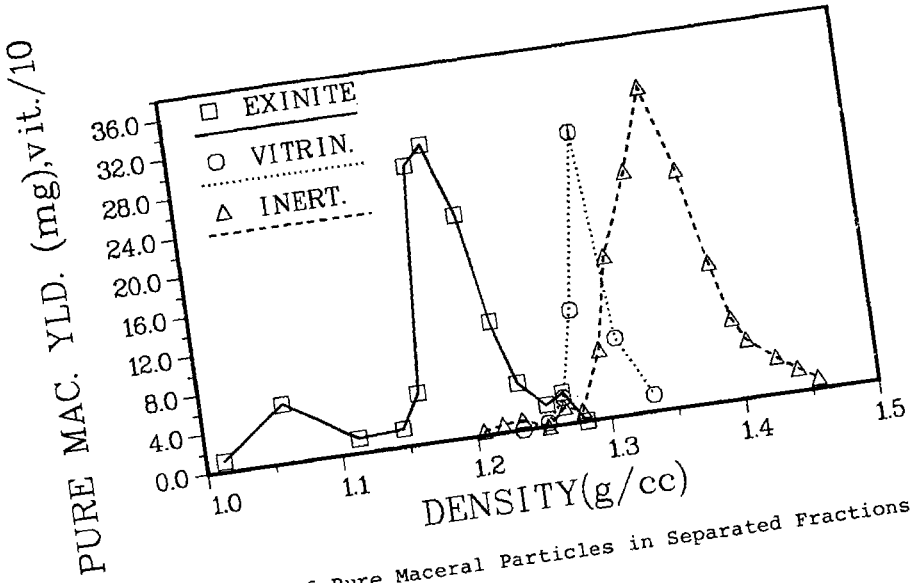

Figure 6. Yield of Pure Maceral Particles in Separated Fractions of PSOC-297.

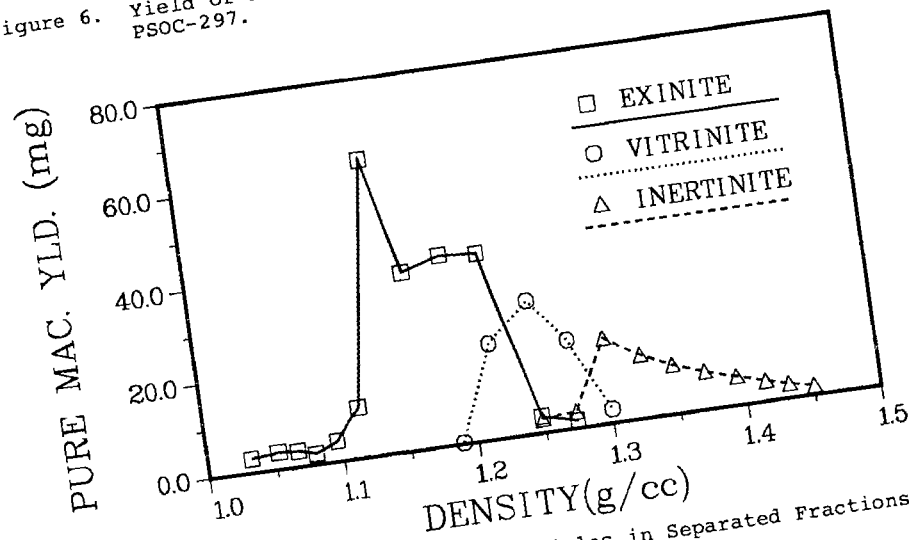

Figure 7. Yield of Pure Maceral Particles in Separated Fractions of PSOC-124.

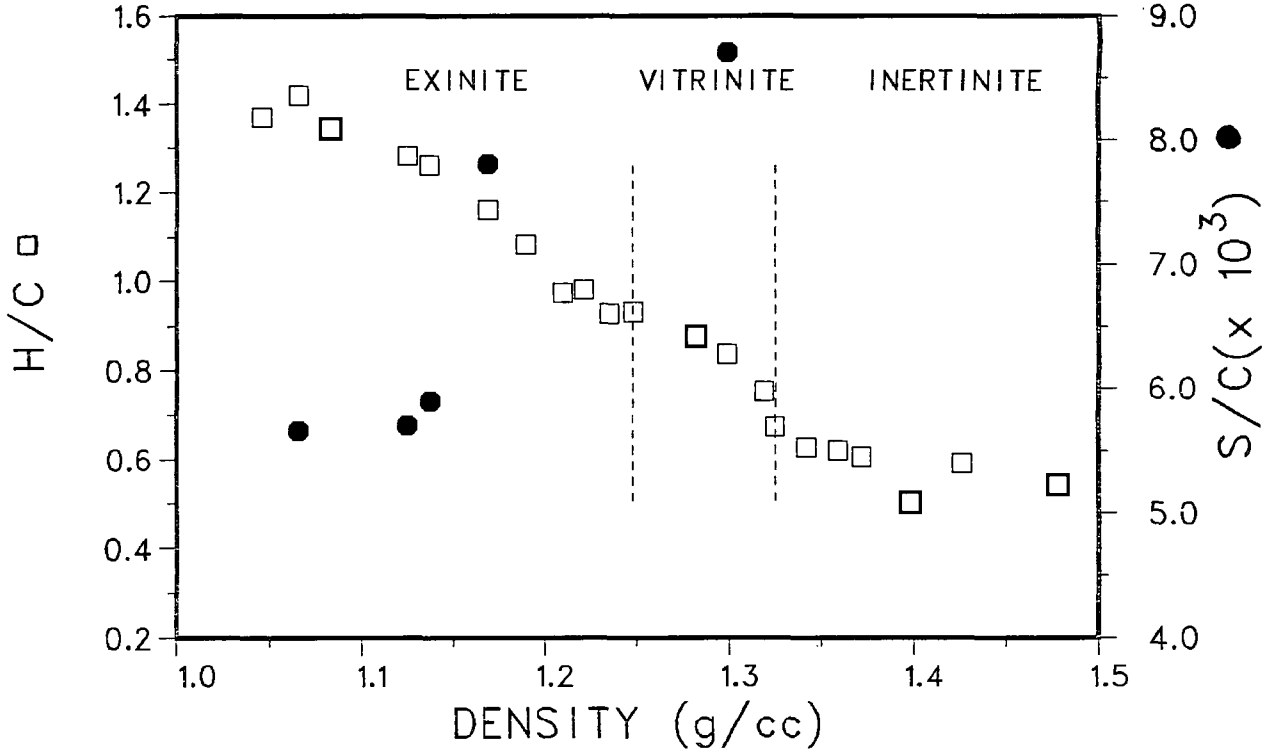

Figure 8. H/C and S/C Atomic Ratios for Separated PSOC-297 Coal.

Rapid Estimation Of % Ash In Coal From % Silicon Obtained Via FNAA, XRF, And Slurry-Injection Atomic Absorption Spectrometry Techniques

by

Donald G. Hicks, James E. O'Reilly, and David W. Koppenaal

Departments of Chemistry, Georgia State University, Atlanta, GA, 30303 and University of Kentucky, Lexington, KY, 40506; and Institute for Mining and Minerals Research, Kentucky Center for Energy Research, Ironworks Pike, Lexington, Ky, 40583.

INTRODUCTION

The ash content of coals is an important classical parameter for their eventual use as fuels, as feedstocks in liquefaction and gasification processes, and in metallurgical processes. For example, it is a fairly common procedure to blend various lots of coal to obtain a more constant ash content when it is used in coal-fired boilers and power plants. Among other parameters, the relative rate of combustion as well as the maximum combustion temperature of aqueous coal suspensions were found by Isaev and Delyagin(1) to be dependent on the ash content of coals used in the study. Other workers have noted that the content of ash and certain minerals in coal can affect the yields from gasifiers and liquefiers.

The conventional method for determining the percent high-temperature ash of coal is simply to burn slowly a representative sample at elevated temperature in a muffle furnace. The method is simple, accurate, and reproducible; but requires a considerable amount of time in the laboratory.

A number of approaches, and refinements thereof, have been reported to be useful for estimating the mineral matter and ash contents of coal from the levels of the major inorganic elements present(2-7). For a variety of reasons, the use of elemental content for the estimation of ash or mineral matter in coals is considerably less exact than, for example, a somewhat similar approach for estimating BTU values(8-10).

Recently, Loska and Gorski(11) and Block and Dams(12) have shown that a reasonable correlation exists between the ash content of coal and the silicon level determined by fast instrumental neutron activation analysis (FNAA) for Silesian and Belgian coals, respectively. They reported that best results came from a logarithmic correlation, % ash = $a(\% \text{ Si})^b$ where a and b are constants. Their mean <u>absolute</u> error for estimation of ash content was about 1.8 % ash, or about 8 % <u>relative</u> error. We have recently developed a very rapid atomic absorption method for analyzing coals for many trace and minor-level elements by <u>directly</u> aspirating aqueous slurries of finely powdered coal into a conventional AA spectrometer(13,14). Because AA spectrometers are so common, it was our desire to see if the slurry-injection atomic absorption spectrometry (SIAAS) method would provide a suitable and fast method for estimating the ash content of some typical U.S. bituminous coals simply from measurement of their silicon concentrations. Comparisons between simple linear plots and log-log plots of data were also of particular interest to us.

This paper reports the results and statistical analyses we have obtained for the correlation of the ash content of a number of eastern Kentucky, western Kentucky(Illinois basin), and West Virginia coals with the silicon content as determined by slurry-injection atomic absorption(SIAAS), X-ray fluorescence(XRF), and fast neutron activation analysis(FNAA). In addition, results are compared with the % silicon and % ash data published by the Illinois State Geological Survey(15, 16) for a wider variety of coals.

EXPERIMENTAL

Coal samples were crushed, pulverized in a swing-mill, and sieved as previously described(13). The high temperature ash values for coals used in this work are from standard 750°C ASTM ashes(17).

The percent silicon in about 20 coals was determined by Drs R. C. Young and W. D. Ehmann of the University of Kentucky Department of Chemistry using FNAA procedures described elsewhere(18). These silicon contents from FNAA were considered to be benchmark values, and were used as standards to calibrate the signals from the XRF and AA spectrometers for determination of Si in these and other coals. The XRF and AA signals were then converted to values of % Si by XRF and % Si by slurry-AA for the various coals. Subsequently, correlations of the % ash with the % Si obtained by the several instrumental techniques were compared.

X-ray fluorescence measurements were performed using a Finnigan 900B energy-dispersive spectrometer fitted with a rhodium target tube, and operated at 14 kV and 0.30 mA. Samples were run as powders and counted for 1000 seconds. Total and net fluorescence counts were acquired for the Si K photopeak (1.74 keV). For SIAAS determinations, coal samples were further ground and sieved by procedures already reported(13). The final slurries aspirated into the burner were 1.5 % wt/vol solids in 0.5 % Triton X-100 surfactant. A 5-cm nitrous oxide/acetylene flame was used, and the analytical wavelength was 251.6 nm. The atomic absorption spectrometer employed was a Varian AA-6 whose standard tantalum nebulizer intake capillary had an inside diameter of 0.400 mm.

RESULTS AND DISCUSSION

To summarize, our results show that a reasonably useful linear correlation can be made between the % high-temperature ash and the % Si for typical Appalachian and Illinois Basin bituminous coals. Figure 1 illustrates a plot for such a correlation involving % Si from SIAAS data for 24 arbitrarily chosen Kentucky and West Virginia coals which range from about 4% to 28% ash. The linear least squares line fit to the data (see Table I) has a correlation coefficient of 0.890; and the standard error of estimate(SEE), the root-mean-square deviation of the y-values for the straight line fit, is 2.4 % ash. Exemplified by Figure 2, similar correlations of % Si by XRF or FNAA vs. % Ash for the same coals result in a roughly similar appearance, but the fits are significantly better as seen by the SEE values of 1.73 and 1.71 in Table I.

The visual appearance of the linear plots such as shown in Figures 1 and 2 are somewhat less satisfying than those of Loska and Gorski(11) and of Block and Dams(12). In the latter cases, however, the plots are log-log and cover a considerably wider range of % ash (about 3% to 40%)! Thus, the deviations from straight line fits appear to be less. But statistically, the fits are more or less equivalent.

Table I presents a comparison of the linear-least-squares fit for Kentucky and West Virginia coals when the % Si is determined by a number of different instrumental methods. The correlations are all roughly comparable---similar slopes, intercepts, standard errors, and correlation coefficients---except for the fact that the fit is significantly worse with the simple SIAAS method for Si determination. This is understandable in view of the facts that SIAAS is not a highly accurate method, and, is somewhat affected by the varying matrix and different particle-size distributions from one coal to another(13). Still, the median relative error in determining % Si by SIAAS is only 10 % for these coals. The larger method errors inherent in SIAAS itself, relative to XRF or FNAA,

apparently add to some degree to the natural uncertainties in the correlation, and decrease the overall fit. However, initial studies with a recently developed acid-slurry-AA method(ASIAAS) for determining silicon(19) have produced % ash-% Si correlations comparable to those obtained from XRF and FNAA data. In this ASIAAS procedure, powdered coal is slurried with a relatively dilute acid mixture (HCl-HF-Triton X-100) for a few minutes in an ultrasonic bath. Further results will be reported at a later date. Similar to previous observations(11,12), we found that relative errors of the worst individual cases seemed to be somewhat larger for coals with lower % ash.

Correlations within a Rank of Type of Coal: Included in Table I are some results for similar correlations using data published by the Illinois Geological Survey(15,16) for a greater number and wider range of coals. These were studied in order to see if significantly better correlations could be obtained within one type or rank of coal than seemed to be the case with the arbitrarily selected set of Kentucky and West Virginia coal samples we used. It was distressing at first to find the very poor correlation for coals from a single source. For example, 15 Harrisburg(No. 5) coals exhibited a correlation coefficient of only 0.417. Apparently, this is primarily a result of the restricted range of % ash values for these coals. However, it is interesting to note that the standard error of estimate (a more meaningful parameter) is actually better for these than any other set of coals. The selection of coals with more widely spaced % Si values covering a wider range of ash values results in better correlations and better appearing plots(11). This notion was tested by arbitrarily selecting one coal within each 0.1 % Si interval from the 172 coals analyzed by the ISGS(15). The correlation (labelled "arbitrary" in Table I) is about as good as any of the others.

Linear versus Logarithmic Correlations: Table II presents the results of logarithmic correlations on the same sets of coals as in Table I, and compares these with previous findings(11,12). On the whole, the logarithmic correlation coefficients for American coals were slightly worse than those from the linear correlations, and there seems to be no particular reason to prefer the former over a simple linear fit. The general conclusion from the results presented in this work is that, regardless of the source or rank of the coal or the rapid method used to measure the silicon content, the % ash of typical American bituminous coals can be estimated by simple linear correlations to within a standard absolute error of about 1.7 % ash---approximately 10 % relative error. This compares with a value of about 1.8 % ash absolute error for Silesian coals(11), and about 8.0 % relative error for Belgian coals(12).

Acknowledgements

The financial support for this work by the Kentucky Institute for Mining and Minerals Research and by Georgia State University is gratefully acknowledged. Special thanks are due Drs. William D. Ehmann and Robert C. Young for neutron activation analyses, and to Dr. Floyd J. Holler for assistance with statistical computer programs.

****

REFERENCES

1. Isaev, V.V.,and Delyagin, G. N., Khim. Tverd. Topl., 1978, 12, 138.
2. Pollack, S.S., Fuel, 1979, 58, 76.
3. Cooper, J.A., Wheeler, B.D., Wolfe, G. J., Bartell, D.M., and Schlafke, D. B., in Advances in X-Ray Analysis, H. F. McMurdie, C.S. Barrett, J.B. Newkirk, and C.O. Rudd, Eds., Vol. 20, Plenum Press, N.Y., 1977, p. 431.
4. Volborth, A., Miller, G. E., Garner, C.K., and Jerabek, P.A., Fuel, 1977, 56, 204.
5. King, J. G., Maries, M.B., and Crossley, H. E., J. Chem. Soc. Chem. Ind. London, 1936, 57, 277.
6. Millot, J.O., Fuel, 1958, 37, 71.
7. Pringle, W.J.S., and Bradburn, E., Fuel, 1958, 37, 166.
8. Ringen, S., Lanum, J., and Miknis, F.P., Fuel, 1979, 58, 69.
9. Lloyd, W.G., and Davenport, D.A., J. Chem. Educ., 1980, 57, 56.
10. Boie, W., Wissenschaftliche Zeitschrift der Technischen Hochschule Dresden, 1952/53, 2, 687.
11. Loska, L., and Gorski, L., Radiochem. Radioanal. Lett., 1972, 10, 315.
12. Block, C., and Dams, R., Anal. Chim. Acta, 1974, 71, 53.
13. O'Reilly, J.E., and Hicks, D.G., Anal. Chem., 1979, 51, 1905.
14. O'Reilly, J.E., and Hale, M.A., Anal. Lett., 1977, 10, 1095.
15. Gluskoter, H.J., Ruch, R.R., Miller, W.G., Cahill, R.A., Dreher, G.B., and Kuhn, J.K., Trace Elements in Coal: Occurrence and Distribution, Illinois Geological Survey Circular 499, 1977.
16. Ruch, R.R., Gluskoter, H.J., and Shimp, N.F., Occurrence and Distribution of Potentially Volatile Trace Elements in Coal: A Final Report, Illinois Geological Survey Environmental Geology Notes, No. 72, 1974.
17. Annual Book of ASTM Standards, Part 19, pp. 438-9, ASTM Standard D1374-73, American Society for Testing and Materials, Philadelphia, 1973.
18. Morgan, J.W., and Ehmann, W.D., Anal. Chim. Acta, 1970, 49, 287.
19. Hicks, D. G., and O'Reilly, J. E., unpublished results.

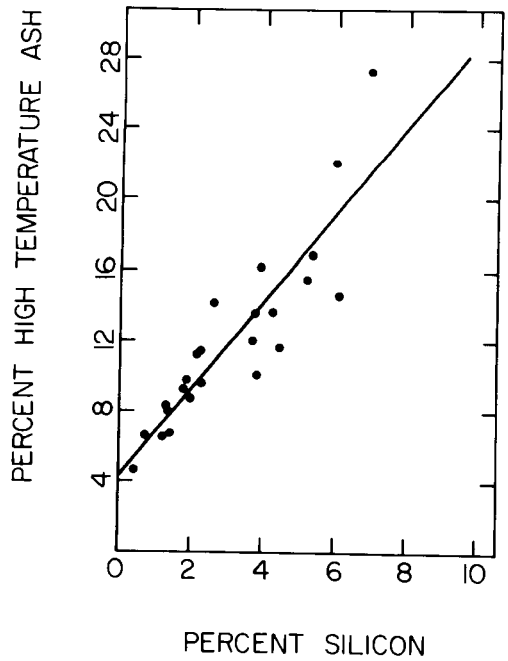

Figure 1: Plot of % high-temperature ash vs. % silicon for some Kentucky and West Virginia Coals. Si determinations by simple slurry-injection atomic absorption spectrometry (SIAAS).

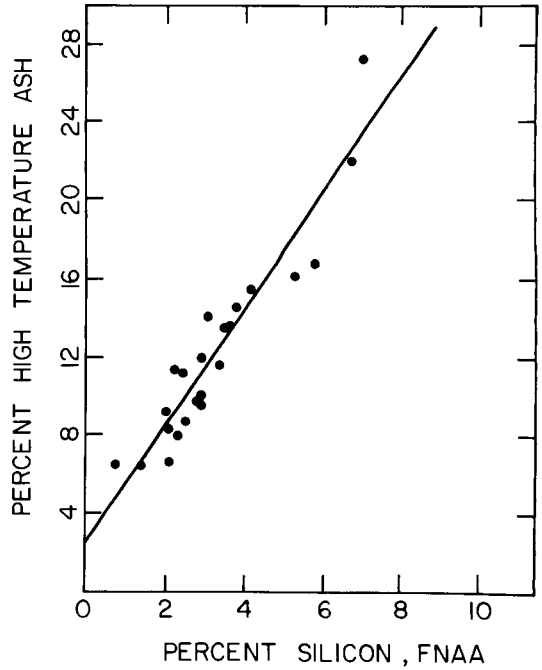

Figure 2: Plot of % high-temperature ash vs. % silicon for some Kentucky and West Virginia Coals. Si determinations by instrumental fast neutron activation analysis (FNAA).

TABLE I: Linear Least Squares Correlations Of Percent Ash vs. Percent Silicon In Some Coals

Type of Coal	Number of Samples	Range of % ash	Method of Si Determination[a]	% ash = p(% Si) + q		SEE[b] (Standard Error of Estimate) as % Ash	Correlation Coefficient	Reference
				slope (p)	intercept (q)			
KY & WV	24	4.6-27.3	SIAAS	2.48	4.33	2.41	0.890	This work
KY & WV	23	6.5-27.3	XRF	2.94	2.88	1.73	0.941	"
KY & WV	23	6.5-27.3	FNAA	3.00	2.69	1.71	0.943	"
ILL(No.5) Harrisburg	15	10.3-14.8	XRF	1.77	7.79	1.18	0.417	15
Western	29	4.1-20.4	XRF	2.76	4.88	1.96	0.856	15
ILL Basin	80	3.3-16.0	XRF	2.31	5.70	1.65	0.659	16
Arbitrary[c]	40	4.1-25.9	XRF	3.02	4.25	1.87	0.924	15

[a]SIAAS = slurry-injection atomic absorption spectrometry; XRF = X-Ray fluorescence; FNAA = instrumental fast (14 Mev) neutron activation analysis.

[b]Standard error of estimate is the RMS deviation in the y-values from the straight line fit.

[c]Data arbitrarily selected for one coal from each 0.1 % silicon interval from the 172 coals listed.

TABLE II: Logarithmic Least-Squares Correlations of percent Ash Vs. Percent Silicon In Some Coals[a]

Type of Coal	Method of Silicon Determination	% Ash = a(% Si)[b]		Correlation Coefficient
		a	b	
KY & WV	SIAAS	6.82	0.525	0.917
KY & WV	XRF	5.82	0.652	0.919
KY & WV	FNAA	5.72	0.663	0.902
ILL(No.5) Harrisburg	XRF	8.85	0.348	0.426
Western	XRF	7.80	0.455	0.845
ILL Basin	XRF	7.20	0.507	0.699
Arbitrary	XRF	7.37	0.547	0.906
Silesian[b]	FNAA	7.63[d] 5.27[e]	0.634 0.89	- -
Belgian[c]	FNAA	4.78	0.930	-

[a] Coals and symbols identified in Table I.
[b] Reference 11; 43 coal samples.
[c] Reference 12; 31 coal samples.
[d] For coals with Si = 4.2 % and above.
[e] For coals with Si = 4.2 % and below.

FORMULAS FOR CALCULATING THE HEATING VALUE OF COAL AND COAL CHAR: DEVELOPMENT, TESTS AND USES

D. M. Mason and K. Gandhi

Institute of Gas Technology
3424 S. State St.
Chicago, Illinois 60616

The heating (calorific) value of coal and char is of great importance in the conversion of coal to other useful forms of fuel, as well as in its direct use. The significance of the correlation of heating value with composition in ordinary fuel usage is shown by the development, as early as 1940, of some 9 different formulas for calculating heating value from the ultimate analysis and 11 formulas for calculating it from the proximate analysis (1). Three additional ultimate analysis formulas have been proposed within the last three years (2,3,4). The correlation is perhaps of even greater importance for the rationalization and modeling of conversion processes now being developed.

Our own work on this problem was carried out for a project on preparation of a "Coal Conversion Systems Technical Data Book," supported by the U.S. Department of Energy and its predecessors.

A data base (including experimental heating values, ultimate analyses and some other parameters) was established, consisting of 121 samples from the Coal Research Section of Pennsylvania State University (5), and 681 samples analyzed by the Bureau of Mines and reported in various state and Federal government publications (6,7,8,9). The Penn State samples, representing large deposits of coal, had been selected for tabulation in the Data Book (10). The data base covers a wide range of coal fields of the United States.

Four formulas were selected for test. They are as follows:

Dulong (1)

$$Q = 145.44\ C + 620.28\ H + 40.5\ S - 77.54\ (O) \qquad 1)$$

Boie (11)

$$Q = 151.2\ C + 499.77\ H + 45.0\ S - 47.7\ (O) + 27.0\ N \qquad 2)$$

Grummel and Davis (1,12)

$$Q = \left[\frac{654.3\ H}{(100-A)} + 424.62\right]\ [C/3 + H - (O)/8 + S/8] \qquad 3)$$

Mott and Spooner (1,13)

$$Q = 144.54\ C + 610.2\ H + 40.5\ S - 62.46\ (O) \qquad (O) \leq 15\% \qquad 4a)$$

$$Q = 144.54\ C + 610.2\ H + 40.5\ S - \left[65.88 - \frac{30.96(O)}{(100-A)}\right](O) \qquad (O) > 15\% \qquad 4b)$$

In the above, Q is the gross heating value in Btu/lb on the dry basis and C, H, S, (O), N, and A are the respective contents of carbon, hydrogen, sulfur, oxygen, nitrogen, and ash in weight percent, also on the dry basis.

For a fair test of the formulas on samples representing commercial coal we eliminated samples with more than 30% ash, leaving a total of 775 samples in the data bank. Results of applying the several formulas separately to the various ranks of coal and also to the combined (all ranks) data are presented in Table 1. The bias (average algebraic difference between observed and calculated values) and the standard deviation after correction for the bias are the most significant criteria. For most of the formulas there are large differences in bias among different ranks of coal, so we have calculated standard deviations for each rank after correcting for the bias shown for that rank. The standard deviation is also given with application of a bias correction averaged over all ranks. Note that the often-used Dulong formula has a substantial bias for all ranks, but of opposite sign for low-rank coals compared with bituminous and anthracite coals. Thus the overall bias is low, but no advantage is gained by its application. Also note that although results from the Boie equation have the highest bias of any, after application of an overall bias correction the results are among the best.

In addition to calculation with the formulas per se, we also calculated heating values by use of Given and Yarzab's modified Parr equation for mineral matter content, and their corrections to obtain carbon, hydrogen, sulfur and oxygen on a mineral-matter-free basis (14). This calculation requires values for pyritic sulfur that were not available for some of the samples. Results obtained with the modified Mott-Spooner equations on 646 samples having pyritic sulfur contents are also shown in Table 1; results from other formulas were improved, but the Mott-Spooner equation gave the best results. Details of this calculation and full results are reported elsewhere (15).

The data bank was also subjected to a least squares regression analysis. Carbon, hydrogen, sulfur, ash, and oxygen terms were significant; nitrogen and cross and square terms were not. To avoid the implied necessity of determining nitrogen, we adopted an oxygen-plus-nitrogen term. The resulting equation, which we refer to here as the Data Book Equation, was as follows:

$$Q = 146.58\ C + 568.78\ H + 29.4\ S - 6.58\ A - 51.53\ (O + N) \qquad 5a)$$

When 100- C-H-S-A is substituted for O+N, an equivalent form is obtained:

$$Q = 198.11\ C + 620.31\ H + 80.93\ S + 44.95\ A - 5153 \qquad 5b)$$

Results from this new formula are also shown in Table 1. The bias for different ranks of coal ranges only from -45 Btu/lb on lignite to 13 Btu/lb on subbituminous coal and does not show a trend with rank. The standard deviation is significantly less than those of the other unmodified formulas, even after improving these by a bias correction. The new formula has about the same accuracy as the Mott-Spooner with modified Parr corrections, but the latter is more complicated and requires pyritic sulfur determination.

The effect of ash content on the accuracy and precision of the formula was investigated, with the results shown in Table 2. For this test, the formula was also applied to the 27 high-ash samples that had been removed from the data bank.

Table 1. TEST OF FORMULAS FOR CALCULATION OF HEATING VALUE

	No. of Samples	Average Absolute Deviation	Bias*	Standard Deviation: Before Bias Correction	Standard Deviation: After Rank Bias Correction	Standard Deviation: After Over-all Bias** Correction
		Btu/lb				
Dulong						
Anthracite	40	137	-123	157	97	146
Bituminous	406	181	-138	221	173	212
Subbituminous	180	174	127	213	170	222
Lignite	149	218	174	255	185	266
All Ranks	775	184	-15	223	—	222
Boie						
Anthracite	40	400	-400	417	100	177
Bituminous	406	253	-248	279	129	129
Subbituminous	180	217	-207	249	138	146
Lignite	149	301	-298	330	138	145
All Ranks	775	262	-256	291	—	139
Grummel and Davis						
Anthracite	40	107	79	134	106	165
Bituminous	406	164	-128	208	164	184
Subbituminous	180	130	46	168	161	185
Lignite	149	127	39	171	167	187
All Ranks	775	146	-44	189	—	184
Mott and Spooner						
Anthracite	40	84	-56	107	91	100
Bituminous	406	160	-134	197	144	149
Subbituminous	180	113	-31	152	149	162
Lignite	149	124	-85	170	147	147
All Ranks	775	138	-96	178	—	150
Mott & Spooner, Modified Parr Basis						
All Ranks	646	106	42	—	—	132
New Formula						
Anthracite	40	73	-14	93	92	93
Bituminous	406	90	10	124	123	124
Subbituminous	180	103	13	140	139	140
Lignite	149	96	-45	137	129	137
All Ranks	775	93	0	129	129	129

* Average observed value - average calculated value
** Bias obtained over all ranks

Table 2. EFFECT OF ASH CONTENT ON THE CALCULATION OF HEATING VALUE

Ash Content, wt %	Number of Samples	Avg. Absolute Difference	Bias*	Standard Deviation
0-10	394	82	6	113
10-20	320	104	−15	144
20-30	61	112	26	141
>30	27	155	20	211

* Average of observed minus average of calculated values

The absence of significant bias, here and among different ranks of coal, indicates that no improvement by change in the formula appears possible as long as it is based on ultimate analysis only. The increase of the standard deviation with ash content can be attributed to the effects of differing ratios of mineral matter to ash, and differing contributions of the mineral matter to determined carbon and hydrogen contents. A computer analysis of the data in which it was assumed that the variance is linear with ash content indicated that the variance increases by 4/2 $(Btu/lb)^2$ per percent of ash, and that the standard deviation on ash-free samples would be 106 Btu/lb.

It is of interest to determine whether the remaining variance can actually be attributed to the laboratory determinations. The latter can be estimated according to —

$$\text{Var (exp)} = \text{Var Q} + 198.11^2 \text{ Var C} + 620.31^2 \text{ Var H} + 80.93^2 \text{ Var S} + 44.95^2 \text{ Var A} \qquad 6)$$

where Var Q, Var C, etc., are variances of the respective determinations. Some precision data have become available from the HYGAS® program at IGT, which can be used for a test.

Sources of variance of the experimental determinations need to be considered for the purpose at hand. The heating value and the analytical determinations (carbon, hydrogen, sulfur, and ash) are all run on a sample of coal (or char) that has been ground finer than 60-mesh sieve size. Thus, the variance from sampling of the coarse sample submitted to the laboratory is not of concern. If the moisture content does not change during all of the sample withdrawals for the various determinations, no variance is contributed by the moisture determination; however, if several days elapse between heating value and carbon-hydrogen determinations, a contribution from this source is likely, either from the change in moisture or from the variance of its redetermination. Variance can also be contributed by day-to-day variations in equipment and operator; thus redetermination on the same day would not serve the purpose. Instead, our procedure consisted of resubmitting from time to time a number of ground samples of coal (in the same 4-oz bottles as originally sampled from) for redetermination of moisture, heating value, carbon, hydrogen, sulfur, and ash. Each reported value for carbon, hydrogen, ash, and heating value is the average of two determinations run at the same time; for sulfur only one determination is made. Completion of the duplicate analysis ranged from 9 to 46 days after completion of the routine analysis. Slight average changes in values from the original analysis to the duplicate, such as an average decrease in heating value of 13 Btu/lb, occurred; the standard deviations were calculated both with and without correction for this bias.

The duplicate differences from this program were examined for outliers. Three sulfur, one ash and one heating value, all with differences between duplicates greater than $3.8\sqrt{2}\,\sigma$, were discarded. In addition, a heating value with a duplicate difference of $2.8\sqrt{2}\,\sigma$, and also having a difference between observed and calculated values of $3.5\,\sigma$ was also discarded. The analysis of the remaining data is presented in Table 3.

The variance contributed to the difference between observed and calculated heating values by the variance of the experimental determinations can now be calculated according to Equation 6. The standard deviations after bias corrections (Table 3) yields the value 64 Btu/lb as the expected σ. This represents 77% of the variance found for a large set of routine HYGAS data on raw bituminous coal discussed later in this paper. The remainder of the variance can be attributed to the effect of outlying laboratory determinations, and the effect of mineral matter.

Table 3. SUMMARY OF HYGAS REPEATABILITY DATA

	No. of Duplicates	Average Value	Bias*	Standard Deviation** Before Bias Correction	Standard Deviation** After Bias Correction
		Btu/lb			
Heating Value	56	11680	13	29	27
		wt %			
Carbon	41	64.07	0.037	0.25	0.24
Hydrogen	41	4.52	0.028	0.051	0.051
Sulfur	55	4.39	-0.011	0.084	0.086
Ash	40	16.77	0.037	0.14	0.14

* Original minus duplicate

** Of reported values, each the average of two determinations run at the same time, except single determinations for sulfur.

TEST AND USES

Data for testing of the new formula were solicited from outside laboratories. Results from two laboratories presented in Table 4 show good precision, but the large bias values suggest the presence of systematic error or difference from the original data.

Results from a third laboratory illustrate an important use of the formula. The experimental data covered a period of several years and were furnished in the sequence in which they were obtained by the laboratory. We eliminated a few samples having over 35% ash or less than 3% oxygen, because the latter are likely to be chars. On the remaining data, the standard deviations obtained from consecutive sets of 50 samples are shown in Figure 1. On the first 650 samples the bias was 32 Btu/lb and the standard deviation was 136 Btu/lb, in good agreement with results on the original data bank. On subsequent samples the results indicate a substantial deterioration in laboratory precision. Thus, a control chart of this kind can serve as a monitor of laboratory performance. Also, the difference between observed and calculated heating values on an individual sample can be used by the laboratory supervisor as a criterion of acceptability of the heating value and carbon-hydrogen determinations. The difference is less sensitive to the sulfur and ash values.

Table 4. TESTS OF NEW HEATING VALUE FORMULA AT OTHER LABORATORIES

Laboratory	Kind of Coal	No. of Samples	Average Absolute Difference	Bias*	Standard Deviation: Before Bias Correction	Standard Deviation: After Bias Correction
			Btu/lb			
A	Bituminous	42	115	−96	157	123
B	Illinois Basin	78	112	−91	139	107
B	Subbituminous	40	81	−50	102	90

* Average observed value minus average calculated value

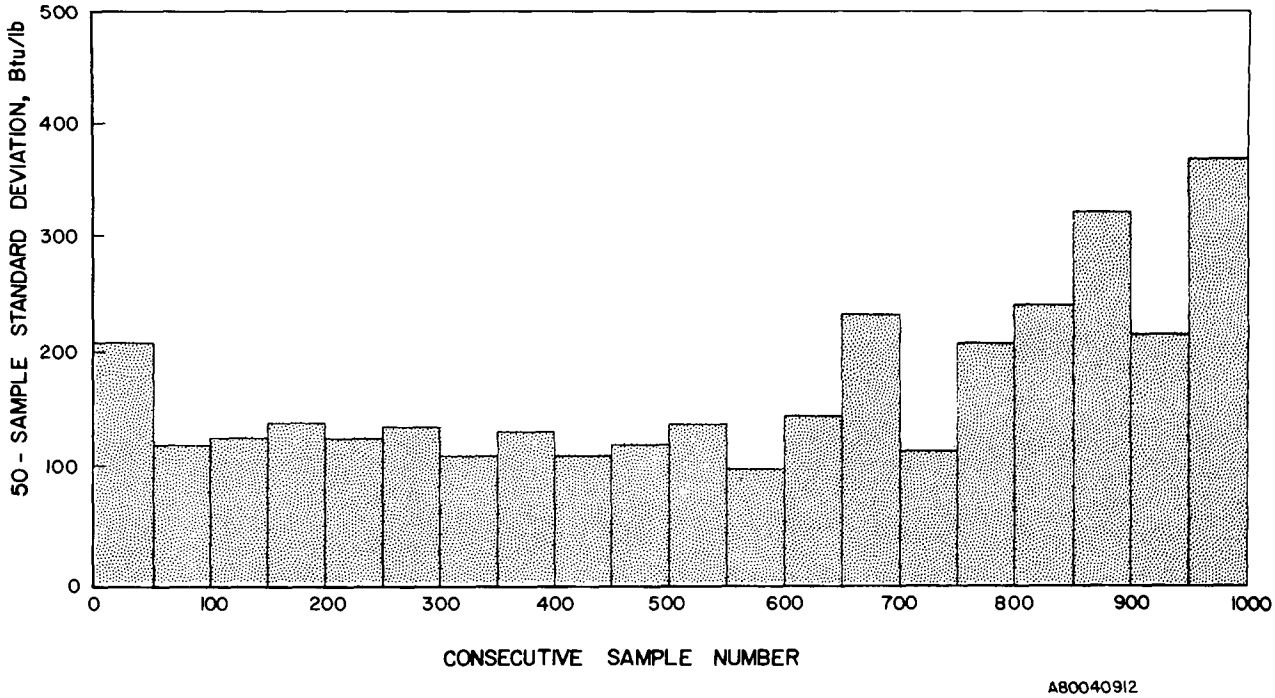

Figure 1. VARIABILITIY OF THE DIFFERENCE BETWEEN OBSERVED AND CALCULATED HEATING VALUE IN ONE LABORATORY

Another important use of a heating value formula is in computer modeling of coal conversion processes. Data on heating value and composition of samples of coal and char obtained at IGT under the HYGAS pilot plant program were analyzed for this purpose. In the HYGAS process, non-agglomerating coals are dried but are not otherwise pretreated. Bituminous coals are pretreated at temperatures of 750°F to 800°F to destroy their agglomerating properties. The resulting product is referred to here as "pretreated coal" rather than "char". Samples referred to as "chars" are from later intermediate stages or are spent (residue) char. Ash in the spent char from the runs on bituminous coal averaged 36%, but ranged up to about 85%. To augment the data from runs on subbituminous and lignite coals, we have added some samples taken from streams that contain feed coal in addition to char, such as the dust collected by a cyclone in the reactor product gas stream. Results are presented in Table 5, together with those obtained on the original data bank.

The most important criterion for use of a heating value formula in a computer model of a coal conversion process is the bias or average difference between observed and calculated values, because it shows how closely the formula represents the properties of the coal. On the 294 samples of raw (untreated) bituminous coals, the calculated values are, on the average, 18 Btu/lb less than the observed values. This differs by only 8 Btu/lb from the value found on the 406 samples of bituminous coal in the original data bank. There is only about a 20 percent chance that the difference is significant; if so, it can be attributed to a slightly lower ash content obtained at IGT, because at IGT the amount of sulfur trioxide in ash is routinely determined and deducted from the reported ash. Ash as customarily determined is likely to contain small amounts of sulfur trioxide.

The standard deviation shown for these coal samples is substantially less than was found on the bituminous coals of the original data bank. The difference may be a result of the limited range of source of the HYGAS samples: all were from the Illinois No. 6 seam and 95% were from a single mine; the ash content averaged 10.7%. (The samples from the repeatability set of data had higher ash, averaging about 17%).

On pretreated bituminous coal the calculated values are, on the average, 157 Btu/lb lower than the observed values. The Data Book formula is thus unsatisfactory for use in a computer model applied to this material; for such use a bias correction can be applied or a formula can be obtained by regression analysis of the pretreated coal data. The difference in bias between the parent and pretreated coal, 139 Btu/lb, can be attributed to a difference in structure (bonding); the formula has already taken into account differences in elemental composition. Such differences in structure include effects of incorporation of oxygen in a different form from that ordinarily present. In other processes the difference in bias may be greater or less, depending on processing conditions such as temperature and presence or absence of oxygen; in the HYGAS process the difference is reduced to about 40 Btu/lb at the stage where the temperature reaches about 1200°F.

On the set of samples of char from bituminous coals the calculated values are, on the average, only 28 Btu/lb less than the observed values; the difference is of about the same order for chars from subbituminous coal and lignite. A more accurate formula could be obtained for the chars from the bituminous coal, but the Data Book formula should be adequate for most practical purposes; the accuracy should be judged according to unit weight of coal feed rather than unit weight of char.

CONCLUSIONS

A new five-term formula for calculating the heating value of coal from its carbon, hydrogen, sulfur and ash content was obtained by regression analysis of data on 775 samples of U. S. coals of all ranks. The standard deviation of the calculated value from the observed value was 129 Btu/lb, compared to apparent standard deviations ranging from 178 to 229 Btu/lb obtained from the Dulong, Boie, Grummel and Davis, and Mott and Spooner formulas. An analysis of the variance of the difference between

Table 5. TEST ON HYGAS ROUTINE SAMPLES OF THE DATA BOOK FORMULA FOR CALCULATION OF HEATING VALUE

HYGAS Data Bank	No. of Samples	Bias[d]	Standard Deviation: Before Bias Correction (Btu/lb)	Standard Deviation: After Bias Correction (Btu/lb)
Bituminous Coal[a]				
Raw Coal	294	18	73	71
Pretreated Coal	572	157	174	76
Chars				
First Stage Hydrogasification	105	58	98	79
Second Stage Hydrogasification	106	2	106	106
Spent Char	570	28	97	92
All Char	781	28	98	94
Subbituminous Coal[b]				
Coal	49	-47	69	51
Chars	80	15	59	57
Mixtures of Coal and Char	66	15	55	53
Lignite[c]				
Chars	80	34	78	77
Mixtures of Coal and Char	44	12	88	77
Original Data Bank				
Bituminous Coal	406	10	124	124
Subbituminous Coal	180	13	140	140
Lignite	149	-45	137	137
All Samples, Including Anthracite	775	0	129	129

[a] From Illinois No. 6 seam. About 1/8 of the samples were from runs on hvBb coal from Saline County, and the remainder from runs on hvCb coal from Christian County.

[b] From the Rosebud Seam, Rosebud County, Montana.

[c] From the Savage Mine, Richland County, Montana.

[d] Average observed value minus average calculated value.

observed and calculated values obtained with the new formula on IGT coal data indicated that at least 77% is contributed by the variance of the experimental determinations; the remainder can be attributed to the effect of mineral matter and outlying experimental determinations.

Application of the formula to coal oxidatively pretreated at 750°F to 800°F to destroy agglomerating properties yields a bias indicating that its heat of formation is higher than expected from elemental and ash composition by about 140 Btu/lb; this is attributed to differences in structure (bonding) of the pretreated coal in comparison to unpretreated coal. The formula gives satisfactory results on higher temperature HYGAS chars, and, with application of a bias correction, on pretreated coal

Thus, the formula is advantageous for use in the computer modelling of coal conversion processes and for monitoring test data on coal and char.

Acknowledgement

The work reported here was conducted as part of a project, sponsored by the U. S. Department of Energy, on preparation of a Coal Conversion Systems Technical Data Book. Use of data obtained under the HYGAS program is gratefully acknowledged.

LITERATURE CITED

1. Selvig, W. A. and Gibson, F. H., "Calorific Value of Coal," in Lowry, H. H., ed., Chemistry of Coal Utilization 1, 139. New York: John Wiley, 1945.

2. Subramaniam, T. K., "How to Calculate Btu Values of Coal," Coal Age, 82, 153-58 (1977) December

3. Lloyd, W. G. and Francis, H. E., Personal Communication, 1979.

4. Lloyd, W. G. and Davenport, D. A., "Applying Thermodynamics to Fossil Fuels," J. Chem. Ed. 57, 56-60 (1980) January.

5. Spackman, W. et al.," Evaluation and Development of Special Purpose Coals, Final Report" ERDA No. FE-0930-2, NTIS, Springfield, Va. 1976.

6. Swanson, V. E. et al., "Collection, Chemical Analysis, and Evaluation of Coal Samples in 1975," U.S. Department of the Interior, Geological Survey, Open-File Report 76-468, 1976.

7. Gilmour, E. H. and Dahl, G. G., Jr., "Montana Coal Analyses," Bur. Mines Geol. Spec. Publ. 43. Butte, Mont. 1976.

8. Glass, G. B., "Analyses and Measured Sections of 54 Wyoming Coal Samples (Collected in 1974)," Geological Survey of Wyoming Rep. Invest. No. 11. Laramie, Wyo. 1975.

9. Sondreal, E. A., Kube, W. R. and Elder, J. L., "Analysis of the Northern Great Plains Province Lignites and Their Ash," U.S. Bur. Mines Rep. Invest. No. 7158. Washington, 1968.

10. Institute of Gas Technology, "Coal Conversion Systems Technical Data Book," U.S. Department of Energy No. HCP/T2286-01, Supt. of Documents, Washington, D.C. 1978.

11. Boie, W., "Fuel Technology Calculations," Energietechnik 3, 309-16 (1953).

12. Grummel, E. S., and Davis, I. A., "A New Method of Calculating the Calorific Value of a Fuel From Its Ultimate Analysis, Fuel 12, 199-203 (1933).

13. Mott, R. A., and Spooner, C. E., "The Calorific Value of Carbon in Coal," Fuel 19, 226-31, 242-51 (1940).

14. Given, P. and Yarzab, R. F., "Problems and Solutions in the Use of Coal Analyses. Technical Report 1." ERDA No. FE-0390-1. NTIS, Springfield, Va. 1975.

15. Institute of Gas Technology, "Preparation of a Coal Conversion Systems Technical Data Book," ERDA No. FE-2286-32, NTIS, Springfield, Va. 1978.

COAL CHARACTERIZATION RESEARCH: SAMPLE SELECTION, PREPARATION, AND ANALYSES

R. C. Neavel, E. J. Hippo, S. E. Smith, R. N. Miller

Exxon Research and Engineering Company P.O. Box 4255 Baytown, Tx. 77520

INTRODUCTION

There are few procedures available to predict process responses or to assess the relative values of coals from fundamental coal properties. Therefore, a comprehensive coal characterization program has been established at Exxon Research and Engineering Company, Baytown, Texas to evaluate coals as process feedstocks. The objective of this program is to relate fundamental coal properties and process response patterns by analyzing and testing a large suite of U. S. coal samples.

This report defines the technical rationale behind the coal characterization program and describes the procedures used in the selection, preparation, and testing of the coal library samples.

RATIONAL APPROACH TO COAL CHARACTERIZATION

The principle goal of a coal characterization research program should be to develop procedures that define the minimal testing required to evaluate coals as process feedstocks. The alternatives available are (1) to test any 'unknown' coal (coal X) empirically in a commercial or small-scale process or (2) to develop information about the fundamental relationships between coal properties and process responses, and to use this information and appropriate analyses of coal X to predict its response.

The empirical technique is direct and provides an unequivocable answer about the response of the tested sample. The results, however, cannot be extrapolated to other samples with different characteristics. This is particularly critical during exploration programs where the coal characteristics may change significantly over the areas being evaluated. Though development of fundamental understanding is more difficult, it provides much greater flexibility in subsequent testing. Only a program designed to relate fundamental properties of a broad range of coals to their process responses has value to the coal community.

Criteria Used in the Selection of a Set of Coal Samples for Research

Coal characterization efforts aimed at predicting coal responses from fundamental properties must follow a rational scientific approach (viz. characterization by rank, type and grade), if they are to yield extrapolatable results[1]. Major differences between "typical" coals in the U.S. are rank-related. Therefore, we employed criteria for selecting our coal samples that maximized coal rank variability. Variations in type, though purposely minimized could not, however, be eliminated and are dealt with as part of this study.

A set of research samples was selected according to the following criteria:

(1) Broad range in rank. In effect, this maximizes variation in organic chemical composition, principally the elements C, H, and O. High rank coals (anthracites) were excluded, because they are of little economic value from a synthetic fuels standpoint.

(2) Vitrinite-rich. Vitrinite is the predominant maceral in most U.S. coals and for that reason its reactivity is of most concern in utilization. Also, the properties of vitrinite vary progressively with rank.

(3) Low in inorganic matter content (preferably less than 10%). This restriction minimizes problems which can arise during analyses and subsequent calculations of the properties of the organic components.

(4) Geographically and geologically diverse (within the continental U.S.). Samples were obtained from the major coal-bearing regions in the United States so as to include different metamorphic histories and geological ages.

(5) Fresh and unweathered.

The optimum range in rank variation of vitrinites is best defined by the classical H/C vs O/C diagram from van Krevelen[2]. When published data (from the Pennsylvania State University coal-data base [3] for high vitrinite (>80%), low mineral-matter coals (<10%) from various regions in the U.S. are plotted on a van Krevelen diagram, a broad band is obtained (shown in Figure 1). From along the length and breadth of this band a random set of coals was identified and then located for collection. Sixty-four samples were ultimately selected for the research study. Two foreign samples were also added to the library. Oistribution of these 66 samples on the van Krevelen plot is shown in Figure 1.

The coal samples were collected by experienced coal geologists directly from freshly exposed seam faces. Where possible, the samples were selected from lithotypes rich in vitrain. Some samples were obtained as run-of-mine samples, providing they were recently mined and free of extraneous rock.

Most samples were collected as coarse lumps (larger than 5-6 cm). Samples were sealed within heavy gauge, polyethylene bags, placed in epoxy-lined containers (when possible, they were placed under water) and shipped. Any information that might ultimately be pertinent to sample quality was logged. Upon receipt, the samples were stored in a cold room (at 30-40°F) until preparation.

SAMPLE PREPARATION

Initial Bulk Sample Preparation

The procedure for the general workup and subsequent characterization of coal samples for this study is summarized by Figure 2. To minimize oxidation during preparation, samples were handled in nitrogen-filled glove boxes (where possible). Maintaining water filled pores minimized exposure of the internal surface to air and prevented irreversible pore collaspe. The initial sample was inspected and a hand specimen was taken for display. Extremely coarse (>5 cm), particles were broken by hammer to about a 5-cm top size. The coal was then washed on a 16 mesh screen (or 100 mesh if the sample was fine) to remove any extraneous mineral matter, debris and fines. Such physical beneficiation to provide sample consistency can be performed when seam-representive samples are not required, as in studies such as this. Subsequently, the coal was surface dried under nitrogen, frozen for at least 4 hours in solid CO_2 ("dry ice"), and then crushed to -4 mesh

using a swing-hammer mill. Freezing the samples minimizes the risk of thermal change, oxidation, and volatile release due to heat generation during size reduction.

The coal was then riffled into 3-kg representative splits. Bottles containing these splits (and all subsequent samples) were placed in a bell jar with the bottle lids loosely in place. The system was evacuated and refilled with nitrogen three times to replace any air. All bottles were capped with tightly fitted lids which were then secured with tape. Sample identification numbers are permanently etched into the bottles. Samples were stored in the manner indicated in Figure 2.

Preparation of a 16 x 100 Mesh Analytical Sample

One of the 3-kg samples of the -4 mesh coal (the "working sample") was stage-crushed using a mechanical gate mill (a "coffee grinder") in a nitrogen filled glove box. After passing through the coffee grinder, the coal was screened on a 16 mesh screen and the top size recycled. The process was repeated until all the sample passed through the 16 mesh screen. This stage crushing maximized the particle size consist of the crushed coal.

The -16 mesh material was wet-screened on a 100 mesh screen by washing repeatedly with water. The fines were discarded. Approximately 70 to 80% of the 3 kg split was retained by this method. Wet screening physically beneficiates the coal by removing fines. Excessive fines are undesirable in certain analytical tests (i.e. HGI, petrography and some process response determinations). Also, removal of fines decreases fusinite and mineral content of the sample, since these components preferentially report to the fines fraction during size reduction.

Excess water left on the 16x100 mesh coal from the washing procedure was removed by placing the wet coal in a 25 cm Buchner vacuum filtration assembly inside of a nitrogen-filled glove box. The aspiration forces nitrogen through the sample and dries the surface of the coal, so that it can be riffled, without exposing the pore structure to air (oxygen).

Four splits containing about 500g of 16 x 100 mesh coal were obtained using a mechanical riffling device. Two splits were stored for future work. The other two fractions were equilibrated in nitrogen at 50% relative humidity and used for all of the analyses. Equilibration at 50% relative humidity is required to obtain reproducible weighings (50% relative humidity is typical for most labs). Nitrogen is used as the equilibrating gas to minimize oxidation. The 50% relative humidity nitrogen was obtained by bubbling nitrogen through water under 2 atmospheres of pressure and subsequently expanding the saturated nitrogen through a regulator to one atmosphere of pressure. The partially moist nitrogen was passed through a manifold into a number of bottles containing coal, and after passing through the coal, was vented. A top loading balance was used to record the weight of each of the bottles of coal as a function of time. When the weight stabilized, equilibration was achieved.

Some coal analyses require coarse-sized coal and other analyses require pulverized (-60 mesh) coals. Splitting the 16 x 100 mesh fraction into a 16 x 60 mesh fraction for coarse analyses and -60 mesh fraction for chemical analysis would not have been valid since coal components segregate to different size fractions. Therefore an aliquot of the 16 x 100 mesh coal was pulverized to -60 mesh.

Preparation of Aliquots for Analysis

Numerous aliquots of about 5g each were riffled in a nitrogen-filled glove box using a rotary riffling device. The rotary system is far superior to other sample splitting methods in that it affords better reproducibility between splits and allows a rapid production of multiple aliquots. Each aliquot was used for only a few tests or analyses. By preparing many aliquots at the outset, oxidation, contamination, or non-representativeness often associated with repeated handling of bulk analytical samples, is avoided.

ANALYTICAL PROCEDURES AND DATA QUALITY

Analyses and tests performed on the samples are shown in Figure 2. Most were performed according to ASTM standardized procedures. Brief descriptions of non-standard tests are described below.

1. Extraction with citric acid and benzene/ethanol azeotrope.
2. Assessment of acidic functionality by $Ca(OH)_2$ and $Ba(OH)_2$ ion exchange.
3. Density by helium pycnometer and by water displacement.
4. Gasification in a small fluidized bed.
5. Pyrolysis in a rapid-heating, fixed bed system. Yields of char, tars, water and gases assayed. Product properties assessed.
6. Liquefaction in small batch system (tubing bomb[4]).
7. Combustibility by burning in a thermogravimetric analyzer (combustion profile technique[5]).
8. Total oxygen by instrumental neutron activation analysis (INAA).

A number of internal checks described below were applied to the standard coal library data to ensure that all basic compositional analyses were accurate and meaningful.

Duplicate Analysis Scrutiny

All standard ASTM tests of elementary composition and for proximate analyses were done in duplicate. Samples were reanalyzed if the differences between duplicates exceeded ±2 standard deviations of the mean difference of all coals. If the rerun was still outside ±2 standard deviations, the test was repeated until the error was corrected. About 10-20% of the standard data required reanalysis, a figure which we believe would be typical for any well-run coal analysis laboratory. The data which were used for subsequent manipulation in the library were the arithmetic averages of two "best" duplicate runs.

Determined Versus Calculated Calorific Value

The calorific value of a coal can be calculated from the elementary composition and this value can be compared to the experimentally determined value as a check on the accuracy of both elemental and calorific value analyses. We checked the coal library data using a combination of three different formulae, two obtained from the literature and one derived specifically from the coal library samples.

---

*All on % dry coal basis except for moisture and calorific value which is Btu/lb on dry coal.

The Mott-Spooner formula calculates a dry, mineral matter-free (dmmf) calorific value (Btu/lb) using elemental analyses on a dmmf basis as:

$$CV_{MS} = 144.54 * C_{dmmf} + 610.2 * H_{dmmf} - 62.46 * O_{dmmf} + 40.5 * S_{org_{dmmf}} \quad (1)$$

If the dmmf oxygen content is greater than 11%, the Mott-Spooner Btu calculation (CV_{MS}) is modified by:

$$CV_{MS}\ (O_{dmmf} > 11\%) = CV_{MS} + [(0.31 * O_{dmmf} - 3.42) * O_{dmmf}] \quad (2)$$

Another formula was derived by the Institute of Gas Technology in Chicago as follows[6]:

$$CV_{IGT} = 146.58 * C + 568.78 * H + 29.4 * S - 6.58 * A - 51.53\ (O + N) \quad (3)$$

where C, H, N and S represent total dry carbon, hydrogen, nitrogen and sulfur respectively (dry basis), and A is the standard ASTM ash yield (dry basis). O+N is obtained by difference (100 - all other factors). The IGT formula gives the calorific value of the whole, dry coal whereas the Mott-Spooner gives the calorific value of the organic matter only. We derived our own formula using a stepwise regression for the 66 coals in the library. The basis for this formula differs somewhat from that used in the IGT or the Mott-Spooner formulae in that it yields a calorific value (Btu/lb) for dry coal from "corrected" dry analyses (an explanation of the corrections is discussed in a later section).

$$CV_{ERE} = 151.31 * C_{org} - 47.87 * O_{org} + 549.74 * H_{org} + 68.96 * S_{pyr} + 47.58 * S_{org} - 400.24 \quad (4)$$

Using the above equations we calculated the calorific values for all 66 coals and compared them to the determined calorific values. If the differences exceeded ±250 Btu/lb, the analyses were evaluated for errors and where appropriate, the samples reanalyzed. Table 3 summarizes the differences between determined and calculated calorific values using the Mott Spooner, IGT, and the Exxon Research (ER&E) formulae.

Table 3

COMPARISONS OF DETERMINED VERSUS CALCULATED CALORIFIC VALUE/(BTU/lb)

Formula	Mean Diff.	Std. Dev.	Value Range Min.	Max.
Mott Spooner (dmmf)	-59.3	113.6	-43.	213
IGT (dry)	-9.2	110.9	-399.	167
ER&E (dry organic)	-7.8	95.4	-298.	205.

All but a few of the coals gave excellent comparisons of calculated versus determined calorific values. We have not been able to determine why the few coals appear as outliers, even after re-analysis.

Elemental Balances

Total oxygen on dry coal can be determined independently using instrumental neutron activation analysis (O_{inaa}). Total oxygen can also be calculated by difference from dry analyses as:

$$O_{diff.} = 100 - C - N - H - S_t - Cl - \text{Ash Elements} \quad (5)$$

where ash elements are the sum of the Si, Al, Fe, Mg, Ca, K, P, Na, and Ti calculated as a percentage of dry coal, and S_t is total sulfur. A comparison of the oxygen by difference against the oxygen by neutron activation serves as an independent check on the accuracy of the combined elemental analyses. The overall mean difference for the 66 coals was -1% with a standard deviation of 0.93 about the mean. The slight negative bias is probably due to the absence of minor and trace elements in the material balances. Several of the samples show significant deviations even though the elementary analysis appears to be valid. We believe the discrepancy may be due to moisture fluctuations or to interferences in the neutron activation analysis of oxygen.

Ash Checks

Ash determinations were done in duplicate on both the 16x100 mesh and the -60 mesh fractions. For all 66 coals, the minimum and maximum differences were -0.43 and +0.30 and the overall mean difference in ash between the two fractions was -0.089. The standard deviation was 0.15, well within the ASTM repeatability limit of 0.3.

CALCULATION OF DATA TO VARIOUS BASES

As-analyzed data are seldom of any direct use. Most raw analytical data must be calculated to some more meaningful basis in order to be effectively employed. All of our data were calculated to the dry basis. Because in most instances we were interested in properties and responses of the organic fraction, data were also calculated to a dry, mineral-matter free basis as described below.

Determination of the Mineral Matter Content

We estimated the inorganic matter (so-called mineral matter) content for the library coals from adjustments to the high temperature ash yield. The formula should apply to coals of all ranks and to coals that contain a variety of inorganic materials. Mineral matter content is calculated using the following relationship:

$$MM = Ash + H_2O_{clay} - 2.5(S_{ash}-S_{SO_4}) + 0.626 * S_{pyr} + CO_2 - O_{ie} \qquad (6)$$

In Equation (6) the high temperature ash yield (Ash) is corrected using terms for the water of hydration of clays (H_2O_{clay}), the net amount of sulfate fixed in the ash ($S_{ash} - S_{SO_4}$) expressed on the coal basis, the decomposition of pyrite ($0.626 \times S_{pyr}$), the decomposition of carbonates to oxides (CO_2 loss) and a correction for the amount of organic oxygen that is retained in the ash (O_{ie}) owing to partial decomposition of humate salts in the lower rank coals. Other reactions of inorganic species during ashing are assumed to be negligible.

All but the H_2O_{clay} and O_{ie} are determined directly. S_{SO_4} refers to sulfate sulfur in the coal; CO_2 is determined according to ASTM D1756. The water of decomposition of clays is estimated using these relationships:

$$H_2O_{clay} = 0.10 * CLAY \qquad (7)$$

$$CLAY = ASH - 1.2452 * S_{pyr} - 1.274 * CO_2 - 1.280 * Fe_{acid\ sol.} - 2.5 * S_{ash} - QTZ - ALK \qquad (8)$$

Expression (8) approximates a clay content (CLAY) by subtracting estimates for the contributions of pyrite, carbonates, iron and sulfur oxides, quartz and any organically derived alkali oxides in the ash. Ten percent of the clay (Eq.7) is

then assumed to be the average water of decomposition. The organically derived alkali oxides (ALK) for use in Equation (8) are estimated from the analyses of the acid soluble alkalies by:

$$ALK = (CaO_{net} + MgO + Na_2O + K_2O)_{acid\ sol.} \quad (9)$$

where CaO_{net} represents all of the acid soluble Ca that is not stoichiometric with the amount of carbonate, estimated from the CO_2 yield as:

$$CaO_{net} = CaO_{acid\ sol.} - 1.274 * CO_2 \quad (10)$$

The ash element analysis can be used to estimate excessive amounts of quartz as:

$$QTZ = 2.1393 * [Si - (2.089 * Al)] \quad (11)$$

Equation (11) assumes that all aluminum is clay-associated and compensates only for coals that contain an exceptionally high content of free SiO_2.

A large portion of the alkali metals in lower rank coals are exchanged to oxygen functional groups. When coal is ashed, at either low or high temperature conditions, these organic/inorganic complexes decompose to yield alkali salts. Therefore, some of the oxygen in the ash is actually derived from organic oxygen. This can be approximated by summing the oxygen that would be stoichiometrically associated with the exchangeable alkali metals present on the coal. These are estimated from acid soluble data by:

$$O_{ie} = [O_{CaO_{net}} + O_{MgO} + O_{NaO} + O_{K_2O}]_{acid\ sol.} \quad (12)$$

The O_{ie} term in the mineral matter Equation (12) should be valid for the total range of coals. Most of the alkali metals in lignites, that are acid soluble, are bound to the organic matter. For the high rank coals, we found that by compensating for carbonate the O_{ie} term in the mineral matter expression is negligible.

Low Temperature Ashing

Mineral matter contents were also determined directly for the coals in the library using low temperature plasma oxidation[7], a technique which produces an inorganic residue from coal in more or less unaltered state. Most of the major minerals do not decompose under carefully controlled LTA conditions. Figure 3 shows a comparison between the calculated and experimental (LTA) mineral matter contents of the coals. In the figure, data points with an "x" refer to low rank coals whose oxygen contents are greater than 16% (dmmf). When these coals are excluded, there is good agreement between the two methods; the mean difference for the 52 higher rank coals is essentially zero (-0.01), but with fair amount of scatter (the standard deviation is 0.85).

As shown in Figure 3, the LTA yield of the high oxygen coals is much greater than the calculated mineral matter content. Lignites and subbituminous coals contain appreciable alkali cations bound to oxygenated functional groups. These tend to inhibit the oxidation process, preventing complete ashing; thus, the LTA yields tend be too high. Also, a substantial amount of combustion gas (as either S- or N-oxides) adds to the weight of the LTA by reacting with the molecularly dispersed alkalies. When these coals are extracted with acid, the alkali cations are removed, and no analytical difficulties are encountered with the LTA

technique. Thus, the best direct measure of the mineral matter content in low-rank coals is the sum of the yield of LTA on acid-extracted coal and the weight fraction of acid-soluble inorganics, or

$$MM_{acid+LTA} = CLTA * (100-A/100) + A \quad (13)$$

where CLTA is the LTA yield on dry, acid-washed coal and A is the weight loss upon acid extraction.

Figure 4 is a plot of the mineral matter calculated from Equation (6) against the mineral matter from the modified LTA method (13). Note that significant improvement is seen with the high-oxygen coals (indicated by "X"). The summary statistics of mean differences indicates that the modified LTA method for estimating the mineral matter content is unaffected by differences in rank.

The formula-derived mineral matter content is applicable to all ranks; to maintain consistency within the library, we used the formula for all calculations to the dmmf basis.

Volatile Matter and Calorific Value

The ASTM volatile matter yield, determined at 950°C, includes components from decomposition of inorganic materials. To obtain an organic volatile content we used a formula modified from Leighton and Tomlinson[8] where

$$VM_{corrected} = VM_{dry} - H_2O_{clay} - 0.41 * S_{pyr} - 0.9 * CO_2 - 0.76 * Cl \quad (14)$$

This formula compensates for volatile loss of clay water, pyritic sulfur, carbonate CO_2, and chlorine.

Calorific value (Btu/lb) determinations should be corrected for contributions due to the exothermicity of pyrite oxidation, thus,

$$CV_{corrected} = CV_{dry} - 55.67 * S_{pyr} \quad (15)$$

Fixed carbon content on the dmmf basis is calculated as:

$$FC_{dmmf} = 100 - VM_{dmmf} \quad (16)$$

Elemental Analyses

Carbon and hydrogen determinations by the ASTM method include carbonate carbon and clay water hydrogen respectively. Corrections to obtain the organic carbon and hydrogen contents are made as:

$$C_{org} = C_{dry} - 0.2729 * CO_2 \quad (17)$$

$$H_{org} = H_{dry} - H_{clay} \quad (18)$$

Where $H_{clay} = 0.1119 * H_2O_{clay}$ estimated from equations (6) and (7).

$$O_{dmmf} = 100 - H_{dmmf} - C_{dmmf} - N_{dmmf} - Cl_{dmmf} - S_{org_{dmmf}} \quad (19)$$

Corrected analyses are multiplied by the factor 100/(100-MM) to convert to the dmmf basis.

To express the calculated organic oxygen on the dry basis (O_{org}) the O_{dmmf} value is multiplied by (100-MM)/100.

CORRELATIONS

The purpose of the coal characterization research program is to establish relationships between fundamental coal properties, derived coal properties, and process responses. Many novel relationships have been found employing multivariate statistical analysis techniques. These results will be reported in publications to follow. Three examples of the kinds of correlations that have been developed are reported below.

Coal density by helium pycnometry is related to the elemental composition as defined by Equation (22).

$$D_{He(dmmf)} = 0.023 * C_{dmmf} + 0.0292 * O_{dmmf} - 0.0261 * H_{dmmf} + 0.0225 * S_{org_{dmmf}} - 0.765 \quad (22)$$

The above expression accounts for 94% of the variance of the densities of the samples (viz. $r^2 = 0.943$).

For those coals exhibiting a free swelling index (FSI) greater than zero, 91% of the variance of the FSI for the samples can be explained according to Equation (23).

$$FSI = 0.875 * C_{dmmf} + 0.859 * S_{dmmf} + 1.304 * H_{dmmf} + 0.347 * R/I - 77.715 \quad (23)$$

In Equation (23), R/I refers to the ratio of reactive macerals (vitrinite, liptinite) to "inert" macerals (fusinite, micrinite) plus mineral matter.

Volatile matter is also strongly correlated with elemental composition ($r^2 = 0.96$) according to the relationship shown in Equation (24).

$$VM_{dmmf} = 1.281 * O_{dmmf} + 12.345 * H_{dmmf} + 1.915 * S_{org_{dmmf}} - 42.251 \quad (24)$$

CONCLUSIONS

Procedures for estimating responses of coals in synthetic fuels conversion processes are practically nonexistent. Consequently, a new look at coal characterization and classification procedures is propitious. We believe that meaningful understanding of the relationships between coal properties can be obtained only through the study of a large suite of carefully selected, prepared and analyzed coal samples. We have, therefore, begun a comprehensive coal characterization research program at the Baytown, Texas, laboratory of Exxon Research and Engineering Company. Sixty-six fresh samples of coal representing the coalification band in an H/C vs O/C plot have been analyzed in detail. Eighty percent of the samples contain <10% mineral matter. Eighty percent also contain >80% vitrinite. Through meticulous preparation procedures designed to minimize exposure to air, through numerous cross-checks of validity of the analytical data, and through calculation of the data to a mineral-matter-free basis we have assembled a data library that is being used to define interrelationships between coal properties. Numerous multivariate correlations have been found indicating strong dependence of properties such as density, free swelling index and volatile matter on elemental composition. Such correlations promise to shed considerable light on the area of coal characterization and classification.

References

1. Neavel, R. C. "Coal Structure and Coal Science: Overview and Recommendations", 178th National Meeting of the ACS, Honolulu, Hawaii, Fuel Div. Preprints, Vol. 24, No. 1, P 73., 1979.
2. Van Krevelan, D. W., Coal, Elsevier Pub. Co., 1961.
3. Spackman, W., Davis, A., Walker, P. J. Jr., Lovell, H. Ll., Essenhigh, R. H., Given, P. H., Vastol, F., and Stefanko, R., "Evaluation and Development of Special Purpose Coals, Final Reports, FE-0390-2, September, 1976.
4. Neavel, R. C., "Liquefaction of Coal in Hydrogen-donor and non-donor Vehicles," Fuel, Vol 55, July, 1976.
5. Wagoner, C. L. and E. C. Winegartner, "Further Development of the Burning Profile." Journal of Engineering for Power, 119-123, April 1973.
6. Fossil Energy Report, FE-2286-32, "Preparation of a Coal Conversion System Technical Data Book", U.S. Dept. of Energy, Prepared by Institute of Gas Technology, IIT Center, 3424 S. State St., Chicago, IL, Feb, 1979.
7. Miller, R. N., Yarzab, R. F., and Given, P. H., "Determinations of Mineral Matter Contents of Coals by Low Temperature Ashing", Fuel, Vol 58, Jan. 1979.
8. Leighton, L. H., and Tomlin, R. C., "Estimation of the volatile matter of pure coal substances", Fuel, Vol 39, P. 133, March, 1960.

FIGURE 1

DISTRIBUTION OF BAYTOWN COAL CHARACTERIZATION LIBRARY SAMPLES ON VAN KREVELEN PLOT

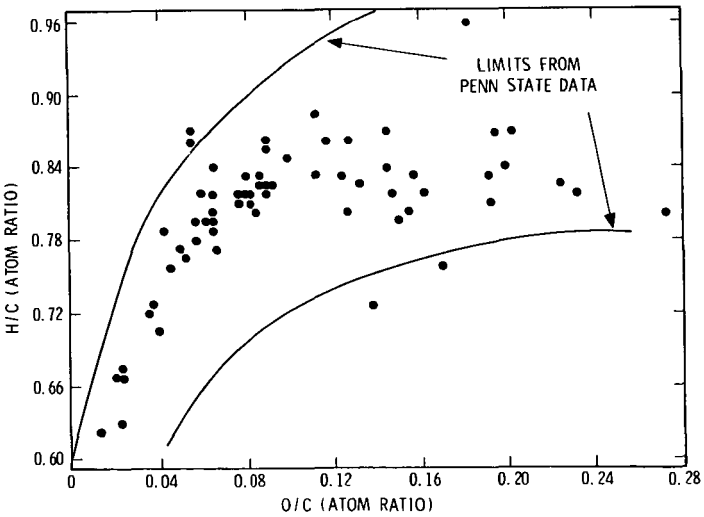

FIGURE 2. BAYTOWN COAL LIBRARY PREPARATION

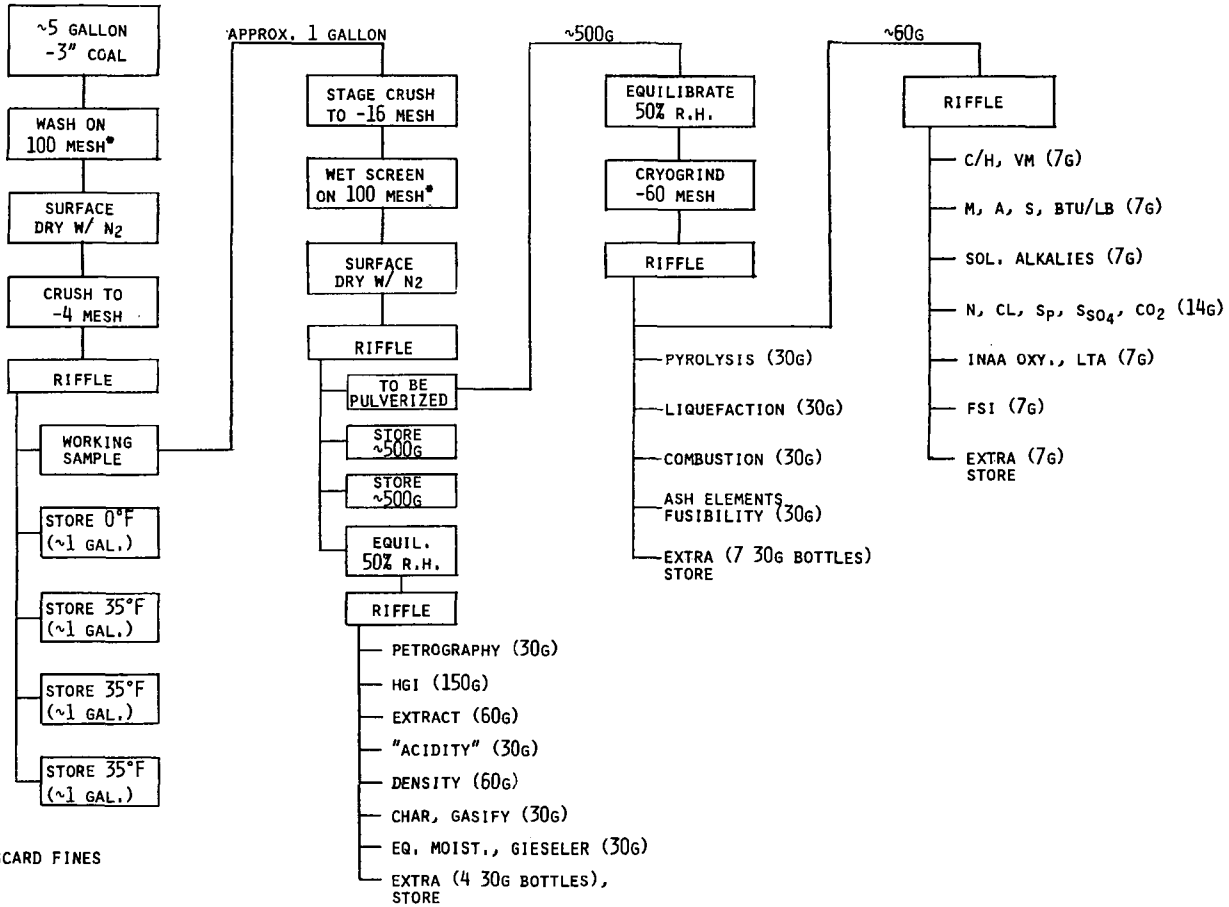

FIGURE 3

RELATION BETWEEN THE LOW TEMPERATURE ASH YIELD AND THE CALCULATED MINERAL MATTER CONTENT

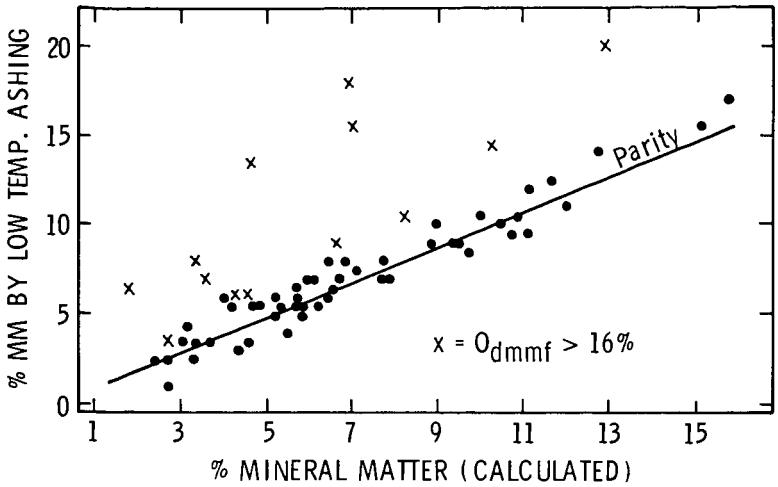

FIGURE 4

RELATION BETWEEN THE MINERAL MATTER CONTENT BY THE ACID MODIFIED LTA METHOD AND THE CALCULATED MINERAL MATTER CONTENT

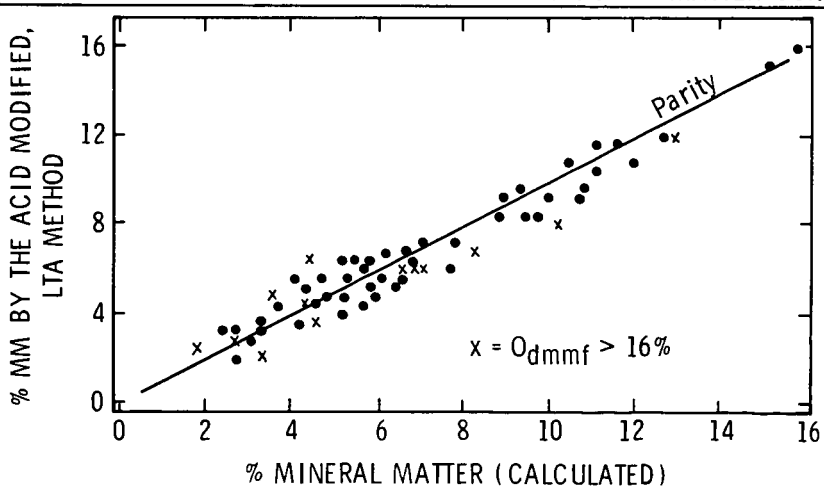

ALKALI CATALYZED CARBON GASIFICATION
I. NATURE OF THE CATALYTIC SITES

Charles A. Mims

Exxon Research and Engineering Company
P. O. Box 45
Linden, NJ 07036

Joanne K. Pabst

Exxon Research and Engineering Company
P. O. Box 4255
Baytown, TX 77520

INTRODUCTION

The published literature regarding the catalysis of gas-carbon reactions by alkali salts spans more than a century.[1] Diverse and sometimes conflicting mechanisms have been proposed to account for the catalytic activity. It is often difficult to make comparisons among the various studies because of differences in temperature range covered, carbon substrate used, and the gas atmospheres employed. The purpose of this study was to unify quantitatively the catalytic effect of potassium salts on the reactions of H_2O and CO_2 with microcrystalline or "amorphous" carbon. These poorly organized carbons are formed from a variety of precursors at temperatures greater than ∿600°C. They consist largely of "graphitic" (or trigonally bonded) carbons in small microlayers.[2] The size of these layers is a function of heat treatment temperature, carbonaceous precursor, and the presence of impurities.

We show that potassium catalyst at one atmosphere and low conversions behaves reproducibly on many of these carbon substrates and in many modes of preparation. Because of this reproducibility and because the alkali dominates the effect of other impurities, this system is in some ways easier to understand than the "uncatalyzed" H_2O-carbon reaction.

EXPERIMENTAL

Most experiments here were performed in a small tube flow reactor at one atmosphere total pressure. The gasification rates were measured under gas compositions far from gas-carbon equilibrium. Most of the rate data are for the H_2O-carbon reaction. Unless stated otherwise, analogous behavior was observed in the CO_2-carbon reaction. Reactivity profiles (instantaneous gasification rates vs. fraction of carbon remaining) generally show constant activity which holds from ∿20% to ∿70% of total burnoff. We take this steady state rate to represent the characteristic rate of the alkali catalyzed reaction when the system is catalyst limited.

CATALYST LOADING RESPONSE

Fig. 1 shows the dependence of the "steady state" rate on the concentration of alkali catalyst. A wide variety of carbon types was examined with both K_2CO_3 and KOH applied. The K/C ratios for the coal chars are corrected for the loss of potassium in reactions with mineral constituents in the coal, principally to form aluminosilicates.

All the data fall near a linear correlation for this range of catalyst loadings. (The rate eventually saturates, as shown later.) The addition of an incremental amount of potassium produces an equivalent response on a wide variety of carbon

types. Equal numbers of reaction centers are formed for each mole of salt. The dispersion is independent of loading. The "activation" energy is independent of catalyst loading, thus supporting the idea that increasing the catalyst concentration simply increases the number of active sites. The linear correlation gives a turnover rate with respect to potassium atoms of 8.2 $hr.^{-1}$ at these conditions ($700^{o}F$, $(H_2O)/(H_2) = 1$). It is also generally found that there is no major dependence of the reactivity on the methods by which the carbons are catalyzed. Provided there is adequate physical contact, a mixture of carbon and the dry powdered K_2CO_3 gives a sample of roughly equivalent activity to one which has been impregnated by a solution (see shaded points in Fig. 1). This has been noted by others.[3] Alternatively, if one attempts to maximize dispersion by ion exchange of potassium onto an oxidized coal[4], the response does not significantly differ (half shaded points in Fig. 1).

CATALYST SATURATION

The gasification rate saturates at a catalyst concentration which depends on the identity of the carbon substrate. Although the reactivity per site is insensitive to the method of impregnation, the number of catalytic sites on coal char can be controlled to some degree by pretreatment. Fig. 2 shows the rate saturation behavior for Illinois coal catalyzed in three different ways. Curve A resulted from carbonizing the Illinois coal first and then adding potassium catalyst (either KOH or K_2CO_3). Similar reactivity to the previous correlation was produced for samples with K/C loadings below 0.05. Above this loading additional alkali did not produce additional catalytic activity. Curve B in Fig. 2 shows rates for a set of K_2CO_3 solution impregnated Illinois coals. Note that the rate now saturates at a K/C ratio of ~0.1. Curve C results from digesting the coal in concentrated KOH solution and then carbonizing. The hope was to stabilize more catalytic sites during carbonization by reaction of a strong base with the coal. As can be seen, higher rates were achieved than in the previous series. When alkali was washed off this char sample and its loading reduced below 0.1, the gasification rates fell on the linear correlation obtained for all the other carbons in Figs. 1 and 2. It is possible in case A that carbons with larger microlayers - and therefore fewer edge carbons - were able to form in the absence of the alkali salts. However, the saturation limit of a particular carbon can be limited by physical as well as chemical effects. We also show gasification rates for SP-1 graphite for comparison. Very few sites are available on this substrate.

K_2CO_3 is predicted to be the thermodynamically stable salt under gasification atmospheres.[5] We heated Illinois coal with K_2CO_3 in which the carbonate carbon was labelled with ^{14}C. The evolution of $^{14}CO_2$ proceeds essentially to completion in 10 minutes at temperatures above ~500°C. No ^{14}C was detected in the form of CO or hydrocarbon products. The reaction temperature of 500°C is far below the decomposition or melting temperature of K_2CO_3. Fig. 3^a shows that the amount of K_2CO_3 which can react with Illinois coal at 700°C is limited. When approximately one potassium atom is present for every 10 carbon atoms in the resultant char, no further CO_2 is liberated from the carbonate. The saturation behavior seen in the K_2CO_3-carbon reaction is reflected in the gasification rate, shown in Fig. 2^b and 3^b. The parallelism strongly suggests that the complex formed in the K_2CO_3-carbon reaction is the site of gasification chemistry. Finally, panel 3^c shows that an important reaction step in gasification, the transfer of oxygen to and from the carbon surface, is catalyzed in an identical manner to the gasification rate. The reaction rate was monitored by the appearance of ^{14}CO in $^{14}CO_2/CO$ gas mixtures. A similar set of experiments performed in H_2O/D_2 and D_2O/H_2 mixtures gave similar results. Oxygen exchange rates on catalyzed activated charcoal are included in panel 3^c to show that the oxygen exchange rates are independent of carbon substrate. We will discuss the relative rates of the various elementary steps and their mechanistic implications in the following paper.

The above indicates a unique, reproducible degree of catalyst dispersion in this system. We obtained evidence that the dispersion is very high from poisoning studies of the H_2O-D_2 oxygen exchange reaction. In the absence of CO_2 this reaction proceeds with measurable rates at 300°C. The loading dependence of this reaction rate is analagous to that of oxygen exchange in $^{14}CO_2/CO$ mixtures and gasification. We may therefore suppose that the catalyst is in the same state of dispersion upon cooling to 300°C as at 700°C. At 300°C the exchange reaction between H_2O and D_2 can be poisoned by addition of HCl. Figure 4 shows the "titration" of reactivity by HCl on a catalyzed Illinois char sample. The reaction is quantitative - no HCl breakthrough is seen until the exchange activity has been poisoned. At the end point, one HCl molecule is adsorbed for every two potassium atoms. The stoichiometry of the poisoning reaction is independent of loading unless the sample has been saturated with catalyst.

If the poisoned system is heated to temperatures >450°C the species can rearrange to form KCl, which can be seen by X-ray diffraction, and liberate the remainder of the potassium for catalysis. The gasification rate at 700°C is then roughly one-half that of the original sample. When subsequently cooled to 300°C the H_2O-D_2 exchange rate is also one-half the original value. This activity can again be titrated in a similar manner (see Figure 4). Thus the catalyst dispersion based on HCl chemisorption is approximately one-half. The high degree of dispersion achieved by K_2CO_3 accounts for the reproducibility seen here.

Alkali salts of strong acids are much less effective catalysts than the carbonate and other salts of weak acids.[1b,d] In a thermochemical sense stable anions of strong acids provide a more attractive environment than the carbon surface for the alkali ion. Thus KCl remains as KCl on the carbon surface at K/C ratios below saturation values. This is confirmed by X-ray diffraction of KCl catalyzed samples. Much of the previous work in the literature can be explained in this framework.

CONCLUSION

Active potassium gasification catalysts are highly dispersed on the carbon substrate. We believe that K_2CO_3 reacts with the carbonaceous material to form groups at the edges of the carbon microlayers. These are the sites of the dominant gasification chemistry on amorphous carbons. This self-dispersion explains the reproducibility seen in this system. The relative catalytic activities of other alkali salts can also be rationalized by their propensity to react with the carbon surface. In the following paper, we will discuss the kinetics of the individual gasification reactions in terms of the discrete site picture presented here.

REFERENCES

1. (a) C. M. Tessi du Montay and C. R. Marechal, British Patent 2548 (1867)
   (b) H. S. Taylor and H. A. Neville, J. Am. Chem. Soc. 43, 2055 (1921)
   (c) F. J. Long and K. W. Sykes, J. Chim. Phys. 47, 361 (1950)
   (d) H. Harker, "Proceedings of the Fourth Conference on Carbon, Buffalo, 1959," Pergamon Press, New York, 1960, pp. 125-139
   (e) J. L. Johnson, Catal. Rev. - Sci. Eng. 14, 131 (1976)

2. R. E. Franklin, Acta. Crystallogr. 3, 107 (1950)

3. W. K. Lewis, E. R. Gilliland, H. Hipkin, Ind. Eng. Chem. 45, 1697 (1953)

4. E. J. Hippo, R. G. Jenkins, P. L. Walker, Jr., Fuel 58, 338 (1979)

5. D. W. McKee and D. Chatterji, Carbon 13, 381 (1975)

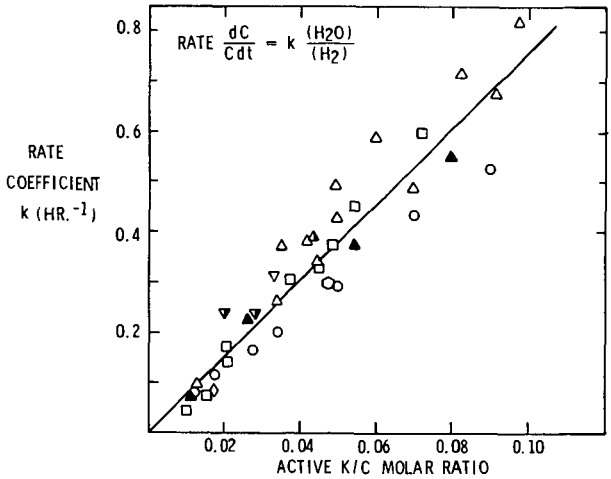

FIGURE 1. DEPENDENCE OF GASIFICATION RATE ON CATALYST LOADING FOR DIFFERENT CARBONS. K/C RATIOS ARE CORRECTED FOR REACTIONS WITH COAL MINERALS. METHOD OF CATALYST IMPREGNATION: OPEN SYMBOLS-SOLUTION-INCIPIENT WETNESS, HALF-SHADED SYMBOLS-ION EXCHANGED, SHADED SYMBOLS-DRY MIXED. △ ILLINOIS, ▽ WYODAK (WASHED), □ ACTIVATED CHARCOAL, ○ SPHEROCARB, ⬡ SPHERON 6, ◊ POLYFURFURYL ALCOHOL COKE

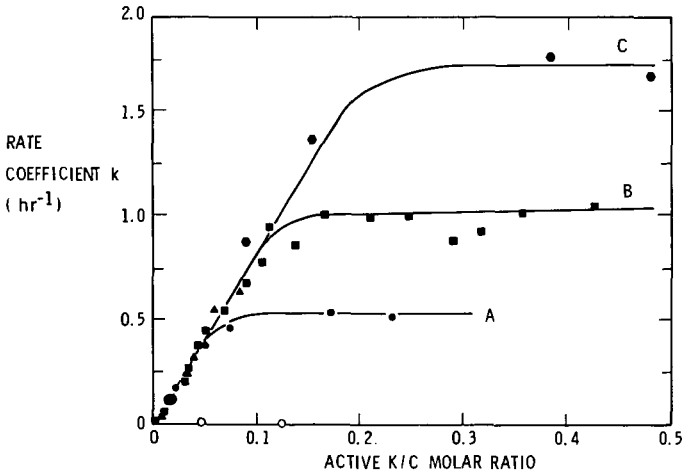

FIGURE 2. GASIFICATION RATE SATURATION CURVES. CURVES A,B, AND C ARE FOR CATALYZED ILLINOIS SAMPLES PREPARED USING DIFFERENT PRETREATMENT TECHNIQUES (SEE TEXT FOR DETAILS). o- SP-1 GRAPHITE.

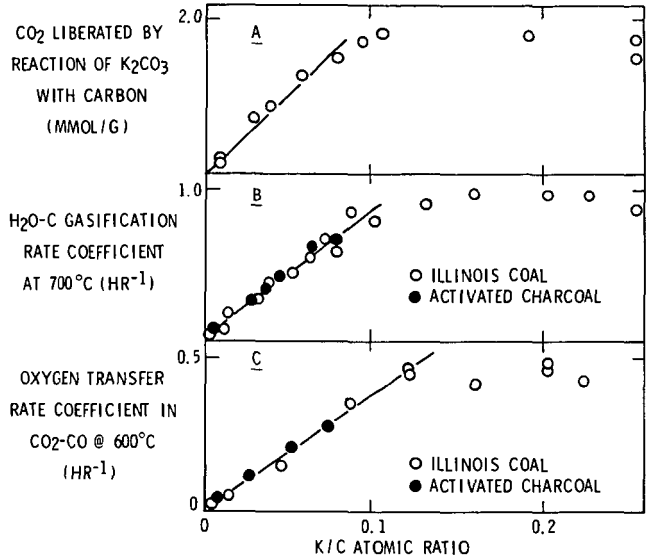

FIGURE 3. COMPARISON OF GASIFICATION RATES WITH K_2CO_3-CARBON REACTION YIELD. O ILLINOIS COAL, ● ACTIVATED CHARCOAL

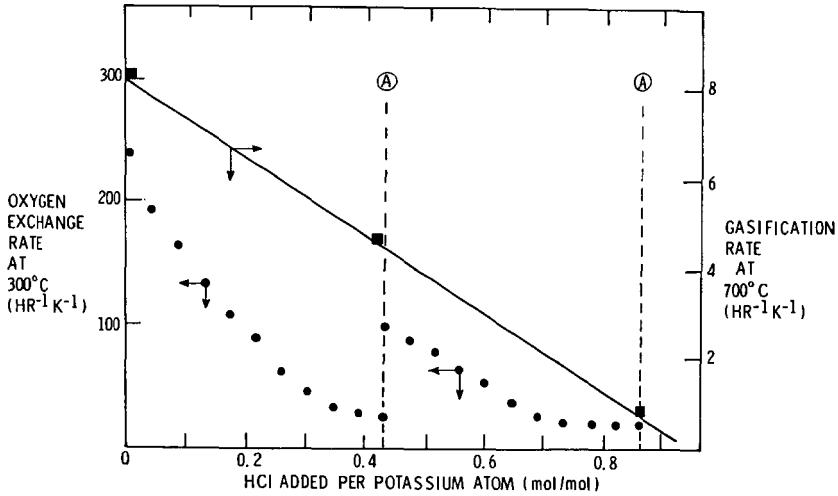

FIGURE 4. HCl POISONING OF POTASSIUM CATALYZED ILLINOIS CHAR. OXYGEN EXCHANGE AT 300°C IS SHOWN AS A FUNCTION OF HCl ADDED. AT POINTS LABELLED Ⓐ THE SAMPLE WAS HEATED TO 700°C AND THE GASIFICATION RATE MEASURED. FOR BOTH RATE MEASUREMENTS, $(H_2O)/(H_2, D_2) = 1$.

ALKALI CATALYZED CARBON GASIFICATION II. KINETICS AND MECHANISM

Charles A. Mims

Exxon Research and Engineering Company
P. O. Box 45
Linden, NJ 07036

Joanne K. Pabst

Exxon Research and Engineering Company
P. O. Box 4255
Baytown, TX 77520

INTRODUCTION

The kinetics and mechanism of carbon gasification have been the subject of many investigations. Kinetic measurements and mechanistic interpretations are often complicated by uncertainties concerning the identity, activity, and number of gasification sites. In the previous paper, a dispersed site picture was presented for catalysis of carbon gasification by potassium. This appears to be a well-defined, reproducible system consisting of a predictable number of essentially equivalent catalytic sites, and is therefore well suited for kinetic studies. We have examined the kinetics of both gasification and oxygen exchange (believed to be an elementary step in gasification) at the catalytic sites. This paper will discuss those results and some mechanistic implications.

EXPERIMENTAL

The kinetic experiments were performed in a small, atmospheric pressure fixed bed reactor charged with about 0.25 g. of catalyzed char or carbon. H_2O from a syringe pump and other gases metered through a gas manifold system were mixed and preheated in the top portion of the reactor. Unreacted H_2O was removed from the product gas which was then fed directly into a GC and/or MS for analysis. Both coals and model carbons were impregnated to incipient wetness with K_2CO_3, dried in a vacuum oven, and devolatilized under N_2 at 700°C for 30 minutes.

RESULTS AND DISCUSSION

OVERALL KINETICS

It is well known that gasification of carbon by H_2O is highly product inhibited. (1) Figure 1 shows that the gasification rate increases linearly with the $(H_2O)/(H_2)$ ratio over a broad range. The impact of product inhibition must be carefully considered when treating the kinetics of these systems in integral reactors. For simplicity, the kinetic data reported in this paper were obtained in a pseudo-differential mode by feeding a mixture of H_2O and H_2 across the carbon bed at low H_2O conversions and at sufficient $(H_2O)/(H_2)$ ratio so that the reactivity of the gas did not change significantly across the bed.

In developing a mechanism for gasification, the strong product inhibition must be explained. The concept of gas/carbon oxygen exchange involving surface carbon oxides as gasification intermediates is the key to many mechanistic schemes. A simple surface oxide mechanism has been discussed frequently in the literature: (2)

$$H_2O + \bar{c} \underset{k_{-1}}{\overset{k_1}{\rightleftharpoons}} \frac{O}{\bar{c}} + H_2 \qquad \text{OXYGEN EXCHANGE} \qquad 1)$$

$$\frac{O}{c} \xrightarrow{k_2} CO + \bar{c} \qquad \text{SURFACE OXIDE DECOMPOSITION} \qquad 2)$$

In the context of the dispersed site picture for potassium catalyzed gasification, $\bar{c}$ is a carbon atom associated with an active catalytic site, and $\frac{O}{\bar{c}}$ is the oxidized form of the active site. Upon decomposition of the surface oxide a new site is regenerated perhaps as the alkali specie becomes associated with another carbon. The number of active sites, Ct, remains approximately constant up to high carbon conversions as reflected by the flat gasification burnoff curves discussed in the previous paper.

According to this and similar mechanisms, the gasification rate is proportional to the number of surface oxides present under gasification conditions, $dc/dt \propto (\frac{O}{\bar{c}})$. This scheme suggests that H_2 inhibits gasification by decreasing the number of surface oxides through the reverse oxygen exchange reaction. (Several other mechanisms have been proposed in which H_2 is thought to block active gasification sites through chemisorption.(3)) If the oxygen exchange reaction is in equilibrium and the number of surface oxides is determined by the equilibrium constant of reaction 1 (i.e. $(\frac{O}{\bar{c}})/(c) = K_1(H_2O)/(H_2)$) then the relative rates of gasification of carbon by different reactants can be predicted by their relative oxygen activities. For example, the relative rates of carbon gasification in H_2O and D_2O at the same $(H_2O)/(H_2)$ and $(D_2O)/(D_2)$ ratio would be given by the ratio of the oxygen exchange equilibrium constants, i.e.

$$\frac{\text{RATE, } H_2O}{\text{RATE, } D_2O} = \frac{K_1, H_2O}{K_1, D_2O}$$

This ratio is equivalent to the equilibrium constant for the reaction $H_2O + D_2 \rightleftharpoons D_2O + H_2$, which can be calculated from thermochemical data and is plotted in Figure 2 as a function of temperature. The data for the measured rate ratios fall very near the predicted line in the temperature range studied. Oxygen activity therefore does appear to be an important factor in determining the gasification rate. This supports the idea that H_2 inhibition occurs through reversal of oxygen exchange rather than by site blocking due to chemisorption.

From the simple surface oxide mechanism represented by Equations 1 and 2, assuming a site balance $Ct = \bar{c} + \frac{O}{\bar{c}}$, a Langmuir-Hinshelwood type rate expression can be derived (2):

$$\frac{d(CO)}{dt} = \frac{k_1\ k_2\ Ct\ (H_2O)}{k_1(H_2O) + k_{-1}\ (H_2) + k_2} \quad . \qquad 3)$$

For agreement with the overall gasification kinetics, this expression must be reduced to a form which reflects the linear dependence of the rate on the $(H_2O)/(H_2)$ ratio. This dictates that the $k_{-1}(H_2)$ term dominate the denominator, in which case the rate equation reduces to

$$\frac{d(CO)}{dt} = k_2 k_1 Ct \frac{(H_2O)}{(H_2)} \ . \qquad 4)$$

The $k_{-1}(H_2)$ term will outweigh the other terms in the denominator if the oxygen exchange reaction is in equilibrium, the equilibrium constant is small, and the subsequent surface oxide decomposition is slow. In addition to providing for the dependence of the rate on the $(H_2O)/(H_2)$ ratio, Equation 4 also reflects the linear dependence of the rate on catalyst loading discussed in the previous paper, and on the oxygen activity of the gas (i.e.K_1).

This simple mechanism based on the concept of oxygen exchange is useful in understanding how a number of factors can influence the gasification rate. For further evaluation of this mechanism, the assumptions which had to be made in order to reduce the rate expression to a reasonable form must be tested. This was done by studying the kinetics of the oxygen exchange reaction.

OXYGEN EXCHANGE

The oxygen exchange reactions can be readily followed using isotopic exchange techniques. For the case of $H_2O/\bar{c}$ oxygen exchange, a mixture of H_2O and D_2 is fed across the carbon bed. Since, as it will be demonstrated, oxygen exchange is very fast compared to gasification, the experiments can be performed at conditions where the gasification rate is negligible. Isotopic scrambling occurs as H_2O and D_2 undergo oxygen exchange with the catalyzed carbon according to Equation 1. In the experiments the water products (H_2O, HDO, and D_2O) were trapped out of the product stream and the gas products (H_2, HD, and D_2) were fed directly into a mass spectrometer for analysis. At gasification conditions, statistical scrambling of the isotopes between the gas and water products was observed, indicating that the reaction was in equilibrium. Under conditions at which the reaction was not at equilibrium, the rate of oxygen exchange was calculated from the rate of appearance of H in the gas products. (4)

Turnover rates (per C atom) for $H_2O/\bar{c}$ oxygen exchange were measured for Illinois char as a function of K_2CO_3 loading (expressed as K/C atomic ratio) and are shown in Figure 3. The gasification rate is plotted as well for comparison. The oxygen exchange rate increases linearly with catalyst loading until saturation which occurs at a K/C atomic ratio of approximately 0.12/1. The figure includes data for several other carbon forms as well. Below catalyst saturation the oxygen exchange rate shows very little dependence on the form of the carbon substrate. In both instances this parallels the behavior of the gasification rate (as discussed in previous paper), very strong evidence that oxygen exchange is occurring at the gasification sites. Although they were measured at a lower temperature, the rates of oxygen exchange were considerably higher than the gasification rates, indicating that the measured oxygen exchange is not rate controlling in gasification.

The kinetics of oxygen exchange occurring at the gasification sites are important in developing and evaluating an overall gasification mechanism. Figure 4 shows that oxygen exchange is first order in (D_2) and essentially independent of (H_2O). In terms of the simple oxygen exchange model, oxygen exchange occurs via Equation 1, and a Langmuir-Hinshelwood type expression can be derived for the rate of oxygen exchange:

$$H_2O + \bar{c} \underset{k_{-1}}{\overset{k_1}{\rightleftharpoons}} H_2 + \overset{o}{\bar{c}}$$

$$\text{RATE} = \frac{k_1 k_{-1}\, Ct\, (H_2O)\, (H_2)}{k_1(H_2O) + k_{-1}(H_2)} \quad . \qquad 5)$$

For the model to be consistent, the conditions imposed on the various rate coefficients in deriving the overall rate expression (Equations 3 and 4) must apply here as well. This requires that the $k_{-1}(H_2)$ term again dominate the denominator, in which case Equation 5 reduces to

$$\text{RATE} = k_1(H_2O)Ct \; . \qquad 6)$$

This predicts that the oxygen exchange rate should be first order in (H_2O), in direct conflict with the data shown in Figure 4. The assumptions which were made in deriving a reasonable rate expression from the simple model were therefore incorrect, indicating that the simple model cannot adequately describe the system. More complex oxygen exchange models can be visualized which could reconcile the data, and these will be the subject of future studies.

Kinetic studies of gasification and oxygen exchange in the CO_2-carbon system have also been performed as part of this investigation. An oxygen exchange mechanism for CO_2 gasification analogous to that discussed here for H_2O gasification has been proposed in the literature (2). Our results do support a strong analogy between the two systems. The kinetic results and mechanistic implications drawn for the CO_2-carbon system were essentially identical to those discussed here for the H_2O-carbon system.

CONCLUSIONS

Oxygen exchange is catalyzed by the potassium gasification catalyst and occurs at the same sites as gasification. Product inhibition of gasification occurs through reversal of the oxygen exchange reaction by the product rather than by chemisorption. This implies the participation of a critical surface oxide in gasification. However, this critical oxide does not react with the gas phase via Equation 1 as the dominant mode of oxygen exchange.

REFERENCES

1. F. J. Long and K. W. Sykes, J. Chim. Phys. 47, 361 (1950)

2. P. L. Walker, Jr., F. Rusinko, Jr., L. G. Austin, Advan. Catalysis 11, 133 (1959)

3. For discussion, see H. H. Lowry, ed., "Chemistry of Coal Utilization, Supplementary Volume," John Wiley and Sons, Inc., New York-London, 1963, p. 929

4. A. A. Orning and E. Sterling, J. Phys. Chem. 58, 1044 (1954)

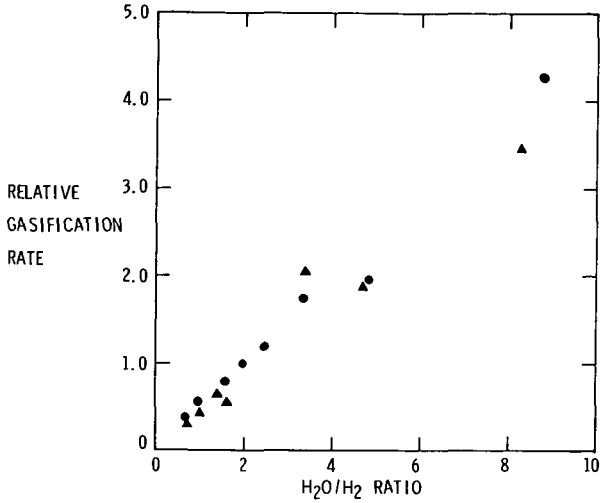

FIGURE 1. PRODUCT INHIBITION OF GASIFICATION RATE. ▲ ILLINOIS + K_2CO_3, ● SPHEROCARB + K_2CO_3 700°C.

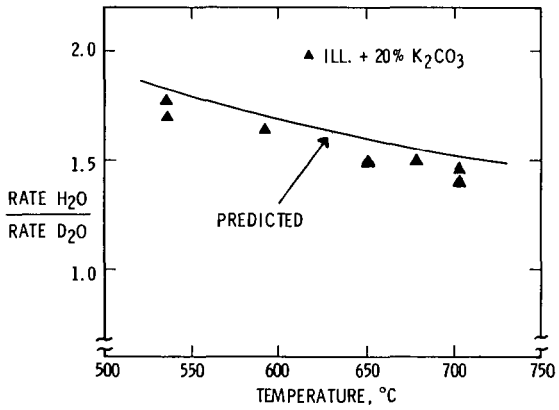

FIGURE 2. DEPENDENCE OF GASIFICATION RATE ON OXYGEN ACTIVITY: RELATIVE GASIFICATION RATES IN H_2O AND D_2O. SOLID LINE - PREDICTED VALUES. ▲ MEASURED VALUES.

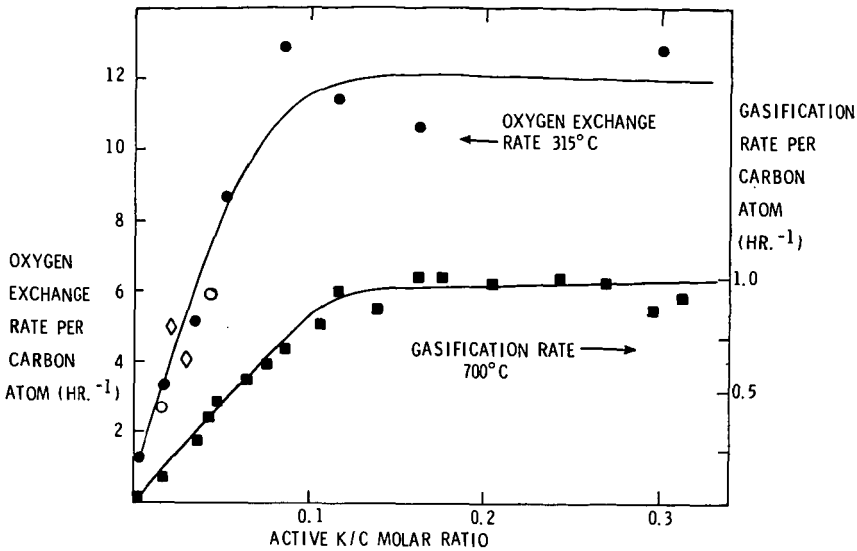

FIGURE 3. DEPENDENCE OF H_2O-D_2 OXYGEN EXCHANGE RATE ON CATALYST LOADING AND COMPARISON WITH GASIFICATION RATE. ●, ■ ILLINOIS COAL + K_2CO_3, ○ ACTIVATED CHARCOAL + K_2CO_3, ◊ SPHEROCARB + K_2CO_3

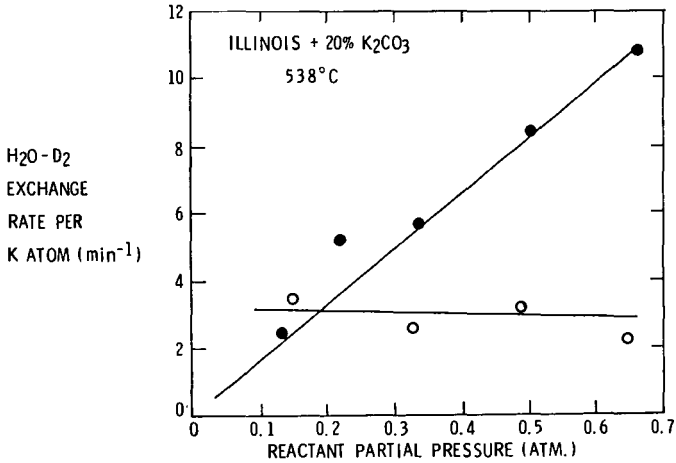

FIGURE 4. DEPENDENCE OF H_2O-D_2 OXYGEN EXCHANGE RATE ON REACTANT PARTIAL PRESSURE. ● D_2, ○ H_2O.

BOTTOMS RECYCLE STUDIES IN THE EDS PROCESS DEVELOPMENT

L. L. Ansell, J. W. Taunton and K. L. Trachte

Exxon Research and Engineering Company
P. O. Box 4255
Baytown, Texas 77520

This paper will present the recent status of developments in moving the Exxon Donor Solvent coal liquefaction technology to commercial readiness. It will discuss results from the operations of totally integrated coal liquefaction pilot plants in which the vacuum tower bottoms are recycled back to the liquefaction reactor system. The paper will give an overview of the EDS coal liquefaction process and will present selected results of the vacuum bottoms recycle studies that have been undertaken to date. In discussing these studies, coal feed flexibility, yield and product flexibility and pilot unit operability will be stressed. Finally, these results will be summarized with a short discussion of the benefits and issues involved in EDS bottoms recycle development.

In the first figure options available with the EDS process involving liquefaction and bottoms processing technologies necessary to provide the required fuel and hydrogen are shown.

In the EDS process, coal is slurried with a hydrogen donor solvent. This slurry is fed in admixture with molecular hydrogen to the liquefaction system. The reaction products are separated by conventional fractionation steps into gases, liquids and a vacuum bottoms stream. Part of the liquid stream is catalytically hydrogenated in a fixed bed, hydrogenation reactor in the presence of molecular hydrogen and becomes the donor solvent. The hydrocarbon gas can be reformed to produce process hydrogen, it can be sold or it can be burned as a process fuel gas. Liquids are the ultimate product from the EDS process and are quality distillates boiling below 1000°F. Options for the vacuum bottoms include partial recycle, feed to a FLEXICOKING unit which produces liquids and process fuel gas or feed to a partial oxidation unit to produce hydrogen or fuel gas. For operations where the vacuum bottoms production is not sufficient to meet the necessary fuel and hydrogen requirements, additional coal can be used as feed to a partial oxidation unit to supplement hydrogen and fuel manufacture.

This paper will address results from the liquefaction step in the EDS process; or in Figure 1, the shaded portion. References will be made to bottoms processing for comparative purposes only.

In the development of the EDS process, extensive use has been made of small integrated coal liquefaction pilot plants of 75 pound-per-day and 1 ton-per-day feed coal capacities. The key features of these pilot plants are shown schematically in Figure 2. In the slurry preparation area, coal is slurried with a recycle donor solvent. The smaller unit uses a batch preparation technique involving manual addition of the solvent, crushed coal and bottoms (if recycled) on a six-hour frequency. The larger 1 ton-per-day unit has continuous slurry preparation. Both units feed from a slurry holding tank using high pressure positive displacement pumps.

The slurry is mixed with hydrogen before preheating and fed to tubular upflow reactors in both units. The reactors are staged to achieve the desired nominal residence time under study and the stages are connected by tubular transfer lines.

The liquefaction reactor effluent is separated by a series of conventional fractionation steps. Gases are separated by high and low pressure flashes. The unconverted coal and mineral matter are separated from the heavier coal liquids by recycle gas stripping in the smaller unit and by vacuum distillation in the 1 ton-per-day unit. Products are

split into naphtha and distillate using fractionation towers on both units. Part of the distillate is used for producing the recycle solvent.

This unhydrogenated distillate is introduced with molecular hydrogen into a conventional fixed-bed catalytic reactor. The hydrogenation conditions are tailored to produce the recycle solvent of the right specification, and this donor solvent is then used for slurrying the crushed coal.

In Figure 3, one of the very important findings obtained early in the bottoms recycle studies is shown. These data show that coal conversion with vacuum bottoms recycle is very sensitive to the liquefaction conditions. In this figure, the pyridine insoluble fraction in the vacuum bottoms, on a DAF coal basis, is plotted against the hours of onstream pilot plant bottoms recycle operations. This data is for West Virginia coal (Ireland mine) and was obtained from operations using the 75 pound-per-day pilot unit. As was discussed above, the 75 pound-per-day pilot unit utilizes a batch slurry preparation technique. This is important because it influences the amount of time required for equilibration of the bottoms stream. This is evident from the very early period of time when the bottoms recycle mode of operations was just starting. During this period, the data show the pyridine insolubles are about 4-5% on a DAF coal basis. As time progresses, the pyridine insolubles are observed to be increasing with time. This is indicative of retrogradive reactions taking place in the liquefaction system and is a result of the necessary hydrogen not being available for quenching the reactive coal fragments. Consequently, the formation of pyridine insolubles increased to an equilibrated level of about 8% as the bottoms recycle operation was continued. In Figure 3, spot samples are shown as points, bars indicate periods during the operation used for material balance purposes. During this period of time there was no observed change in coal conversion over that observed from coal-only operations due to these retrogradive reactions taking place. After returning to coal-only operations in which the recycle of the bottoms was discontinued, the pyridine insolubles in the bottoms dropped back to their previous level of around 4-5%.

The data was initially puzzling but in fact helped in understanding the phenomena that were occurring. Earlier work had suggested the sensitivity of bottoms recycle to hydrogen availability. By increasing pressure and solvent-to-coal-to-bottoms ratio a continuation of the low pyridine insoluble content in the bottoms product was realized. This is also shown in Figure 3 and comes from the fact that additional hydrogen is being supplied from the gas phase as molecular hydrogen and from the liquid phase due to the higher level of donatable hydrogen present with the solvent. At the higher solvent rates and higher pressure that were employed in this successful bottoms recycle experiment, the coal conversion did increase. Discussion of the additional conversion from bottoms recycle will be presented in detail subsequently.

This study has been expanded from the West Virginia coal to include other coals including an Illinois No. 6 coal and the Wyoming coal. These data along with conventional coal-only data are shown in Figure 4.

In Figure 4, the 1000°F$^+$ liquefaction conversion on a DAF coal basis obtained from the integrated pilot plants is presented. Here both the coal-only and bottoms recycle operations under EDS liquefaction conditions are shown. High conversions for all the coals in the range of 55-65% DAF coal are obtained with coal-only operations with the exception of the Illinois No. 6 Burning Star coal. These include bituminous, subbituminous and lignitic coals and confirm the fact the EDS process on a coal-only basis is applicable to a wide variety of coals. The initial data on the bottoms recycle operations show substantial increases in the conversion of the coal for three of the coals: the Illinois No. 6 and West Virginia bituminous coals and the Wyoming subbituminous coal.

In Figure 5, results are provided that show the liquid yields for the conversion conditions that were discussed previously. Despite the fact that there are differences in liquefaction liquid yields for each of the coals, additional liquids can be recovered from the FLEXICOKING operation on the bottoms to give total liquids of about 45-55% of DAF coal for all of the EDS program coals. For bottoms recycle, liquid yields of the same magnitude are achieved from the liquefaction step. Additional data will be forthcoming to define what additional liquids can be recovered from FLEXICOKING of vacuum bottoms from bottoms recycle operations.

In summary, pilot plant studies have successfully confirmed that the EDS process is flexible to process a wide variety of coals. In the 75 pound-per-day unit all of the EDS project coals have been processed to high yields of liquid products. In the 1 ton-per-day unit, investigation of three EDS project coals has confirmed the liquid yields from the smaller unit. Additional studies to investigate the remainder of the coals are planned using the 1 ton-per-day pilot plant.

Initial pilot plant studies indicate that bottoms recycle may be an attractive mode of operations. This is based on data from the 75 pound-per-day unit for three EDS project coals--the Illinois, the West Virginia, and the Wyoming coals and data from the 1 ton-per-day unit for the Illinois and Wyoming coals. Additional discussion of these data will follow.

The pilot unit data indicate there is a syngerism between higher pressure and bottoms recycle which leads to the higher conversion and liquid yields. Small autoclave studies, although not covered here, indicate bottoms recycle is generally applicable under EDS conditions to all the coals discussed here.

In Figure 6, data showing the product distributions from bottoms recycle operations with Illinois No. 6 bituminous coal from the Monterey No. 1 mine is presented. The product yields in wt % based on the dry coal fed to the unit are shown for different operating conditions and for the different units. Comparison is made between a previous base set of coal-only operations which resulted in a liquid yield of approximately 34% on dry coal. These yields were achieved for coal-only conditions at 840°F, 60 minutes residence time, at 1500 pounds pressure. In the bottoms recycle mode of operation at 2000 psi an additional 7% liquids and an additional 10% C_1-C_3 gas is obtained. This is counterbalanced by increased hydrogen consumption of about 3 wt % on coal. These data have been taken from operations of the 75 pound-per-day unit and similar results are obtained from the operations of the 1 ton-per-day unit as shown in the companion figure. Here we do have a direct comparison at the higher pressure. Notice that the increase in liquids is maintained along with the increase in C_1-C_3 gas. As would be expected, the corresponding increase in hydrogen consumption is there also. In data from both pilot units, an increase in the amount of C_4-400°F naphtha is observed compared to coal-only operations.

In Figure 7, similar data are shown but for the Wyoming subbituminous coal from the Wyodak mine. The product yields for coal-only and bottoms recycle conditions from both the 75 pound-per-day unit and the 1 ton-per-day pilot unit are shown. Here the liquefaction conditions have been changed to 800°F, 100 minutes. From the 75 pound-per-day unit and for coal-only operations at 1500 psi approximately 29% liquids are obtained, for coal-only operations at 2500 pounds the liquids are increased to about 34%. For bottoms recycle at 2500 pounds an additional 7% liquids were recovered to total 42% based on dry coal. The increase in liquid yields is accompanied by a significant increase in the fraction in the C_4-400 naphtha and also in the C_1-C_3 gas. As would be expected these increases are accompanied by an increase in hydrogen consumption as was observed with the Illinois Monterey coal. The data from the 1 ton-per-day unit gives similar total liquid yields of around 43%. The product distribution is slightly different in that there is less of the C_4-400 naphtha and less of the C_1-C_3 gas. Here the comparison is data from 2000 pounds pressure operation with the data from 1500 pounds pressure operation for the Wyodak coal.

The results in Figure 8 are presented to show a wide range of flexibility with the bottoms recycle mode of operation to alter the product slate from essentially an all naphtha slate to one in which the naphtha content is approximately 50%. One set of data are from the 75 pound-per-day unit and one set from the 1 ton-per-day unit and it is expected that there will be slight differences in comparison but the general theme of the flexibility to change the product slate significantly is valid. Notice that the high liquid yields that were shown previously are maintained at the 42-44 wt % on a dry coal basis. The all naphtha product slate shows accompanying high C_1-C_3 gas yields. For the naphtha/fuel oil product slate, the naphtha is only about 50% and the 400-1000°F liquid is on the order of 50%. For the operating conditions leading to this product slate, the gas is substantially reduced.

In summary, the EDS bottoms recycle operations impact on the yield and product flexibility that can be obtained in the EDS process. Bottoms recycle operations provide increased liquid yields of about 8-10 wt % on dry coal and there is a general trend toward a lighter product slate. Bottoms recycle has provided product flexibility. Results showing an all-naphtha product and a naphtha/fuel oil product have been presented. Additional studies are currently underway aimed at a naphtha/distillate product. This would produce a product of all 700°F$^-$ material; part of which would be naphtha, part of which would be 400-700 distillate. The bottoms recycle mode of operations has been shown to be applicable to three coals--two bituminous coals and a subbituminous coal. As mentioned previously, based on small scale bench liquefaction studies, bottoms recycle should be applicable to all coals that are being investigated in the EDS project. This is an additional target of the current studies.

It is now appropriate to return to the discussion of the vacuum bottoms produced from coal-only and bottoms recycle operations. As discussed previously, in the initial studies of bottoms recycle operations for the West Virginia Pittsburgh seam coal, increases in pyridine insolubles due to retrogradive reactions were occurring at conditions not optimium for bottoms recycle operations. The results shown in Figure 9 are for the Illinois No. 6 bituminous coal from both the 75 pound-per-day pilot unit and the 1 ton-per-day pilot plant. For all operations, the pyridine insolubles are approximately the same; in the range of about 16% of the 1000°F$^+$ organics in the vacuum bottoms. The asphaltenes which are the benzene soluble fractions of the bottoms are on the order of 25-55% of the bottoms and the preasphaltenes are on the order of 55-25% of the bottoms. The use of bottoms recycle at the higher pressure significantly improves the quality of the bottoms as shown by the increase in asphaltene content of the bottoms when compared to the coal-only bottoms. This has led to better pilot plant operations and improved bottoms handling properties.

Additional data of this same nature is shown in Figure 10 for the Wyoming subbituminous coal. Here again comparison of data for both the 75 pound-per-day pilot unit and the 1 ton-per-day pilot plant is presented. For the 75 pound-per-day pilot unit, the data at 2500 psi show additional increases in the asphaltene content when bottoms recycle is compared to coal-only operations. In this figure, the pyridine insolubles for Wyodak bottoms are higher than for the Illinois bottoms and are approximately 20% of the DAF 1000°F$^+$ bottoms. There is significant change in the asphaltene content based on the increased pressure; note that in the data from the 75 pound-per-day pilot unit, the asphaltenes increase from about 20% to about 43% for coal-only operations by increasing the pressure from 1500 psi to 2500 psi. Additional improvements in the bottoms quality is obtained by incorporating bottoms recycle into the operations. A similar relationship for the 1 ton-per-day unit is observed although the coal-only data at 2000 psi is not available.

In Figure 11, the results of the improved bottoms character is shown. The data in this figure show the vacuum tower bottoms viscosity in poise, measured at 550°F

and 21 reciprocal seconds shear rate as a function of the amount of liquids that are left in the vacuum tower bottoms. These liquids are characterized as nominally boiling in the 850-1200°F temperature range. Figure 11 shows two distinct sets of data: one for coal-only at 1500 pounds and one for bottoms recycle at 2000 pounds.

In Figure 11, data from two different pressure levels are being compared. The effect of higher pressure on coal-only data would be to move the coal-only curve directionally toward the bottoms recycle curve. Based on a small amount of additional data, these data sets are not expected to be identical. The data shown on this slide indicate that the conditions of the vacuum tower may be relaxed to give a similar amount of liquids in the bottoms for both coal-only and bottoms recycle but have a substantial decrease in bottoms viscosity for bottoms recycle.

In Figure 12, similar data for Wyoming subbituminous coal is shown. There is some overlap in the two data sets which was not observed with the Illinois coal operations. The viscosities for bottoms recycle derived bottoms are considered to be comparable or lower than those for coal-only derived bottoms. Here there is considerable scatter observed for the coal-only viscosities. This is contrasted to relatively tight band of data for bottoms recycle operations. This consistency of the bottoms recycle data compared to coal-only data on viscosities is indicative of the relatively uniform vacuum tower operation during bottoms recycle. The bottoms produced from bottoms recycle operations with Wyoming coal have essentially the same viscosity as the bottoms from the Monterey coal under coal-only conditions.

Alternative to operating the vacuum tower in a manner to deliver products with a single liquid content there is the opportunity to deliver bottoms at a specified viscosity. For this case, the bottoms from bottoms recycle operations will have less liquid associated with them compared to the bottoms from the coal-only operations. This would lead to additional liquid recovery for bottoms from bottoms recycle as opposed to the coal-only case.

In summarizing, operability advantages have been observed during bottoms recycle studies. Smoother pilot plant operations have been observed due in part, to higher asphaltene content of the bottoms which implies fewer degradative reactions. The vacuum tower operations have been more stable which probably follows from the lower bottoms viscosity and higher asphaltene content. Record operating times in both the 75 pound-per-day unit and the 1 ton-per-day unit have been achieved with bottoms recycle.

Overall, there are benefits from bottoms recycle operations but there are still concerns that must be addressed. Bottoms recycle operations result in higher conversions for three different coals. Bench scale laboratory studies imply general coal applicability of the bottoms recycle mode of operations, and the additional coals are under investigation. Product slate flexibility has been demonstrated and naphtha and naphtha/fuel oil product slates produced from operations of the integrated coal liquefaction pilot plants. Operating conditions for naphtha/distillate product slate are under investigation. Significant pilot plant operability benefits of longer, smoother operations due to the improved bottoms character have been observed. These benefits should translate into operability advantages for the larger 250 ton-per-day pilot plant.

Commercial application of EDS bottoms recycle will require reassessment of the process bases. The increased hydrogen consumption will require rebalancing of the hydrogen/fuel supply. The processability of higher ash containing streams will require further definition. Due to the additional recycle stream, higher investment and operating costs will result. Here the reduction in bottoms production implies only one bottoms processing technology would be necessary, but development of alternative bottoms processing technologies should be pursued to ensure flexibility and reliability. The lower bottoms production will also allow a decoupling of process fuel and hydrogen production which should improve startup, operability and the service factor of a commercial facility.

FIGURE 1

OPTIONS AVAILABLE WITH THE EDS PROCESS

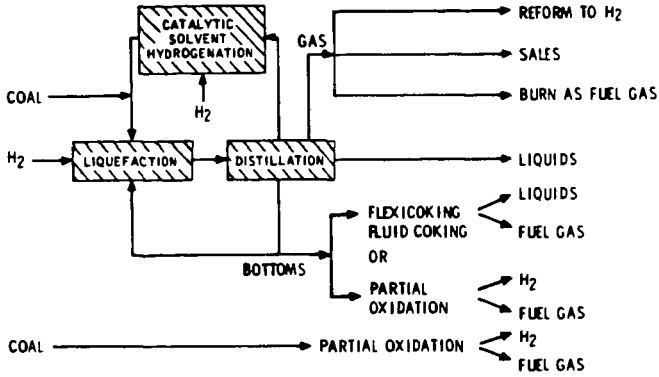

FIGURE 2

EDS COAL LIQUEFACTION PILOT PLANTS

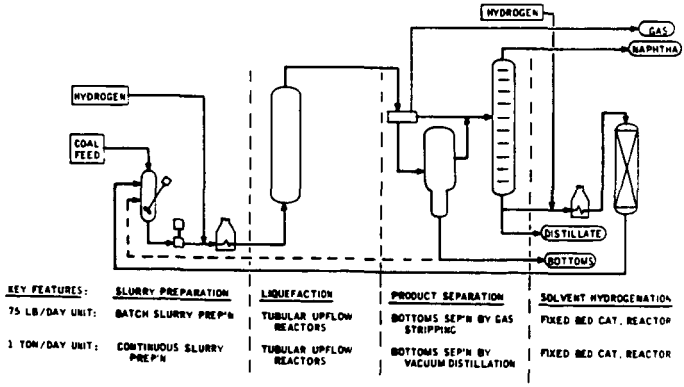

FIGURE 3

COAL CONVERSION SENSITIVE TO LIQUEFACTION CONDITIONS WITH BOTTOMS RECYCLE OPERATIONS

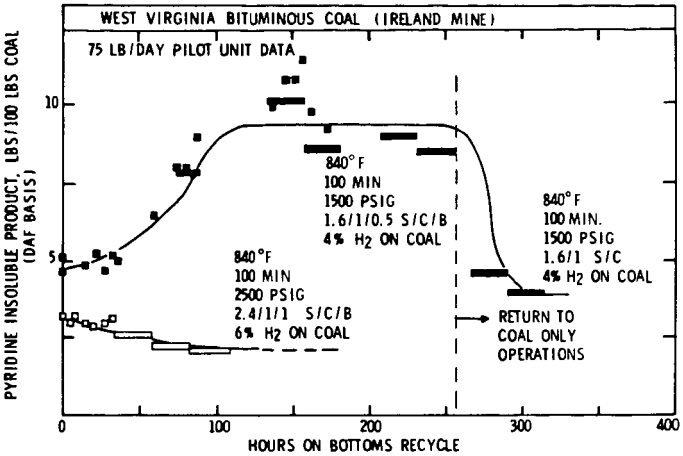

FIGURE 4

COAL RANK EFFECT ON CONVERSION

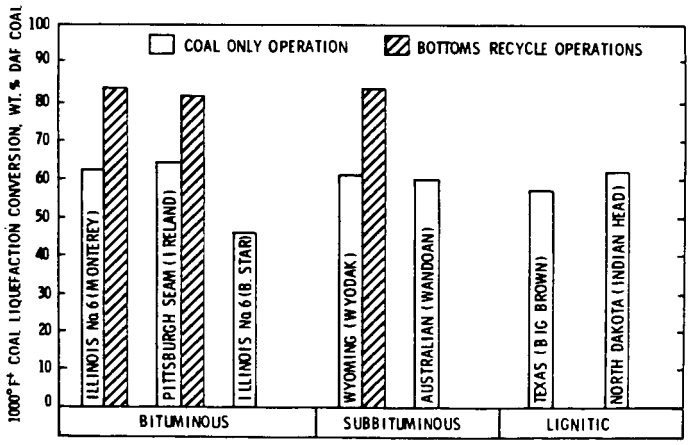

FIGURE 5

COAL RANK EFFECT ON LIQUID YIELDS

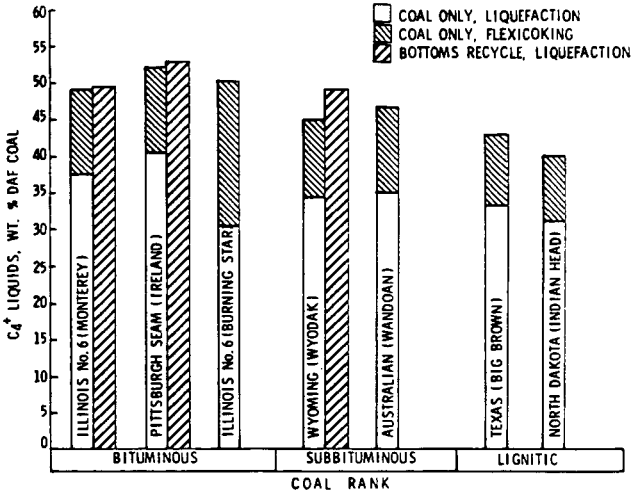

FIGURE 6

EDS BOTTOMS RECYCLE IMPROVES LIQUID YIELD AND PRODUCES A LIGHTER PRODUCT SLATE

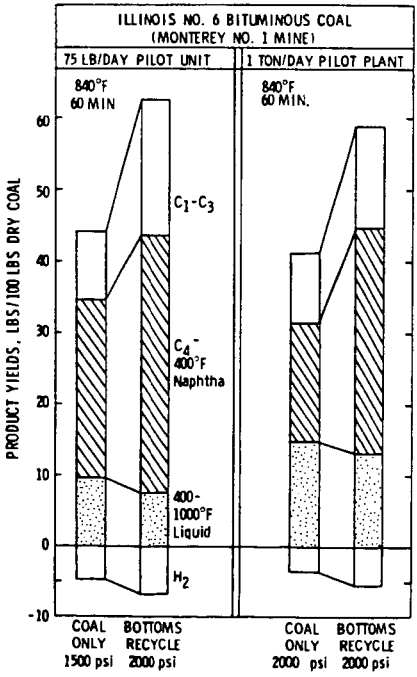

FIGURE 7

EDS BOTTOMS RECYCLE IMPROVES LIQUID YIELD AND PRODUCES A LIGHTER PRODUCT SLATE

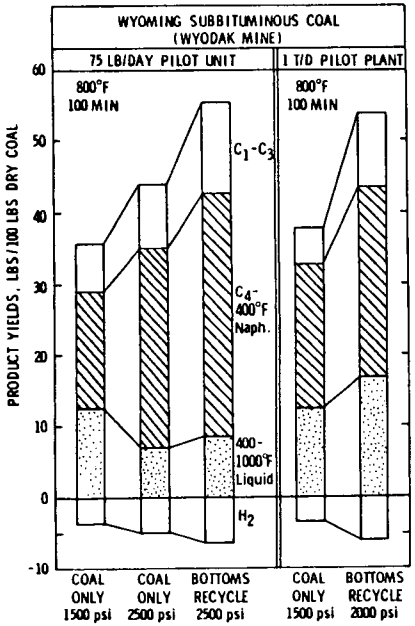

FIGURE 8

PRODUCT SLATE FLEXIBILITY ENHANCED WITH EDS BOTTOMS RECYCLE

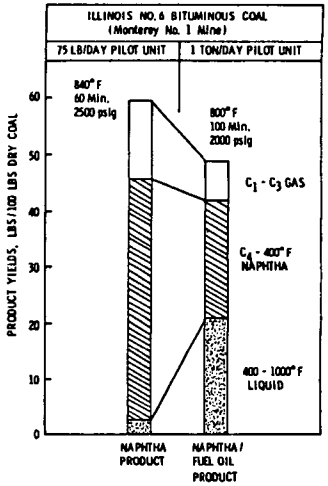

FIGURE 9

BOTTOMS RECYCLE IMPROVES SOLUBILITY OF BOTTOMS PRODUCT FROM BITUMINOUS COAL

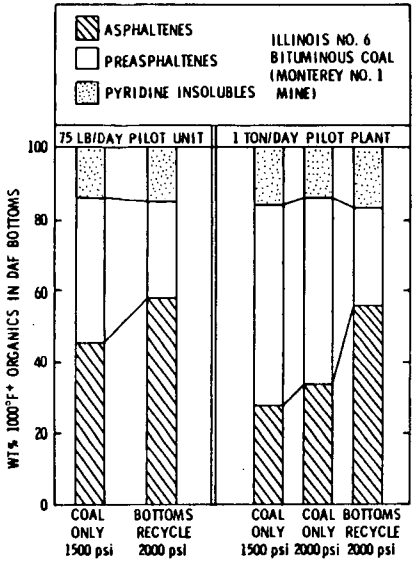

FIGURE 10

BOTTOMS RECYCLE IMPROVES SOLUBILITY OF BOTTOMS PRODUCT FROM SUBBITUMINOUS COAL

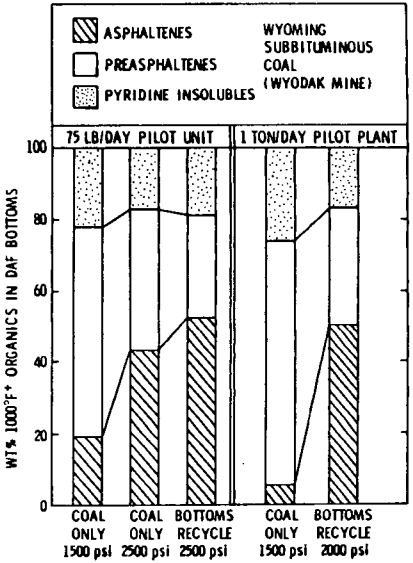

FIGURE 11

EDS BOTTOMS RECYCLE WITH BITUMINOUS COAL PRODUCES BOTTOMS PRODUCT WITH LOWER VISCOSITY THAN COAL-ONLY BOTTOMS

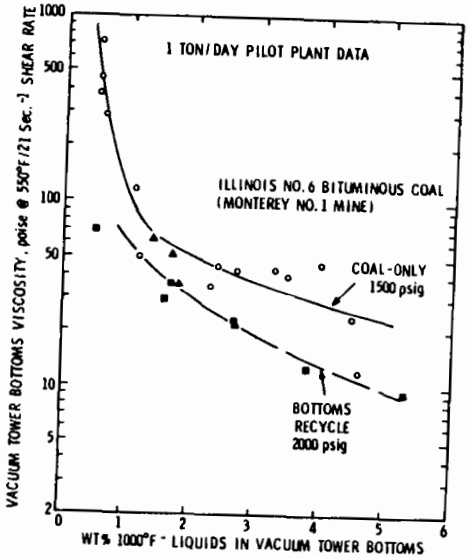

FIGURE 12
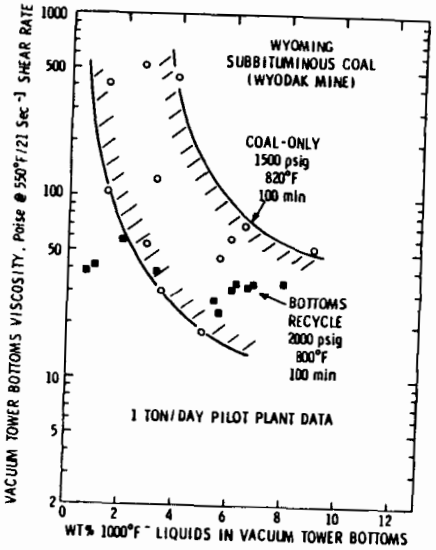
EDS BOTTOMS RECYCLE WITH SUBBITUMINOUS COAL SHOWS BOTTOMS VISCOSITY COMPARABLE TO COAL-ONLY OPERATIONS